FUNCTIONAL STUDIES OF MICRORNAS IN THE POST-DEVELOPMENTAL *DROSOPHILA* BRAIN – INSIGHTS INTO PHYSIOLOGICAL HOMEOSTASIS AND BEHAVIOR

DEVIKA GARG

B Tech
Indian Institute of Technology Kanpur

THESIS SUBMITTED FOR THE DEGREE OF

DOCTOR OF PHILOSOPHY (PHD)

DEPARTMENT OF BIOLOGICAL SCIENCES
NATIONAL UNIVERSITY OF SINGAPORE
2013

DECLARATION

I hereby declare that this thesis is my original work and it has been written by me in its entirety. I have duly acknowledged all the sources of information, which have been used in the thesis. This thesis has also not been submitted for any degree in any university previously.

Devika Garg

April 2013

Om Gurave Namah.

ACKNOWLEDGEMENTS

First of all I would like to thank my PhD advisor, Stephen Cohen, for giving me the great opportunity to work in his lab, for allowing exploration, for his encouragement and support, understanding and excellent scientific guidance through good and bad phases of my projects. I appreciate his honesty, patience and great scientific enthusiasm, and particularly his keen scientific intuition that allows following one hypothesis over another.

I am grateful to the members of my thesis advisory committee, Stephen Cohen, Joanne Yew, Adam Claridge-Chang and Christoph Winkler, for having accompanied and supported me all through my PhD, providing useful feedback and suggestions.

I am grateful to my collaborators, Jayantha Gunaratne, Mohd Farhan, and Rudy Behnia who provided help with experiments when they were most required. Thanks also, to the entire scientific community at TLL and IMCB Singapore, for help with scientific suggestions, and reagents.

Thanks to all members of the Cohen lab, former and present, who have made my work environment a pleasant, stimulating and often fun place to spend most of the day. Thanks to Sébastien Szuplewski, Jishy Varghese, Chen Ya-Wen, Ville Hietakangas, Malou Ramos-Pamplona, Valerié Hilgers, Weng Ruifen, Zhang Wei, Zhang Rui, Hong Xin, Ge WanZhong, Pushpa Verma, Jan Kugler, Héctor Herranz, David Foronda, Marita Buescher, Lim SingFee, Sherry Aw, Lynette Foo, Tan KahJunn, and Song Shilin. Special thanks to the Jishy, who helped me greatly in learning fly genetics, and gave me lots of guidance and support throughout my PhD. Special thanks to Zhang Wei, Hong Xin, Yawen and SingFee for being such great friends. Thanks to Ajay Sriram Mathuru, whose infectious enthusiasm for all things science made our discussions so entertaining.

Moving to Singapore and away from family and friends has been made a lot easier by the constant cheering-up that was delivered from a distance or, on many occasions, in person, by the people close to my heart. I thank Manu for traveling across the world to visit me. Thanks also to Deepti, Rashmi mom, Veena mom, and Swati for keeping the distances so small.

I am very thankful to the friends I made in Singapore for making my time away from home so enjoyable. Thanks to my flatmates Ekta, Shruti, life would have been really dull without you. Thanks to Pritha&Nitin, Kavita, Vignesh, Arnika&Prashant, Sumeet, Abhishek, Dipanjan, Nikhil, Vinay, Reena bhabhi and Alka aunty. Thanks to Chander Mehta uncle, for being so genuinely interested in fly research.

Nothing I have ever achieved would have been possible without the great support and love of my family. There are no words to express my appreciation, love and gratitude to my parents, Atul and Rashmi Garg, my parents-in-law, Rakesh and Veena Bansal, my sister Deepti, my brother Pratyush, my sister-in-law, Gita and my ever-inspiring grandparents, Baleshwar Das and Swarajya Garg.

Finally, thank you Manu, for your unconditional love and endearing support, for being so close over so many miles.

TABLE OF CONTENTS

Permission to re-use Figure 3.1a from Dr William Stark.

Summary

Organisms interact with their environment through gene networks embedded in their neuronal networks. Post-transcriptional gene regulation by miRNAs can provide an important and additional layer of regulatory complexity in these networks. This thesis work explores the role of one *Drosophila* miRNA, *miR-285* in the post-developmental brain, using *miR-285* loss of function mutants. In the first part, I have explored the role of *miR-285* in the *Drosophila* eye – loss of miR-285 results in light-dependent loss of photoreceptor integrity. In the second part, I have studied age-related functions of *miR-285*.

Interestingly, *miR-285* acts to 'promote' age-related impairment in the male nervous system. Mutants lacking *miR-285* are protected from age-progressive behavioral decline and live longer. *miR-285* targets genes at multiple steps in the pathway for extracellular superoxide metabolism. Mutants show elevated superoxide flux, elevated ROS signaling and are protected against oxidative stress. Interestingly, *miR-285* is expressed at higher levels in young males than in older males. Young mutant males show reduced reproductive success. Thus, regulation of superoxide metabolism in the nervous system appears to be required for reproductive fitness, at the cost of accelerated decay of brain function in male *Drosophila*.

LIST OF TABLES

LIST OF FIGURES

LIST OF SYMBOLS AND ABBREVIATIONS

Ago	argonaute
CREB	cAMP response element-binding protein
Dcr	Dicer
DP	Deep pseudopupil
EcR	Ecdysone receptor
FRT	Flp Recombination Target
GO	gene ontology
GTP	Guanosine triphosphate
Loqs	Loquacious
miRNA	microRNA
miRNP	microRNA associated ribonucleoprotein complexes
nt	nucleotide
ORF	Open reading frame
RISC	RNA induced silencing complex
RNA	Ribonucleic acid
RT-PCR	Reverse Transcription-polymerase chain reaction
SD	Standard deviation
SILAC	Stable isotope labeling by amino acids in cell culture
UTR	untranslated region

Chapter 1 Introduction

1.1 Gene regulatory networks

Gene regulatory networks are very important in controlling various developmental and homeostatic processes in plants and animals. These networks are in place at several levels, starting transcriptionally, where promoter-enhancer elements are decorated with binding sites for transcription factors that act singly or many times in conjunction with activators or repressors. By this way, the cell regulates gene expression at the most upstream level. Transcription is an energy intensive process; it's no surprise then that many major transcription factors lie downstream of signaling pathways that are either directly sensing nutrition or metabolic states, or are closely receiving input from them. The second level of regulation occurs post-transcriptionally, at capping, splicing, polyadenylation or RNA editing. All of these processes act to either stabilize the nascent transcript or create variation apart from the genetic code. Gene silencing by small RNAs is also very prevalent – miRNAs, siRNAs, piRNAs are transcribed by RNA pol III, and silence mRNAs by binding via sequence complimentarity and destabilizing them. The regulatory action of small RNAs can add an additional layer of genetic complexity that is important under many circumstances.

1.2 What are miRNAs?

In the history of the study of gene regulatory networks, miRNAs evaded discovery until 1993, stealthily functioning as important parts of the biological

machinery. The first published description of a miRNA gene appeared in 1993: in *C. elegans*, the small RNA lin-4 was identified as a regulator of larval development timing and found to control the expression of lin-14 messenger RNA (mRNA) (Lee et al., 1993; Wightman et al., 1993). The discovery of let-7, another small regulatory RNA, in *C. elegans* (Pasquinelli et al., 2000), and of its homologues in other organisms including mammals (Pasquinelli et al., 2000) opened the field of miRNA research. Since then, hundreds of miRNAs have been identified in many multi-cellular organisms, and numerous studies have revealed the diversity and biological impact of this class of non-coding RNAs.

miRNAs are small 19-22nt-long non-coding RNAs with important regulatory roles in post-transcriptional regulation of animal development and homeostatic processes. They target mRNA transcripts that have binding sites satisfying certain parameters (sequence complimentarity, binding energy etc), for translational inhibition or degradation. In this manner, they can exclude translation of certain mRNAs spatially and temporally depending upon their own transcriptional regulation. Sometimes, miRNAs can work to fine-tune their target mRNA levels, keeping them within a certain optimum range. These kinds of mechanisms can either be a part of the developmental program itself, or be important for maintaining robustness in the face of environmental fluctuations. Recent work has shown that both possibilities exist in natural systems.

miRNAs are found in all plant and animal genomes, and are expressed widely in tissues. Sequencing efforts show that miRNAs account for approximately 1% of all genes in any organism (Lim et al., 2003). Many of them are very well conserved across animal species, entailing important functions in development, physiology, morphology and behavior. The *Drosophila melanogaster* genome encodes 333 miRNAs (Griffiths-Jones et al., 2008, miRBase v19) that are believed to target approximately 30% of the protein-coding genome (Ruby et al., 2007b).

1.2.1 Why post-transcriptional gene regulation?

Post-transcriptional control seems wasteful at the first glance. The cell would save more energy by the efficient use of fewer mRNAs. However, there is ample indication that evolution may not always optimize efficiency; and the added layer of control by miRNAs may actually be useful in gene regulatory networks, providing a fast and sometimes a reversible switch on the target mRNA. In other cases, targeted degradation of mRNAs from the cell is also necessary to define certain differentiated states; for example, the zygotic miR-309 cluster clears the maternal mRNAs in the *Drosophila* embryo, to promote the maternal-to-zygotic transition (Bushati et al., 2008). miRNAs are present in diverse spatio-temporal profiles, and have a lot of regulatory potential, making it important to study their function.

1.3 microRNA biogenesis

1.3.1 miRNA transcription

miRNAs are encoded by short sequences in the genome, which maybe located intergenically, or within the intron of a protein-coding gene. miRNA locus of the former kind have an independent promoter; whereas intronic miRNAs are transcribed with the host gene. These miRNA genes can be monocistronic, dicistronic or polycistronic in nature. Upon transcription by RNA polymerase II, pri-miRNA transcripts are capped and polyadenylated, these are sometimes several kilobases long and contain hairpin loops that comprise the future mature miRNA (Fig 1.1).

1.3.2 miRNA hairpin generation

The pri-miRNA is cleaved into ~70nt hairpin pre-miRNAs inside the nucleus by the RNAse III enzyme 'microprocessor' complex Drosha/Pasha (Lee et al., 2003) followed by export into the cytoplasm (Fig 1.1). pre-miRNAs may also be directly produced from 'mirtrons' located in host-genes as introns with a hairpin structure by the spliceosome complex, thus bypassing Drosha/Pasha processing (Ruby et al., 2007a).

1.3.3 Export into cytoplasm and maturation

Upon export into cytoplasm by Exportin 5, a Ran-GTP dependent nuclear export factor, the pre-miRNA is further processed into a mature miRNA/miRNA* duplex by Dicer-1, another RNase III-type enzyme. miRNA* is the complementary miRNA sequence. The fully processed mature

miRNA is loaded onto the RNA-induced silencing complex (RISC) complex with Argonaute-1 and other associated proteins (Fig 1.1). *Drosophila* has two Dicers, Dicer-1 for miRNA processing and Dicer-2 for endogenous short-interfering RNA (siRNA) processing respectively (Saito et al., 2005) (Lee et al., 2004). *Drosophila* has five Argonaute family members (Argonaute1, Argonaute2, Argonaute3, Aubergine and Piwi). *Drosophila* Ago1 has been shown to functionally associate with Dicer-1 while Ago2 does so with Dicer-2 (Okamura et al., 2004). The fact that purified Ago-miRNA complexes mainly contain single-stranded miRNAs suggested a mechanism to unwind the duplex before loading (Martinez et al., 2002). The loading preference on one strand over the other seems to be dependent on the thermodynamic stability of the two ends of the duplex: the strand that enters the RISC is the one paired less strongly in the 5'-end (Khvorova et al., 2003; Schwarz et al., 2003). Subsequently, one of the 2 strands in the mature miRNA is released and degraded and the remaining guide strand directs the RISC complex to complementary mRNAs and silences them. The mature RISC complex together with the miRNAs is also called miRNA-ribonucleoprotein complex (miRNP). The majority of these particles are diffused in the cytoplasm. Upon stress induction, miRNAs are slightly enriched in stress granules (Mollet et al., 2008). Additionally, there is some indicative evidence that Importin 8 interacts with Ago proteins in miRNPs and targets them to cytoplasmic P-bodies (processing bodies), where most mRNA turnover takes place (Liu et al., 2005; Weinmann et al., 2009).

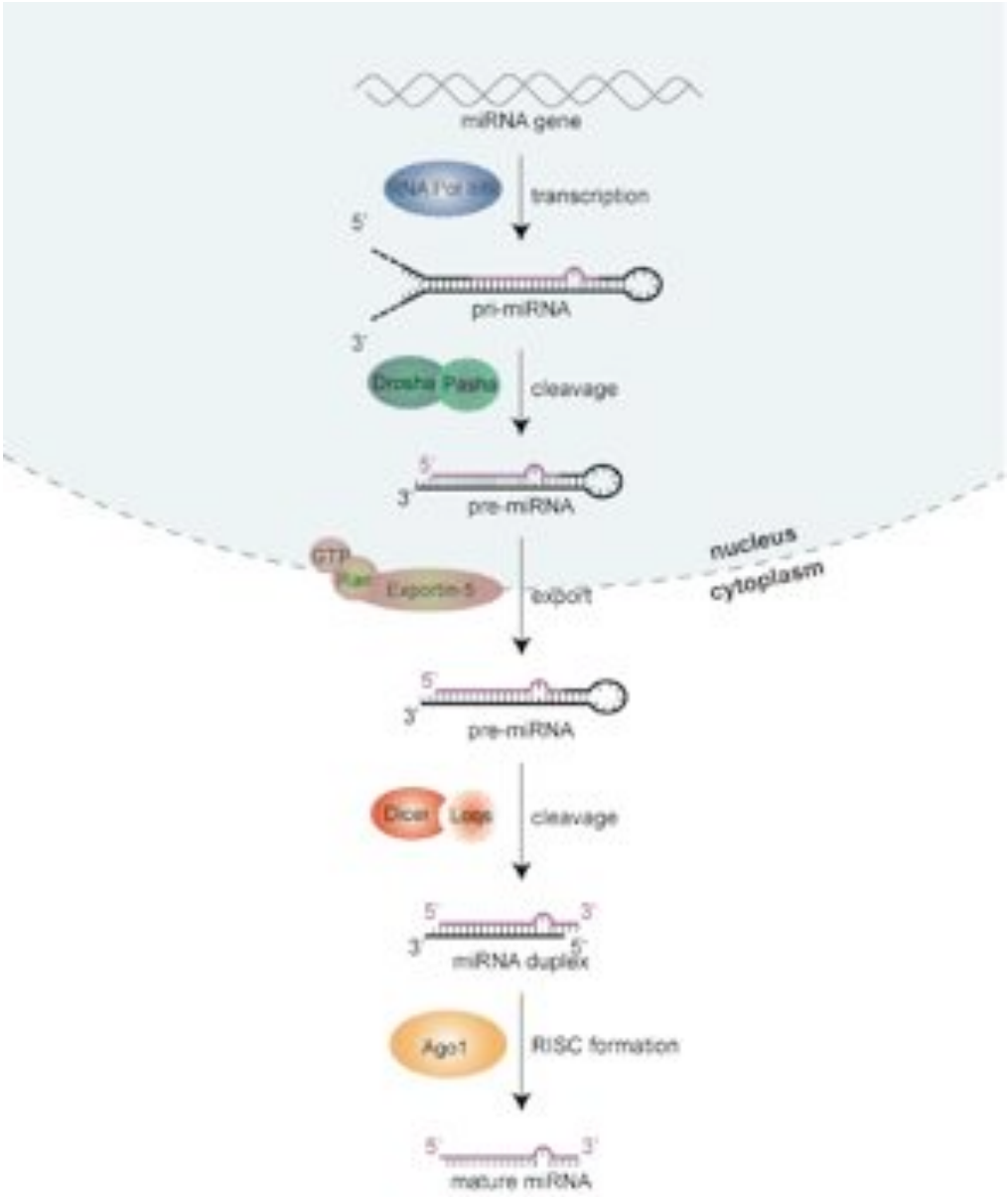

Fig 1.1 Schematic representation of miRNA biogenesis in *Drosophila*. The pri-miRNA is transcribed in the nucleus by RNA Polymerase II or III and undergoes 5'and 3' cleavage by the Drosha/Pasha complex. The generated pre-miRNA is exported into the cytoplasm by Exportin-5 via a Ran-GTP dependent mechanism. Removal of the loop structure by Dicer/Loqs leads to formation of the mature miRNA:miRNA* duplex, which is incorporated into the RISC complex. The miRNA* strand is the complementary strand to the miRNA sequence, and is generally degraded, while the mature miRNA serves as a guide to direct regulation of mRNA expression (See Section 1.3.3).

1.3.4 Non-canonical biogenesis pathways

While canonical pathways generate most miRNAs, an array of alternative strategies has emerged recently, including animal pathways that are independent of Drosha or Dicer (Westholm and Lai, 2011; Yang and Lai, 2011). For example, mirtrons are short hairpin introns whose splicing defines their pre-miRNA hairpin ends (Okamura et al., 2007) (Ruby et al., 2007a), thus bypassing Drosha. Still other RNases can substitute for Drosha to cleave pre-miRNA hairpins from longer precursor transcripts, such as RNase Z (which processes tRNAs) (Bogerd et al., 2010), or the Integrator complex (which processes snRNAs) (Cazalla et al., 2011). Interestingly, there is a reverse example - Drosha cleavage of the mammalian mir-451 generates a 42-nt-long hairpin that is too short to serve as a Dicer substrate. Instead, pre-mir-451 bypasses Dicer, and is loaded directly into Ago2 and relies on its 'slicer' activity for maturation (Cheloufi et al., 2010) (Cifuentes et al., 2010) (Yang et al., 2010). In all cases, an RNase-III enzyme is required. However, Maurin et al suggest that there may be yet another non-canonical pathway that is completely RNase-III independent (Drosha/Pasha and Dicer) where RNase Z or the Integrator complex combined with the 'slicer' activity of Ago2 may be sufficient to generate functionally mature miRNAs (Maurin et al., 2012). While they do not report any endogenously occurring miRNAs taking such a biogenesis route, they provide proof-of-principle for existence of such a pathway.

1.4 Mechanism of miRNA action

1.4.1 Binding - Seed region

Loaded onto the RISC, miRNAs act as guide molecules to find target mRNAs based on sequence complimentarity. Notably, perfect pairing is rare among animal miRNAs, whereas it is predominant in plant miRNAs. miRNAs in animals usually bind to target mRNAs via imperfect complimentarity: target sites have been grouped into several categories- 'canonical', 'seed-only/marginal' and '3'compensatory/atypical' (Brennecke et al., 2005) (Bartel, 2009). Canonical sites have perfect Watson-Crick complimentarity to a small subsequence of the mature miRNA called the 'seed' region is critically required for binding (Lewis et al., 2003); (Doench and Sharp, 2004); (Brennecke et al., 2005) (Krek et al., 2005). This region is of primary importance in the miRNA:target interaction, imparting thermal stability, and is often very highly conserved among miRNAs across species. It spans from nt 2-8 or 1-7 from the miRNA 5' end, imparting the strongest inhibition of target mRNA expression. Seed-only or marginal sites refer to matches to nt 2-7 or 3-8 of the miRNA seed region. These 6-mers have reduced efficacy. In '3'compensatory' or atypical sites, 3' compensatory sites exist in miRNA-target pairs with insufficient 5' seed pairing, creating an efficient and functional site (Brennecke et al., 2005).

Computational algorithms have been developed to predict miRNA regulatory targets, based on sequence determinants, thermodynamic stability and evolutionary conservation of sites. These algorithms and experimental reporter evidence show that miRNA binding sites are primarily enriched and most

conserved in 3'UTRs, but growing evidence suggests that sites in ORFs of mRNAs are also functionally relevant (Schnall-Levin et al., 2010). The sites in ORFs show significant conservation above background, however, targeting in ORFs appears to be weaker than 3'-UTR targeting. In *Drosophila*, computational evidence suggests binding sites in 5'-UTRs too (Lee et al., 2009).

1.4.2 Mechanisms of mRNA repression

1.4.2.1 mRNA cleavage

Following the binding of the target mRNA to the RISC complex, translation inhibition, mRNA destabilization or mRNA cleavage may take place (reviewed in (Valencia-Sanchez et al., 2006). The mechanism depends upon sequence complimentarity of the mRNA-miRNA pair. Perfect pairing leads to cleavage of the target mRNA; however this is rare for animal miRNAs, and more common for plant miRNAs. In this mechanism, mRNAs are targeted for endonuclease cleavage, referred to as 'Slicer' activity. One requirement for slicer activity additional to perfect base pairing is that Ago2 must be present within the RISC (Liu et al., 2004) (Meister et al., 2004) (Hutvagner and Simard, 2008). Ago2 has an RNaseH-like domain and contains critical residues to carry out cleavage.

1.4.2.2 mRNA degradation

mRNA destabilization is the predominant mechanism of action for metazoan miRNAs, and this is independent of slicer activity (reviewed in (Bartel, 2009).

It has been suggested that miRNAs recruit Ago/GW182 complexes to the target site, leading to the recruitment of decapping enzymes and deadenylation enzymes to initiate mRNA degradation program (Behm-Ansmant et al., 2006a; Behm-Ansmant et al., 2006b). This comes from evidence in eukaryotic cells that mammalian Argonaute proteins are concentrated in P-bodies (sites of mRNA decapping and degradation) and can co-immunoprecipitate with decapping enzymes (Jakymiw et al., 2005); (Liu et al., 2005); (Pillai et al., 2005); (Sen and Blau, 2005).

1.4.2.3 Translational inhibition

Greater than 80% of miRNA-mediated silencing takes place via mRNA degradation (Guo et al., 2010a). This is supported by the observation that microarray profiling of change in mRNA levels upon miRNA over-expression or depletion largely correlated with quantitative proteomic change upon miRNA misexpression (Baek et al., 2008; Guo et al., 2010b; Selbach et al., 2008). However, there are some examples showing changes in target at the protein level, but not at the mRNA level (Behm-Ansmant et al., 2006b; Guo et al., 2010b). Some of these examples were explained by a ribosome drop-off model in which the ribosome falls off the target mRNA while still translating, resulting in premature termination. In a more recent study, it has been suggested that miR-430 reduces the rate of initiation on target mRNAs rather than altering the ribosomal density by causing drop-off (Bazzini et al., 2012).

Hence, the mode of miRNA-mediated target repression could be rather complex, involving multiple mechanisms at mRNA and/or protein translation

level. The mechanism of action may even differ for the same miRNA in a context-dependent (spatio-temporal or target mRNA) manner, for example depending upon the co-expression of the various mode-specific enzymes/protein complexes.

However, it has recently been hypothesized that any mRNA degradation is initiated by translational inhibition at the initiation step followed by decapping and decay (Bazzini et al., 2012; Djuranovic et al., 2011). Additionally, because translational inhibition and transcript decay are very closely linked events in the cell (reviewed in (Coller and Parker, 2004), therefore any translationally inhibited mRNA will likely undergo decay unless it is actively protected from doing so. So, translational inhibition is hypothesized to be a default state of the target mRNA – it may or may not be followed by transcript decay.

1.4.3 miRNA turnover

Alterations in miRNA expression patterns under many disease conditions has caused them to get roles as potential 'biomarkers' for disease prognosis (Hu et al., 2012; Port et al., 2011; Ziu et al., 2011). Studies also reveal that some miRNA levels are regulated temporally even under normal physiological conditions in various cells and tissue types (Noren Hooten et al., 2010; Pandey et al., 2011; Somel et al., 2010). Many miRNAs change expression levels and patterns with development, or post-development (during aging). However, very little is known about the mechanisms of miRNA regulation and miRNA turnover has come under scrutiny only in recent years (reviewed in (Kai and

Pasquinelli, 2010; Ruegger and Grosshans, 2012). Both cis-acting elements and trans-acting proteins and RNAs are being discovered that affect miRNA half-life.

1.4.3.1 miRNA stabilization

Several studies show that Argonaute proteins stabilize mature miRNAs in a slicing-independent manner (Diederichs and Haber, 2007; O'Carroll et al., 2007). A recent report shows direct evidence for this interaction (Winter and Diederichs, 2011). Transcriptional inhibition by actinomycin reduced half-lives of multiple endogenous miRNA guide strands in cells lacking Ago2. This effect was reversible upon the reconstitution of Argonaute expression. Correspondingly, over-expression of Argonaute proteins decelerated miRNA degradation and increased miRNA half-life (Winter and Diederichs, 2011). Ago2 mediated stabilization is further corroborated by the finding that endogenous target binding is also protective of miRNAs in *C. elegans* (Chatterjee et al., 2011). Recently, GW182 has also been identified to have a protective role by stabilizing mature miRNAs (Yao et al., 2012).

Protective modifications on mature miRNAs can also affect stability. It was recently demonstrated that 3′ adenylation can have a stabilizing effect on animal miRNAs. Although the addition of adenines has been detected on many different animal miRNAs, a functional consequence of this modification by Gld2, a cytoplasmic non-canonical poly(A) polymerase, has been established for miR-122 in liver cells (Katoh et al., 2009). A recent study has also demonstrated that Gld2 3’ monoadenylates specific miRNAs, and

stabilizes them. Sensitivity to monoadenylation and stability depends on nucleotides in the miRNA 3′ end (D'Ambrogio et al., 2012).

1.4.3.2 miRNA destabilization

Along with stabilization, active degradation is also important for miRNA homeostasis. In animals, the 5′-to-3′ exonuclease XRN-2 (Rat1p in yeast) catalyzes degradation of mature miRNAs (Chatterjee and Grosshans, 2009). Another enzyme, the exosome 3′–5′ exoribonuclease complex was identified as the primary nuclease involved in miR-382 decay (Bail et al., 2010). It is likely that several miRNAs are actively destabilized depending upon their mature sequences. Perfectly complementary targets can also destabilize and degrade miRNAs.

1.4.3.3 circular RNAs – miRNA reservoirs

Two papers published very recently by (Hansen et al., 2013; Memczak et al., 2013) describe highly stable, circular RNAs that bind several copies of a microRNA to terminate suppression of mRNA targets.

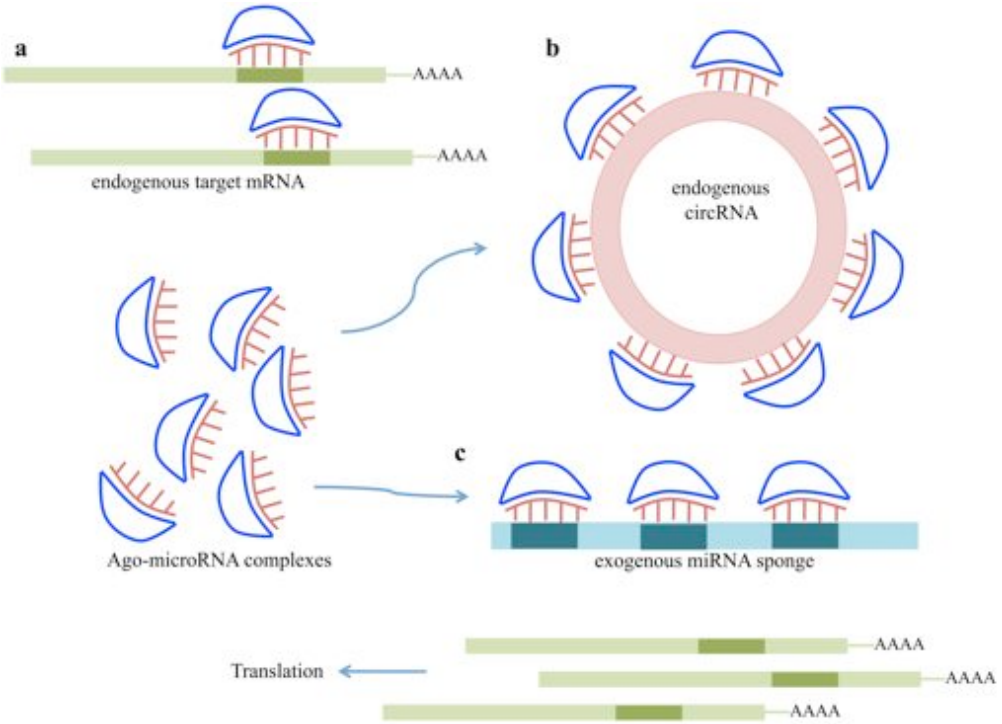

Fig 1.2 circularRNAs and miRNA sponges. **a** Ago-miRNA complexes can target endogenous mRNAs in a normal setting, **b** presence of circRNAs or miRNA sponges can sequester miRNAs from their endogenous targets, relieving their repression.

The circular RNA (circRNA) reported, called CDR1as by Memczak et al. and ciRS-7 by Hansen et al., contains roughly 70 evolutionarily conserved binding sites for miRNA-7 (miR-7) and forms a complex with AGO proteins. Essentially, these function like endogenous sponges (See Section 1.6.3.2), sequestering miRNAs from their targets, and at the same time, stabilizing them by protecting their 3' and 5' ends from RNA exonuclease enzymes. Hence, circRNAs act as miRNA reservoirs, keeping them stably bound until circRNA destruction, which would release a shower of miRNAs that would be free to target multiple mRNAs with the shared binding sequence (Fig 1.2).

1.5 miRNA-target relationships

1.5.1 miRNAs in gene-switches, and as tuning molecules

miRNAs repress their target genes. The peculiarity of miRNAs in the context of cellular activity is their ability to simultaneously control many genes. They have been classified as switch targets and tuning targets (Fig 1.3) (Bartel and Chen, 2004).

In the case of binary 'switch' targets, miRNAs may exclude the target completely from the tissue of expression, resulting in a mutual exclusion of miRNA and target mRNA. Sometimes, miRNA and the switch target mRNA may both be present together, and the miRNA may act to limit the target levels, as excess target mRNA or protein might be deleterious to the tissue where it is expressed. In the classical switch interaction that was described for the field-founding miRNAs *lin-4* and *let-7*, target expression is essentially abolished in the tissue where the miRNA is expressed (Caygill and Johnston, 2008; Lee et al., 1993; Moss et al., 1997; Reinhart et al., 2000; Sokol et al., 2008).

In the case of 'tuning' targets, both excess or too little of the target gene can lead to harmful phenotypes, in which case a miRNA can act to 'tune' target levels. *miR-8* has been shown to tune or modulate its target gene Atrophin in *Drosophila* nervous system: both loss and gain of Atrophin function leads to increased apoptosis in the brain (Karres et al., 2007). In the mammalian haematopoietic system, *miR-150* is highly expressed in mature B cells (Zhou et al., 2007). Loss of function and gain of function experiments show that

miR-150 downregulates its target c-Myb in a highly dose-dependent way. *miR-150* knock-out mice display an increase in B cell progeny, which is likely due to mild c-Myb over-expression (Xiao et al., 2007). Interestingly, a reduction of c-Myb RNA levels as modest as 30-35%, caused by ectopic expression of *miR-150*, has grave phenotypical consequences, which include a partial block of B cell development (Xiao et al., 2007; Zhou et al., 2007).

In other cases, miRNAs can act to reinforce established processes that are already under transcriptional or post-translational control. By maintaining transcript levels below levels that are functionally relevant, i.e., setting a threshold for target expression, miRNAs add a level of precision to developmental decisions.

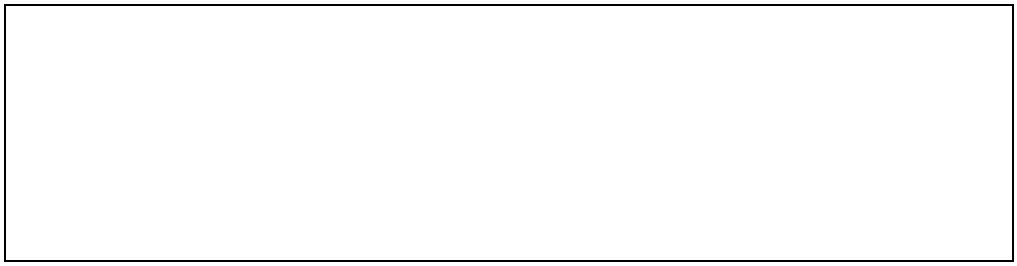

Fig 1.3 miRNA-target relationships. Target mRNA levels (blue) decrease as miRNA levels (orange) increase. Dashed lines represent critical thresholds of target mRNA; the upper line indicates the level that would be undesirably high in the cells that express the microRNA (miRNA), the lower line indicates the level below which the protein no longer exerts its effect.

1.5.2 miRNAs as noise buffers

Additionally, miRNAs also have a role in buffering noise in biological systems, both developmental noise and noise from environmental fluctuations

in the form of stress. miRNAs are often part of gene regulatory networks – feedback and feed forward loops that impart stability in the face of intrinsic and extrinsic noise (Herranz and Cohen, 2010). One example is that of the feedback loop between miR-14 and the ecdysone signaling receptor (EcR) in *Drosophila*. EcR regulates itself, and miR-14 represses it. In turn, EcR represses miR-14 levels. Mutual repression keeps them both in a steady state until a hormonal cue activates EcR, which shuts off miR-14 transcription. The pre-existing miRNA decays slowly, permitting the cell to distinguish between sustained ecdysone-induced EcR activation vs that by transcriptional bursts. This positive auto-regulatory loop acts to protect the animal against initiating a large-scale EcR-dependent transcriptional program without the proper hormonal cue (Varghese and Cohen, 2007).

1.6 Studying miRNA functions

1.6.1 Hints from miRNA-expression profiling

In the last decade, since the discovery of the first miRNA lin-4 in *C. elegans*, (Lee et al., 1993; Wightman et al., 1993), the number of studies have skyrocketed, both in terms of miRNA discovery as well as for implicating miRNAs in diverse physiological processes, in normal and disease conditions. miRNAs are widely expressed and function in almost every imaginable biological process. miRNA expression profiles of various tissues in different conditions often result in the possibility of using them as biomarkers. However, most of these studies do not address the question whether these 'biomarker' miRNAs are the cause or the consequence of the observed conditions.

1.6.2 miRNA biogenesis mutants

Apart from miRNA expression profiling, there are studies from flies, mice and worms detailing functions of miRNAs using genetic manipulation. Studies abolishing all miRNA function by disrupting their biogenesis using total and conditional Dicer mutants have underscored the importance of miRNAs in a variety of processes like germ line development, stem cell division, DNA damage repair, neurogenesis, neurodegenerative disorders, muscle development, immune cell development (Choi et al., 2008; Damiani et al., 2008; Davis et al., 2008; Dorval et al., 2012; Hatfield et al., 2005; Hebert et al., 2010; Kim et al., 2007; Sadegh et al., 2012; Schaefer et al., 2007; Tang and Ren, 2012; Zhang and Bevan, 2010). A recent study also showed a correlation of decline in Dicer expression with decreased stress tolerance in adipose tissues in humans, mice and worms. Dicer loss of function mutations in *C. elegans* reduce lifespan and stress tolerance, while overexpressing Dicer confers stress resistance to the animals (Mori et al., 2012).

1.6.3 miRNA gain of function

Just as any other gene, miRNA gain of function experiments could also be expected to shed light on their biological function. However, there is a major caveat associated with such experiments. Many genes contain miRNA-binding sites, but they may not be targeted by the miRNA under natural physiological conditions of miRNA expression. Over-expressing miRNAs even if only in their native expression domains could lead them to target physiologically

irrelevant mRNAs, generating confounding phenotypes. miRNA mis-expression out of their normal spatial and temporal expression context can be even more misleading due to the same reasons.

1.6.3 miRNA loss of function

1.6.3.1 Targeted homologous recombination

Functional loss of miRNA activities in different model organisms has shown to exert distinct impacts on the organism's viability and development. While most of individual miRNA deletions in *C. elegans* are not reported to affect the animal's survival nor cause much phenotypical abnormality, a number of miRNA knockouts in flies and mice have been reported to cause defects in animal development, survival and behavior (Brennecke et al., 2003; Ge et al., 2012; Hilgers et al., 2010; Karres et al., 2007; Klein et al., 2010; Miska et al., 2007; Poy et al., 2009; Rasmussen et al., 2010; Sokol et al., 2008; Teleman et al., 2006; Varghese and Cohen, 2007; Varghese et al., 2010; Ventura et al., 2008; Wang et al., 2008; Weng and Cohen, 2012; Zhao et al., 2007). miRNA function can be probed directly and effectively by using miRNA knockouts as this ensures complete loss of miRNA activity in an intact animal. Direct deletions also ensure that other regions of the genome are unaffected.

Borrowed from yeast genetics, the technique of targeted homologous recombination has been successfully applied to a few model organisms including yeast, mouse and recently in the fly (Chen et al., 2011; Rong et al., 2011; Rong and Golic, 2000, 2001, 2003; Weng et al., 2009). Briefly, a P-element based FRT targeting construct is designed to contain an eye color

marker gene (mini-white) flanked by two homology arms that are about 3.5-4kb in length, and identical to upstream and downstream flanking sequences of the miRNA locus in *Drosophila* genome (Fig 1.4). By P element-mediated transformation, a transgenic donor line is generated based on eye color. This targeting construct (homology arms with mini-white gene) is linearized into an extrachromosomal DNA molecule, which then undergoes homologous recombination with the miRNA locus with less than 1% efficiency (Jones et al., 2007; Manoli et al., 2005). To improve efficiency, the bacterial phage ΦC31 integrase has been used in the system called RMCE (recombinase-mediated cassette exchange). ΦC31 integrase catalyzes recombination between two non-identical recognition sites, attP and attB, and produces two new sequences, attL and attR (Groth et al., 2004). The RMCE method allows directional site-specific exchange between a plasmid "donor cassette, attB" and the genomic "acceptor cassette, attP" at relatively high targeting efficiency (up to 25% of success rate) (Bateman et al., 2006). This vector in principle could allow targeting events happening more than once in the same locus and the mini-white gene could be swapped by any sequences of interest (eg GFP, miRNA, miRNA target genes), that are under control of the endogenous miRNA promoter activity. While RMCE doesn't increase efficiency in terms of initial targeting, it does allow retargeting with greatly improved efficiency.

Genetic knockouts of miRNAs in mice work well using similar methods as in *Drosophila*. A miRNA knockout ES library has recently been generated using RMCE targeting strategy for 392 mouse miRNAs with high germline

transmission rates (Prosser et al., 2011). Yet another library has been published recently with conditional, reporter-tagged knockout mice for 162 evolutionarily conserved miRNAs (Park et al., 2012).

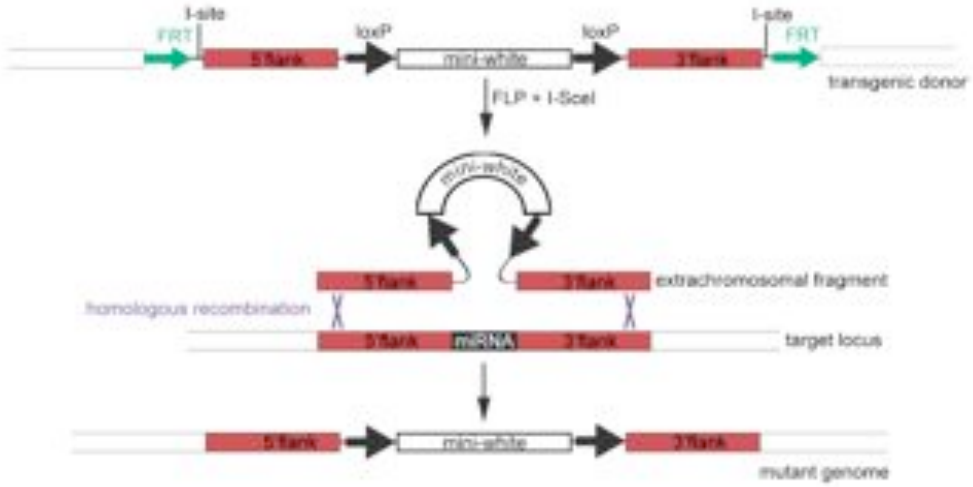

Fig 1.4 Schematic representation of targeted homologous recombination. The transgenic donor construct is excised and linearized in presence of FLP recombinase and I-SceI nuclease and can recombine with the chromosomal target locus, replacing the miRNA hairpin sequence with the mini-white marker gene.

1.6.3.2 Sequestering miRNA function using a 'sponge'

miRNA mutant generation is a tedious process that takes approximately 6 months in flies and longer in mice. Also, in order to study miRNA functions with spatio-temporal constraints, conditional knockouts are needed, requiring additional generations of crosses. Secondly, many *Drosophila* miRNA knockout lines are lethal or semi-lethal during development, making the assessment of miRNA functions in adult tissues very difficult (Chen YW et al., unpublished observation). Therefore, a method providing spatio-temporal control over depleting miRNA function could potentially reveal phenotypes that may not be possible in whole-animal knockouts.

miRNA ‘sponges’ offer great advantages and broad applicability in studying miRNA functions in vitro and in vivo. A sponge is a transcribed artificial RNA sequence containing multiple consecutive binding sites for one miRNA or the whole miRNA family, as defined by identical seed sequences (miRNA 5’ nucleotide position 2-8) of the miRNA. A sponge sequence is typically designed to contain 5-10 repeated sequences that are complementary to the mature miRNA. When sponge RNAs are expressed, they presumably sequester miRNAs upon binding, thus prevent targeting on the endogenous mRNAs. Thus, the sponges ‘soak up’ miRNAs, creating a total or partial loss-of-function status in tissues of sponge expression (Fig 1.4). We and others have successfully used the sponge system to study miRNA functions in *Drosophila* (Becam et al., 2011; Herranz et al., 2012a; Herranz et al., 2012b; Loya et al., 2009). The application of miRNA sponge in vertebrates is also well demonstrated in many studies (reviewed in (Ebert and Sharp, 2010).

Unlike genetic knockouts, the effectiveness of sponges depends critically both on the expression levels of sponge and the usual miRNA expression level. Some miRNAs are highly abundant in certain cells/tissues, in which case a partial reduction in miRNA activity by expressing the sponge may not be able to reveal any phenotype. Therefore, although sponges are versatile tools for studying miRNA functions, a careful assessment of the effectiveness of the sponge construct is required before any conclusions can be made from such studies.

1.7 Target Identification

1.7.1 Computational predictions

Based on sequence complimentarity, computational predictions are the first tool to use for target discovery. Over the years, several bioinformatics programs have been developed that predict miRNA targets based on parameters such as complimentarity, binding energy, secondary RNA structures, thermodynamic stability, and also evolutionary conservation of the seed sequence. Some of the most frequently used ones are TargetScan, Pictar, miRanda, mirWIP, PITA and MinoTar. Seed match and evolutionary conservation have been common among the majority of prediction algorithms, while other parameters like hybridization energy, site accessibility and UTR context features vary from one to another.

Although there is a lot of overlap, there is also significant variation in target predictions from all these programs. This comes from slight differences in prediction algorithms. For example, Minotar and TargetScan both require an exact 7-8 base pair match at miRNA seed region while the other programs allow mismatches and/or G:U base-pairing to different extents (Friedman et al., 2009; Lewis et al., 2005; Lewis et al., 2003; Schnall-Levin et al., 2010).

1.7.2 Biochemical methods

Biochemical methods for target identification often involve unbiased genome-wide profiling at the mRNA and/or protein levels. Microarray sampling is done from cells and tissues with either over-expression or deletion of the

miRNA of interest. Change in mRNA profiles is a reliable readout for miRNA activity because studies suggest that miRNAs predominantly affect target mRNA stability. This method has aided target discovery in several studies (Karres et al., 2007; Varghese et al., 2010). Also, experimental studies have shown that mRNA level change correlates well with proteomic change (see Section 1.4.2). Next-generation RNA sequencing might provide a more comprehensive quantification of mRNA copy number as compared to microarray (Xu et al., 2010).

Another way to identify targets is to compare the profiles of mRNAs that associate with Ago2 protein in miRNA mutant and control animals using immuno-precipitation (IP) of the Ago/GW182 complex (Beitzinger et al., 2007; Easow et al., 2007; Hendrickson et al., 2008; Hong et al., 2009; Karginov et al., 2007). Coupled to mRNA array or RNA sequencing platforms, this method could be an effective way to address physiological interactions between miRNAs and their targets within the RISC effector complex.

Though the majority of target mRNA changes correlated well with changes in protein level, there are well-documented evidences of certain miRNA targets that change mainly at the protein level (Behm-Ansmant et al., 2006b); Chen *unpublished findings*). Therefore, measurement of target protein level by quantitative proteomics could be a more direct measurement of miRNA action on its targets and perhaps also reveal crucial changes in pathway activity caused by a miRNA. Differential isotope labeling of proteins in vivo via

SILAC (stable isotope labeling by amino acids in cell culture) (Mann, 2006; Ong et al., 2002; Sury et al., 2010) or of peptides in vitro via di-methyl labeling (Boersema et al., 2009) followed by mass spectrometry are two useful techniques to compare miRNA and wild type mutant protein profiles. SILAC has been used extensively in cell culture, but recently it has also been applied in vivo in *Drosophila* (Sury et al., 2010). Feeding larvae with food enriched in heavy and light lysine enables stable protein labeling in these animals, which can be readily tested. This is in contrast to the di-methyl labeling strategy, which involves isotope labeling of peptides after protein extraction. The former method has a wider coverage, improved efficiency and has a better internal control for labeling; as compared with the latter which has considerable amount of protein loss during the several steps involved.

Overall, together these methods for differential protein quantification, combined with methods for estimating differentially regulated mRNAs provide a strong experimental starting point from which to identify potential miRNA targets. Additionally, based on the gene regulatory patterns, they can also provide clues into the nature of biological processes the miRNA might regulate. Genes identified from these methods can be further verified using quantitative RT-PCR and Western blots. It is interesting, however, that potential target genes identified from biochemical methods often do not match computationally predicted genes. One reason is that most of current major prediction programs do not consider whether the miRNA and targets are co-expressed in the same cell types.

1.7.3 Genetic methods

Targets shortlisted via computational and biochemical methods require further experimental validation. The shortlisted targets can be confirmed by their genetic interactions with the miRNA. They may phenocopy the miRNA mutant when over-expressed in the right tissues in an otherwise wild type genetic background. The binary UAS-Gal4 system can be utilized for this purpose – several enhancer-promoter (EP) lines are available on FlyBase, which can be used for such over-expression analysis. The second method is to reduce the expression level of putative target genes in the miRNA mutant animals and test for rescue of mutant phenotypes.

1.7.4 Target reporter assays

A gene that interacts genetically with the miRNA may or may not be a direct target of the miRNA. To confirm direct miRNA-mediated regulation, it is important to test the actual binding of the miRNA to the target. A reporter assay system is a cell-based assay, typically consisting of the reporter gene, which produces a biofluorescent or bioluminescent protein like GFP or luciferase with the 3' end fused to a 3'UTR sequence containing candidate miRNA binding sites. The miRNA of interest is often co-expressed together with the reporter. Given the fact that miRNAs could target protein coding regions or 5' UTRs, one can also engineer the site sequences into the open reading frame or 5' UTR of the reporter gene to mimic the targeting location in vivo (Hafner et al., 2010; Schnall-Levin et al., 2010). In order to demonstrate the importance of miRNA-target base pairing, the predicted sites, particularly the nucleotides targeted by miRNA seed region, are mutated to

disrupt the binding. It has been shown that one single base mutation at miRNA seed pairing region could significantly affect targeting efficiency (Brennecke et al., 2005). If the gene were a direct target, mutating the miRNA binding sites would relieve the miRNA-mediated repression on the reporter expression.

1.9 Conclusions

miRNAs are a class of genes that regulate gene expression in a wide range of mechanisms. Some miRNAs appear to be key players in specific pathways and are crucial for development and homeostasis, while others confer robustness to existing transcriptional and post-translational mechanisms and enforce cellular or tissue identity. miRNA transcription, processing and function are subject to activatory and inhibitory modulation by other cellular components, thus creating a complex network of interactions that the cell exploits in a context-dependent manner. Further deciphering the mechanisms underlying specific and global functions of miRNAs, using a combination of genetic, bioinformatics and molecular biology approaches, will help our understanding of cellular and organismal physiology.

1.10 miRNAs and the nervous system

Organisms interact with their environment through sensory systems (afferent) and also through motor output (efferent). These interactions are dependent on the neuronal connections, internal energy status, and the gene expression profiles of the sensory cells, the neurons, and the motor output cells. There is

an intricate meshwork of gene networks, sensing and responding to the environment. Specifically, synaptic plasticity is a key feature of nervous system function. Post-transcriptional regulation by miRNAs can provide an additional mechanism, with potentially faster kinetics for gene expression modulation at the synapse, making them important players in this system (reviewed in (McNeill and Van Vactor, 2012). Indeed there are studies pointing towards such roles for miRNAs (Edbauer et al., 2010; Zovoilis et al., 2011).

1.10.1 Nervous system expression

A third of miRNAs in most metazoan genomes are expressed in the nervous system, often in spatially and temporally regulated patterns (Bak et al., 2008; Berezikov et al., 2011; Berezikov et al., 2006; Chiang et al., 2010; Kapsimali et al., 2007; Landgraf et al., 2007). To date, several hundred microRNAs have been identified in human and chimpanzee brain (Berezikov et al., 2006; Landgraf et al., 2007). The number of studies cataloging miRNA profiles in whole-brains and sub-brain populations both in developing and adult brains using arrays and deep-sequencing platforms has seen a tremendous rise in recent years (Hua et al., 2012; Li et al., 2013; Ling et al., 2011; Moore et al., 2013). miRNA profiling at the single cell-type resolution has also started recently. For example, by combining immunoprecipitation of tagged, transgenic Ago2 with the cell-type-specific Cre/Lox system in mouse (a method called ‘miRAP’), it has been possible to identify the miRNA ‘finger prints’ of different GABAergic interneurons and excitatory pyramidal cells

from neocortex or Purkinje cells from cerebellum. In addition to spatial regulation of mRNA transcripts, temporal regulation adds another layer to miRNA-mediated regulatory complexity. For example, a recent profile of hippocampal miRNA levels after contextual conditioning in vivo showed significant changes in miRNA pattern between 1, 3, and 24 hr post-training compared to animals that received NMDA-receptor antagonist prior to training (Kye et al., 2011). Thus, there are now significant numbers of studies showing that miRNAs are spread far and wide in the neuronal space-time landscape.

1.10.2 Neural development and physiology

Global depletion of miRNAs by using mutations such as *dicer*, that compromise miRNA biogenesis often mask nervous system-related phenotypes – for example, mouse Dicer mutants die before neurulation (Bernstein et al., 2003), so a conditional knockout approach is needed. Cell type-specific removal of Dicer from a variety of mouse neuronal cell types has revealed defects in neuronal survival during development and in mature neurons. Depletion of all microRNAs in this way can lead to progressive loss of these cells and to behavioral defects reminiscent of the phenotypes seen in the pathologies of neurodegenerative disorders (Choi et al., 2008; Damiani et al., 2008; Davis et al., 2008; Kim et al., 2007; Schaefer et al., 2007). Glial cell defects may also profoundly influence neuronal survival (Ilieva et al., 2009; Prinz et al., 2011). Indeed, neurodegeneration ensues after targeted deletion of Dicer in astrocytes (Tao et al., 2011), oligodendrocytes (Shin et al., 2009), and Schwann cells (Pereira et al., 2010; Verrier et al., 2010; Wu et al., 2012).

Detailed studies of miRNAs have begun to suggest extensive roles for miRNAs not only in cell survival but also in the formation of synaptic connections, circuit maturation, and the activity-driven plasticity of these connections. Some of this evidence came from knockout mutations of the microprocessor genes – a clonal genetic screen in *Drosophila* identified DGCR8/Pasha and Dicer1 as crucial components in wiring specificity (Berdnik et al., 2008). Additionally, hypomorphic alleles of *drosha* and *pasha* in *Drosophila* resulted in adults with overtly normal development but reduced synaptic transmission in the photoreceptor neurons (Smibert et al., 2011). As a whole, studies of the core miRNA-processing pathway have focused attention on miRNA function in neural circuits, but mechanistic insights into such functions require analysis of individual miRNAs and the target genes they control. Indeed, studies of individual miRNAs are emerging, demonstrating specific roles during neuronal maturation, connectivity and plasticity. For example, miR-137 controls early neural differentiation (Silber et al., 2008) as well as later steps in developmental plasticity (Szulwach et al., 2010). miR-34a negatively regulates dendritic growth and synaptic function by targeting synaptic components (Agostini et al., 2011).

1.10.3 Animal behavior

1.10.3.1 Genes and Behavior

Behavior is the final output of metazoan nervous systems, making the study of animal behavior naturally fascinating. The study of animal behavior or ethology, came into being during the 1930s with the work of Dutch biologist Nikolaas Tinbergen and by Austrian biologists Konrad Lorenz and Karl von

Frisch. Even after a new understanding of genetics and the discovery of the DNA structure and genes, the idea of behavior being hard-wired in the genome was still regarded as radical for a fairly long time. Molecular concepts and methods were slow to penetrate the discipline of brain and behavior, where physiologists, ethologists and behavioral geneticists were struggling with the complexity of genetically heterogeneous pools, multigene effects, and pleiotropism.

In the late 1960s, Seymour Benzer, long considered the father of behavioral neurogenetics, presented and crystallized the concept of genes regulating behavior with his seminal studies in behavior using *Drosophila*, bringing the reductionist approach into this field (Harris WA 2008; (Dudai, 2008; Greenspan, 2008). Benzer isolated several mutants affecting fly phototactic behavior in his first paper on fly behavior (Benzer, 1967). The continued efforts of his lab yielded a collection of single-gene mutations affecting behaviors as complex as courtship, memory, circadian rhythms, and modifying sensory perception, nerve conduction, and neural development. Since then, the field has opened up with thousands of papers studying the genetic basis of various behaviors in mice, flies and worms in carefully set up behavioral paradigms including foraging, mating, exploration, communication, learning, memory, anxiety and fear, just to name a few. Even though there are many single-gene mutations with major consequences on behavior, the one gene – one behavior concept initially proposed by Benzer turns out to be rather simplistic, since there is usually more than one gene acting in concert to produce a certain behavioral output. Single-gene mutations

are still only tiny bits to explain how the brain controls behavior, specifically disease-relevant behaviors. But with the development of new methodologies for brain imaging, genetic and genomic analyses, molecular engineering of mutant animals, novel routes for drug delivery, and sophisticated cross-species behavioral assessments, it is now possible to study behavior relevant to psychiatric and neurological diseases and disorders on the physiological level, and to elucidate the complex genetic mechanisms associated with them.

1.10.3.2 miRNAs and behavior

A few early behavioral studies emerging from flies, bees and mice assign miRNAs important roles for regulating behavior. Learning and memory are processes central to synaptic transmission and plasticity. Extensive dendritic remodeling occurs during memory formation, via activity-dependent transcription factors such as c-Fos and CREB. Studies have identified miR-132 as being regulated by CREB in activity-regulated plasticity (Nudelman et al., 2010), and over-expression of miR-132 in mouse forebrain neurons showed a marked increase in dendritic spine density (Hansen et al., 2010). Additional studies (Mellios et al., 2011; Tognini et al., 2011) also indicate that a fine balance of miR-132 is required for plasticity. Additional miRNAs are also being discovered to have roles in learning and memory - miR-128b, miR-124 and miR-34c are three such examples (Agostini et al., 2011; Yang et al., 2012; Zovoilis et al., 2011).

Circadian rhythms are controlled by an internal circadian oscillator, which receives input from light cues. Several proteins in the clocking pathway are

tightly regulated according to the daily rhythms, and also via the internal clock. Recent work by a number of groups has revealed a role for miRNAs in clock physiology. Initial studies in *Drosophila* profiled miRNA expression and found oscillations in miR-263a and miR-263b that were observed in wild-type flies but absent in clock mutants (Yang et al., 2008). In a later study, Kadener et al found that abolition of miRNA biogenesis led to both an increase in circadian-regulated gene expression and a disruption of circadian-regulated behavioral rhythms, revealing a role for miRNA in clock timing (Kadener et al., 2009). Recently, miR-279 was also identified in driving rest-activity rhythms in *Drosophila* through regulation of the JAK/STAT pathway (Luo and Sehgal, 2012).

Sleep and circadian rhythms are intimately connected. It is no surprise that miRNAs miRNA levels in brain are altered by sleep deprivation, and over-expression of miR-132 in vivo decreases duration of non-REM sleep while simultaneously increasing duration of REM sleep during the light phase (Davis et al., 2011).

One very interesting 'miRNA-mediating behavior' story comes from honeybees (*Apis mellifera*). Bees are eusocial insects, with a highly ordered social system and division of labor. Worker bees give up their reproductive potential and serve to build and maintain the hive, serve the reproducing queen bee, and take care of the brood. However, interestingly, what worker bees do depends on how old they are – they begin with brood-nursing, secreting beeswax and attending to the queen. As they grow older, they assume the role

of grooming and ventilating the nest and packing pollen. Towards the end of the worker bee's life, she becomes a forager, exploring to collect nectar and pollen for her colony. Greenberg et al identified a genetic basis to this stereotypical behavior – some miRNAs are upregulated in heads of older worker bees, enabling their foraging behavior (Greenberg et al., 2012). Interestingly, these miRNAs are shared with wasps and ants, other eusocial insects, suggesting that miRNAs are important regulators of social behavior not just for the bee but also over evolutionary time. Overall, this study suggests that miRNAs can be powerful remodelers of behavior, imparting the ability to switch behavioral states with change in their temporal expression patterns.

miRNA knockout studies also suggest that miRNAs can affect courtship behavior in *Drosophila* males (Weng et al., 2013) and have a variety of effects on negative geotaxis, phototaxis, and anxiety-related behavior (*unpublished data*, Cohen Lab). One thing is clear, the playing field of miRNAs in mediating behavior is very large and we have only begun to explore.

Chapter 2 Materials and Methods

2.1 Fly genetics

Flies were reared on standard media at 25°C. All crosses were carried out at 25°C. Flies were grown and maintained in vials containing standard agar cornmeal medium (1.2% agar, 1.8% dry yeast, 1% soy flour, 2.2% turnip syrup, 8% malt extract, 8% corn powder, 0.24% methyl-4-hydroxybenzoate). Stocks were kept at 18°C and flipped every 45 days.

2.1.1 Generating the miR-285 mutant flies

miR-285 mutant flies were generated by targeted homologous recombination. The downstream homology arm was amplified using TTCGAGAATGTCTGCTCCACT and TTCGATTTGACACTTCGCTG as forward and reverse primers and cloned into the AscI site of pW25 (Weng et al., 2009). The upstream homology arm was amplified using AGTGGCAGGGCAAGTAGGTA and CAACCTGTGTGGATGGAGAA as forward and reverse primers and cloned into the NotI site. Targeting was carried out as described (Chen et al., 2011). Briefly, the donor construct was inserted into the genome by P-element-mediated transformation. Transgenic 'donor' males were mated to females expressing a site-specific recombinase (FLP) and a site-specific endonuclease (I-SceI) to generate a linear extra-chromosomal DNA molecule. Homologous recombination between the donor and the homologous chromosomal target locus resulted in the replacement of the endogenous miRNA gene with mini-white. Progeny were screened for w+

and removal of the *miR-285* hairpin was confirmed by PCR on genomic DNA using GGTGACTAAAGACCCGGTCAACGA and AGTGGCAGGGCAAGTAGGTAGCTCC as forward and reverse primers. The *miR-285* mutants were backcrossed for 6 generations into the parent line w^{1118}, followed by 4 generations into w-CS.

2.1.2 Generating rescue, Gal4 and EGFP transgenes

The rescue transgene comprised ~3kB of genomic DNA spanning the *miR-285* locus, delimited by flanking loci (Fig 3.4a) cloned into the pAttB vector. Cloning of the same region, but lacking the miRNA hairpin, was used as the control rescue transgene. Gal4 and EGFP constructs were generated by replacing the miRNA sequence in the rescue transgene. All the three transgenes were introduced in the genome by site-specific integration at 51D, Bloomington Stock 24483 (Bischof et al., 2007).

2.1.3 Generating UAS-miR-285 transgenic flies

The *miR-285* hairpin was amplified from genomic DNA using AGCGGCCGCAACGAGATGGCTTGCACTTT and AGCGGCCGCCTGACATCGCACCCATAC as forward and reverse primers. Cloning of the *miR-285* hairpin was done into the pUAST vector containing attB sequences and gypsy elements to prevent site-specific effects on transcription. UAS-*miR-285* was integrated at the 22a and attp16 sites in the genome. The 22a insertion was used for all experiments.

2.2 Fly strains

The deficiency line *Df(3L)BSC120* was used to remove one copy of the endogenous *miR-285* locus. *Df(2R)BSC358* was used to remove the endogenous *Sod3* locus. Deficiency strains were obtained from the Bloomington stock center. All UAS-RNAi lines were obtained from the VDRC stock center.

2.3 RNA analysis

2.3.1 RNA extraction

RNA was isolated using the manufacturer's protocol (Trizol, Invitrogen). Briefly, flies were flash frozen in liquid nitrogen and 20-30 heads were collected per sample. Heads were ground by a pestle in 1000 μL TRIzol, followed by further shearing and homogenization using a syringe. The homogenate was vortexed with 200 μL chloroform. Phase separation was performed by high-speed centrifugation. RNA was precipitated from the aqueous phase with isopropanol, washed with 70% ethanol and resuspended in water. RNA samples were digested with DNAse using a kit according to the manufacturer's protocol (Promega). Samples for measuring mature miRNA levels by qPCR were not treated with the on-column DNase Qiagen protocol.

2.3.2 RT-qPCR

2.3.2.1 mRNA RT-qPCR

SuperscriptIII (Invitrogen) for reverse transcription and Power SYBR Green (Applied Biosystems) reagents were used for qPCR of mRNAs according to

manufacturers' protocols. Briefly, RNA samples from three biological replicates were reverse transcribed and qPCRs were setup in 96-well plates in the ABI7500 real time thermal cycler (Applied Biosystems) following manufacturers' protocols. GAPDH, rp49 and actin42 were used as controls for target qPCRs. qPCR primers are in Table 2.1.

1	CGAGAAGGGAGATCTGACCA	CG9027 F
2	ACATGACGCACCTCGTGA	CG9027 R
3	CCATGTTCTACCCCATGTCC	Prx2540-2 F
4	ACCTTGAGGCGATCAGTCAG	Prx2540-2 R
5	CGCTTTCGCAACCACTGT	CG3835 F
6	CTGCACGTTGTCGGTGAT	CG3835 R
7	TCAACGAGATCTTGGCACAG	Cyp6a23 F
8	GAGCTCGTACAGGGCAAATC	Cyp6a23 R
9	TCACCTCCTGGCAGTTATCC	CG7227 F
10	CGATGCTTTCGTTTACAGAGG	CG7227 R
11	CTGCTCAAAGGCGCACAG	CG10924 F
12	GAATGGAGAGGAAGCGACAG	CG10924 R

Table 2.1 qPCR primers for target genes. F denotes forward primer, R denotes reverse primer.

2.3.2.2 miRNA RT-qPCR

Primer sets designed to amplify mature *miR-285* and reference genes were obtained from Applied Biosystems. The reverse transcription and real-time PCR reactions were performed using the TaqMan MicroRNA assay kit (Applied Biosystems) according to the manufacturer's protocol. *U14*, *snoR442* and *U27* were assayed as references for *miR-285* but *U27* (small nucleolar RNA) was used as an endogenous control because it showed maximum stability across samples.

2.3.2.3 RT-qPCR primer sequences

All RT-qPCR primers were designed using the Primer3Plus program (http://www.bioinformatics.nl/cgi-bin/primer3plus/primer3plus.cgi). The optimal parameters were set as follows: primer length 20nt, product length 80-120nt, annealing temperature 60°C, GC content 50%, no predicted primer dimers. RT-qPCR primers used are listed in Table 2.1.

2.3.3 Microarray

RNA samples were prepared from three independent replicates (~50 heads each) of homozygous mutant and control flies (w^{1118}) (RNA~3ug/sample) with newly eclosed mixed gender flies (day 0-1). Labeling and hybridization on Affymetrix 2.0 microarrays was performed by the EMBL Gene Core facility according to Affymetrix protocols. Data were analyzed using the CARMAweb 1.5 suite. (https://carmaweb.genome.tugraz.at/carma/). Raw data were pre-processed and normalized using the Affymetrix standard method MAS5. Raw p-values were determined using moderated t-statistics provided by the limma package and adjusted by multiple hypotheses testing using the Bonferroni method (carmaweb1.5) (Rainer et al., 2006). The median value of each biological triplicate was used to determine whether a gene was up regulated. Cut-off thresholds were 1.5-fold change in expression, and p-value <0.05. Gene Ontology analysis was done using DAVID (http://david.abcc.ncifcrf.gov/).

2.4 Protein analysis

All proteomics work was performed by Siok Ghee Ler and Jayantha Gunaratne at IMCB.

2.4.1 Preparation of peptides

Frozen fly heads (50 each from wild-type and mutant) were crushed, vortexed and sonicated for 5 min in 50 mL of SDT buffer (4% w/v) SDS, 100mM Tris/HCl pH7.6, 0.1M DTT) in separate vials. Lysates were collected after centrifugation at 16,000x g at RT for 20 min. Protein was measured using the RCDC assay kit (BioRad). Filter-aided sample preparation (Wisniewski et al., 2009) was performed on 100 mg of lysates. 8M urea in 0.1 M Tris/HCl pH 8.5 (UA buffer) was added to the lysate and transferred to Millipore 30 kDa Amicon filter units. Buffer exchange was carried out twice with UA before alkylation with 50mM iodoacetamide (IAA) in the dark for 20 min. Trypsin (porcine, modified sequencing grade; Promega) digestion (1:100) in 40mM ammonium bicarbonate (ABC, Sigma-Aldrich) was performed in the filter at 37°C overnight. Peptides were eluted by centrifuging at 14,000xg for 10 min at RT, with two additional elution using 40mM ABC.

2.4.2 On-column stable isotope dimethyl labeling

The dimethyl labeling was performed as described (Boersema et al., 2009; Hsu et al., 2003) with modifications. The digested peptide mixture was acidified with 100 mL of 1% trifluoroacetic acid (TFA) before proceeding to dimethyl label on C18-SD solid phase extraction cartridges (3M Empore™).

The columns were conditioned with methanol followed by 0.1% TFA/70% ACN and 0.1% TFA. Peptides from each sample were divided into two equal portions and loaded separately onto conditioned columns. After washing with 0.1% TFA, the 'medium' reagent [45mM sodium phosphate buffer pH 7.5, 0.2% formaldehyde (CD2O) (20%, 98% D, Isotec) and 0.3M sodium cyanoborohydride ($NaBH_3CN$, Fluka)] and 'heavy' [45 mM sodium phosphate buffer pH 7.5, 0.2% formaldehyde (13CD2O) (20%, 99% 13C, 98% D, Isotec) and 0.3M sodium cyanoborodeuteride ($NaBD_3CN$, 96% D, Sigma-Aldrich] reagents were passed through the columns. For "Forward" labeling, medium reagent was passed through a column with the wild-type digest and heavy reagent was passed through the column with the mutant digest. For "Reverse" labeling, medium and heavy reagents labeled the reciprocal digests. After washing with 0.1% TFA, labeled peptides were eluted with 0.1% TFA/70% ACN and mixed before concentration using a speed vacuum concentrator. A small amount of the reaction was used to check label incorporation by mass spectrometry analysis. The rest were mixed as follows: Forward Experiment: 'medium' labeled wild-type sample with 'heavy' labeled mutant sample. Reverse Experiment: 'heavy' labeled wild-type sample with 'medium' labeled mutant sample.

2.4.3 Isoelectric Focusing (IEF)

IEF was performed on Agilent 3100 OFFGEL Fractionator (Agilent, G3100AA). Briefly, after rehydrating the 13 cm ImmobilineDryStrip pH 3-10 (Scimed) with a 12-well frame attached in a tray, the peptide mixture was loaded equally among the 12 wells. The 12-well frame was covered with a

cover seal and electrodes were fixed onto the tray on wet electrode pads before attaching the tray onto the fractionator. Glycerol was added as cover fluid to the left and right electrode before running a total of 50 kVh with gradient. Collected fractions were subjected desalting using C18 stage-tip as follows. 3 pieces of the solid phase extraction disks, C18 membrane discs (3M Empore) were packed into a 200 µL pipette tip. The stage tips were conditioned first with methanol followed by 80% ACN/0.1% formic acid (FA) and 0.1% FA with centrifugation. During the conditioning, the flow rates of the stage tips were determined. Sample was then loaded onto the stage tip and centrifuged at the determined flow rate. The stage tip was then washed with 0.1% FA before peptides were eluted with 80% ACN/0.1% FA. Eluted peptides were concentrated in speed vacuum concentrator for 15min and topped up with 0.1% FA to a total volume of 20 ml before introducing into the mass spectrometer.

2.4.4 Mass Spectrometry and Data Analysis

Vacuum dried peptide samples were reconstituted in 0.1% FA and analyzed using nanoHPLC (Proxeon, Thermo Scientific) coupled to a LTQ Orbitrap XL (Thermo FisherScientific). Peptides were trapped onto a C18 pre-column and separated on an analytical column using 2% AcN/0.1% FA as Solvent A and 80% AcN/0.1% FA as Solvent B. A 120 min gradient ranging from 5% to 50% solvent B, followed by a 5 min gradient ranging from 50% to 100% Solvent B at the flow rate of 250 nL/min was used. Survey full scan MS spectra (m/z 300–1400) were acquired with a resolution of r = 60,000 at m/z 400, an AGC target of 1e6, and a maximum injection time of 500 ms. The ten

most intense peptide ions in each survey scan with an ion intensity of >2000 counts and a charge state ≥2 were isolated sequentially to a target value of 1e4 and fragmented in the linear ion trap by collisionally-induced dissociation using a normalized collision energy of 35%. A dynamic exclusion was applied using a maximum exclusion list of 500 with one repeat count, repeat, and exclusion duration of 30 s. Data were searched using MaxQuant version 1.2.0.18 by uniprot DROME fasta (18787 sequences). Database searches were performed with tryptic specificity allowing maximum two missed cleavages and two labeled amino acids as well as an initial mass tolerance of 7 ppm for precursor ions and 0.5 Da for fragment ions. Cysteine carbamidomethylation was searched as a fixed modification, and N-acetylation and oxidized methionine were searched as variable modifications. DimethylLys4, DimethylNter4, dimethylLys8, dimethylNter8 were selected as light and heavy labels respectively. Maximum false discovery rates were set to 0.01 for both protein and peptide. Proteins were considered identified when supported by at least one unique peptide with a minimum length of six amino acids. Proteins up regulated >1.5 fold in the mutant samples relative to control in at least 3 biological replicates were selected.

2.5 Data integration for *miR-285* target search

Target sites were identified using the online site calculator, RNAHybrid http://bibiserv.techfak.uni-bielefeld.de/rnahybrid/. Briefly, all available transcript sequences of genes up regulated in the microarray and proteomics data were downloaded from FlyBase. These were probed for *miR-285* binding sites using RNAHybrid manually. The criteria for a good predicted site

(Brennecke et al., 2005) were base-pairing from 2 to 8bp from the miRNA 5' end, single GU pairs were allowed. Both coding sequences and 3'UTRs were thus analyzed.

2.6 Cell transfection and luciferase assays

Complete wild type and mutated *Sod3* (546bp) and *Prx2540-2* (663bp) CDS were cloned into the 3'UTR of luciferase under the control of a tubulin promoter. S2 cells were transfected in 24-well plates with 250 ng of tubulin promoter-*miR-285* plasmid DNA or the empty tubulin-promoter vector, 25 ng of firefly luciferase DNA or *Sod3/Prx2540-2* CDS or mutant luciferase reporter DNA and 25 ng of *Renilla* luciferase DNA as a transfection control. Transfections were performed using Cellfectin II reagent (Invitrogen) according to the manufacturer's protocol, with triplicate technical replicates in at least three independent experiments. Dual luciferase assays were performed 60 h post-transfection according to the manufacturer's protocol (Promega) in an Infinite 200 multimode reader (Tecan).

2.7 Lifespan assays

For all lifespan assays, flies were collected upon eclosion; male and virgin females were aged separately in groups of ~20 flies/vial. The vials were transferred every 3 days to avoid death due to spoilt food conditions. Survival counts were taken every 3 days. These experiments were done with siblings in 3 biological replicates of 3 starting vials with ~20 flies/vial i.e. ~180-190 flies.

Analysis was done using Kaplan Meier Statistics and the log-rank test, using OASIS (http://sbi.postech.ac.kr/oasis/surv/) (Yang et al., 2011).

2.8 Behavior assays

For all behavioral assays, the targeted knock-out allele was used in *trans* to the deletion *Df(3L)BSC120* to minimize effects of genetic background. The heterozygous knockout mutant was used as a control unless otherwise indicated. Flies were collected upon eclosion and kept and aged in groups of 20 to avoid any behavioral variations associated with social conditions. All assays were performed during a fixed time window in the afternoon to minimize circadian variation.

2.8.1 Climbing assays

2.8.1.1 Setup

Climbing assays were performed in long cylindrical tubes (~ 20cm pipette tubes) on groups of 20 male or female flies. Flies were tapped down and the number of flies at the top 5 cm (n_{top}) and bottom 5 cm (n_{bottom}) of the cylinder were counted after 30 seconds. Each genotype was tested with 3 biological and 5 technical replicates.

2.8.1.2 Analysis

Climbing index was calculated as $½(n_{tot}+n_{top}-n_{bottom})/n_{tot}$) (Feany and Bender, 2000). The climbing index was tested for statistical significance using the Student's t-test. Error bars indicate standard deviation.

2.8.2 Phototaxis assays

2.8.2.1 Setup

Two empty fly food vials used for the assay, the base of one was colored black. Flies were transferred into one vial, and the second vial was taped to the open end, thus creating a lighted and a darkened end (Koh et al., 2008). Phototaxis assays were performed in these transparent vials using groups of 20 flies. Flies were exposed to a focused light source (~2000 lux) at one end of the vial, while the other end of the vial was kept dark. Flies were tapped to one end horizontally and the number of flies that moved towards the light n_{light}, and the number that stayed at the dark end n_{dark} were counted after 30 seconds. The experiment was repeated in the dark as a control.

2.8.2.2 Analysis

Phototaxis index was calculated as $½(n_{tot}+n_{light}-n_{dark})/n_{tot}$) in the experimental (with light) and the control (without light) conditions. In cases where the control phototaxis index showed a bias towards the left or right side of the vial, data from that cohort was discarded. The phototaxis index was tested for statistical significance using the Student's t-test. Error bars indicate standard deviation.

2.8.3 Locomotor assays

2.8.3.1 Setup

Locomotor assays were performed on groups of 20 flies using the *Drosophila* Population Monitors (Trikinetics). Equal numbers of flies were transferred into clean long glass vials (12.5 cm length, 2.5 cm diameter) without using carbon dioxide. The vials were inserted into the monitors, and the monitors placed into a behavior chamber with constant temperature and humidity (25°C, 70%). Monitors were placed uniformly in the chamber, allowing for uniformity of light. Flies were monitored over a period of 1.5 hours, but only the later one-hour data was used for analysis to account for acclimatization of the flies to the new surroundings. Activity is measured by the fly interrupting an infrared beam in the test chamber, and recorded as number of beam breaks per hour, per group. Activity plots were recorded using the DAMSystem 308 software (Trikinetics) and binned into 5 minutes intervals over the 1-hour assay period.

2.8.3.2 Analysis

100 flies (5 biological replicates) were tested per sample. Each biological replicate was tested 3 times for recording technical variation. Activity counts were normalized to the control for each experiment. Activity was tested for statistical significance using the Student's t-test. Error bars indicate standard deviation.

2.8.4 Ether resistance assays

Two drops of ether (Sigma) were put on a cotton plug and were used to knock out flies. Flies were anesthetized within 10-30 seconds in cohorts of 10 flies for each genotype. The time to recovery was recorded using a timer. Flies were also observed for the presence of ether-induced leg-shaking behavior (Wang et al., 2000).

2.8.5 Courtship assays

For all courtship assays, socially naïve animals isolated at late pupal stages were used.

2.8.5.1 Paired courtship assays

Single male-female courtship assays were performed and video-recorded in courtship chambers as described (Demir and Dickson, 2005). Videos were analyzed for courtship latency (time to courtship initiation), copulation latency (time to copulation). n ~ 20 biological replicates for each genotype and combination. Statistical analysis was done using the Mann Whitney test.

2.8.5.2 Mate-choice assays

Mate-choice assays were performed and video-recorded in 35mm petri dishes customized for use as courtship chambers, to allow adequate space for courting. Briefly, a small hole was made to allow fly transfers into the dish using a soldering iron in the cover of the petri dish and BluTac was used to seal it off.

2.8.5.2.1 Male mate choice assay

Wildtype and mutant males were paired with a CS virgin and a CS non-virgin, and courtship videos were recorded for ~30 mins. CS females were 'dotted' on their wings using a marker one day before the mate-choice assay. One set were mated with CS males and one set was kept virgin. The non-virgin females were tested an hour post-mating. Virgins and non-virgins were marked in an equal number of trials, to exclude bias due to the mark. Videos were analyzed for the amount of time the male spent actively courting (following, singing, licking or attempting copulation) either the virgin or the non-virgin. Approx 20 biological replicates for each genotype and combination. Statistical analysis was done using the Fisher's exact test.

2.8.5.2.2 Female mate choice assays

A WT female was paired with two males of differing genotypes and courtship videos were recorded for ~30 mins. CS virgin females were used for this assay. Males of one genotype were 'dotted' on their wings using a marker one day before the mate-choice assay (males of each genotype were marked in an equal number of trials, to exclude bias due to the mark). Videos were analyzed for the female's choice for copulation. Approx 20 biological replicates for each genotype and combination. Statistical analysis was done using the Fisher's exact test.

2.9 Deep pseudopupil assays

Deep pseudopupils were visualized as described previously (Stark and Thomas, 2004). Briefly, flies were anesthetized with CO_2 and immobilized on a glass microscopic slide using clear nail polish. Heads were oriented to expose the dorsal region. Because of the regularity of receptor structure in each ommatidium and of the angle between ommatidia, there is a magnified virtual image about 80 μm in diameter of the rhabdomere tips superimposed from all the ommatidia sampled (typically 25, depending on the numerical aperture of the microscope objective) about 150 μm behind the surface of the eye; this is the deep pseudopupil. For counting, deep pseudopupils in *Drosophila* were viewed with a compound microscope at 5x maginification. Observation of the deep pseudopupil of red-eyed flies required illumination from below (antidromic), using a narrow, bright light source with a transparent, elevated stage for the flies. The deep pseudopupil of white-eyed flies was viewed with illumination from above (orthodromic). For imaging, a Zeiss LSM 510 confocal microscope was used at 488 nm.

2.10 Semi-thin adult *Drosophila* retina plastic sections

Plastic semi-thin sections of adult fly retina were prepared as described (Gaengel and Mlodzik, 2008). Briefly, flies were anesthetized with CO2, and decapitated. One eye was cut away to allow penetration of fixation solutions. Samples were fixed with 2% glutaraldehyde followed by 4% osmium tetroxide. Following fixation, samples were dehydrated with increasing concentrations of ethanol. Samples were embedded in Durcupan ACM resin (Sigma D-0166). Eye sections were prepared after mounting the embedded

samples, and microscopic analysis was done using an electron microscope at the IMCB EM core facility.

2.11 Western blotting

Heads were taken from 10-15 2 day old adult flies and homogenized in SDS sample buffer followed by incubation at 98°C. Heat denatured protein samples were run in 10%~12% SDS-PAGE at a constant voltage of 100 V till the lowest marker (20kDa, Progema) reached the end. The gels were then transferred to a nitrocellulose membrane in ice-chilled transfer buffer (25 mM Tris, 192 mM glycine, 0.025% SDS, 20% methanol) at a constant current of 200 mA/membrane for 50 min. The blocking buffer (5% non-fat dry milk in 1 x PBST [137 mM NaCl, 2.7 mM KCl, 10 mM Na2HPO4 · 2H2O, 2 mM KH2PO4, 0.1% Tween-20]) was used to block the membrane for 1 hour at room temperature. After that, primary antibodies were added and incubate overnight at 4°C. The next day, 1X PBS-T wash buffer was used to wash the membrane for 3 times, each for 15 min before addition of HRP-conjugated secondary antibodies. After incubation of secondary antibody in blocking buffer for 1.5 hours, the membrane was treated with horseshoe peroxidase (Promega) for 2 minutes before detection of chemilluminescence.

Antibodies to *Drosophila* AKT and pAKT S505 were used for immunoblots at 1:1000 and 1:3000, respectively (product # 9272 and 4054, Cell Signaling). Anti-Kinesin was used at 1:2000 as a loading control.

2.12 Immunohistochemistry

Adult brains were dissected in ice cold PBS and fixed in freshly diluted 4% paraformaldehyde (PFA) for 20 min at room temperature on a mild rocker. Samples were washed 3x with PBT (PBS+0.1%Tween-20) for 20 min each. This was followed by blocking in BBT (PBT+5%NGS) for 1 hour at room temperature. Samples were incubated in primary antibody for 2 nights at 4°C. They were washed thrice with PBT and incubated with secondary antibody for 2 hours at RT. After washing, they were equilibriated in VectaShield mounting medium (Vector Labs) before mounting for imaging. Rat anti-elav, mouse anti-Rh1, mouse anti-repo and mouse anti-brp (nc82) were from DSHB, and used at 1:400, 1:200, 1:20, and 1:400 dilutions, respectively. DAPI was used at the dilution of 1:2000.

2.13 Measurement of SOD biochemical activity

Total SOD activity was measured from adult fly heads (day 3-5) and the assay was performed according to the manufacturer's protocol (Dojindo Molecular Technologies Inc.). Briefly, adult heads were flash-frozen and homogenized

2.14 Oxidative Stress assay

3-5 day old flies were starved for 5 hours on 1% agarose in groups of 20 before being subjected to oxidative stress by feeding with 5% hydrogen peroxide, 2.5% sucrose in 1% agarose. Controls were fed 2.5% sucrose in 1% agarose. Flies were counted for survival every 6 hours.

2.15 Electroretinograms ERGs

ERGs were performed in the Desplan lab using previously described methods (Dolph et al., 2011). 10 flies were tested for every different age and genotype. Flies were immobilized in 0.8% agarose. The recording electrode was placed on the corneal surface of the eye. The reference electrode was inserted lightly into the thorax. Flies were given a 1s light stimulus, and the current was measured using the rig.

Chapter 3 Results

3.1 The miRNA knockout library

The Cohen lab has produced a library of miRNA knockouts by targeted homologous recombination in *Drosophila*, for 131 conserved miRNAs. Including clustered miRNAs, there are 98 knockout fly lines (Chen et al, *in preparation*). Most of the miRNA knockout animals are viable as adults.

3.2 *miR-285* and Vision: retinal degeneration screen

miRNAs are thought to have roles in neuronal degeneration, based on several miRNA expression profiling studies of diseased tissues (Gandhi et al., 2013; Junn and Mouradian, 2012). Such studies do not distinguish whether changes in miRNA profiles are a cause or a consequence of neurodegeneration. However, functional studies of miRNA mutants have highlighted the importance of miRNAs in neurodegenerative processes (Karres et al., 2007; Liu et al., 2012).

To isolate miRNA mutants potentially linked to neurodegneration, I chose to screen the miRNA mutant collection for mutants showing retinal photoreceptor degeneration. I chose a simple method for this screen, which is to score for the presence or absence of deep pseudopupils in the eye. Each *Drosophila* compound eye is composed of ~ 800 ommatidia, with every ommatidium containing one rhabdomere. The rhabdomere is the light-sensing unit found in the 8 photoreceptors R1-R8. The ordered structure of the insect

compound eye is such that the orientation of the rhabdomeres leads to formation of the deep psuedopupil, roughly 150 microns below the surface of the eye (Fig 3.1a) (Franceschini and Kirschfeld, 1971a, b). Visualizing deep pseudopupils has been a useful tool to identify mutations involved in genes related to visual transduction and photoreceptor maintenance. Loss of the deep psuedopupil (DP) is an early marker for loss in structural integrity in the highly ordered photoreceptor lattice, and is a marker for possible retinal degeneration (Katz and Minke, 2009). Fig 3.1b shows the method to visualize DP, and the image of an intact DP in a Canton-S fly eye.

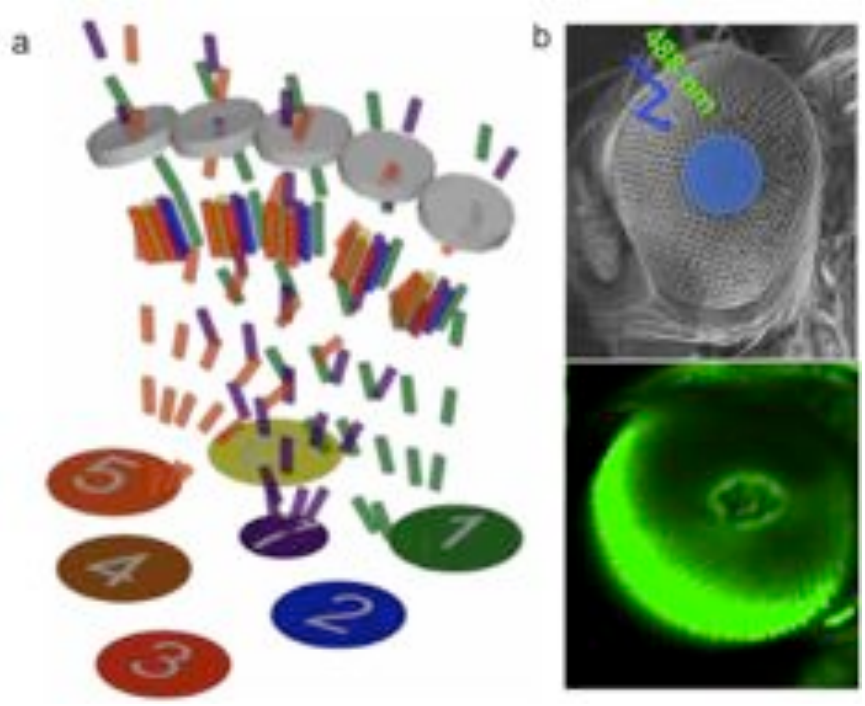

Fig 3.1 a Schematic of deep pseudopupil (DP) formation. Gray discs represent ommatidia, color-coded cylinders depict R1-R8 photoreceptors. Light passing through the photoreceptors (colored dashed lines) results in DP formation. Copied with permission from Dr William S Stark. **b** Experimental setup for DP visualization involves 488 nm monochromatic light (above), and the resulting DP in a Canton-S fly (below).

3.2.1 Dicer depletion leads to loss of deep pseudopupils

Before screening the mutant library, I tested whether a general depletion of miRNAs by knocking down their biogenesis using Dicer-1 RNAi could lead to a loss of deep psuedopupils. I used the eye-specific rh1 Gal4 driver to knockdown Dcr-1. The stronger GMR driver resulted in gross morphological changes in the eye, and hence, was not used. Under normal 12:12 day/night condition (~400 lux), Dcr-1 depletion did not result in disappearance of the DP. However, under constant bright light of ~3000 lux, Dcr-1 depleted flies showed a loss of DP at 5 days after eclosion (Fig 3.2).

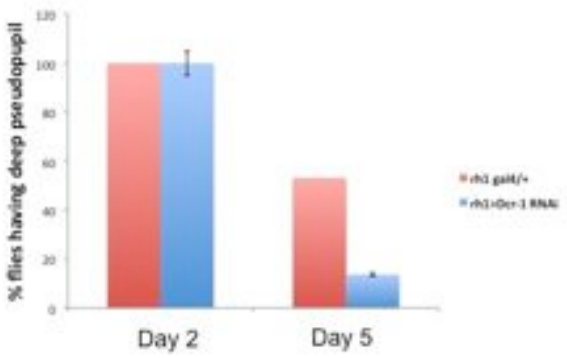

Fig 3.2 Graph shows loss of deep psuedopupil in Dcr-1 RNAi flies as compared with the Gal4 driver alone as control. Flies were kept under constant light of ~3000 lux. Error bars represent SEM.

3.2.2 Screen summary

I screened the unpublished collection of mutants for the miRNAs most highly enriched miRNAs in adult *Drosophila* heads (Ruby et al., 2007b). I isolated 3 candidate mutants, *miR-285*, *miR-284* and *miR-7*, which caused the pseudopupil to disappear by 5 days post-eclosion. *miR-7* mutants showed a complete lack of the pseudopupil from the time of eclosion. *miR-7* has been

previously identified to have a role in photoreceptor differentiation (Li and Carthew, 2005) and hence is likely to have impaired ommatidial structure, resulting in the lack of the DP. The *miR-284* phenotype was non-specific because restoring *miR-284* in the mutant using UAS-*miR-284* in the Rh1-expressing cells did not rescue the DP (Fig 3.3). The *miR-285* phenotype could be rescued (see next section); hence I continued work with *miR-285*.

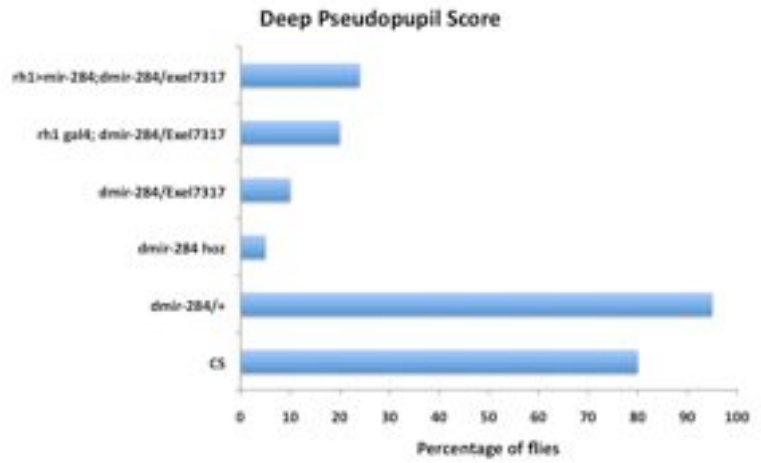

Fig 3.3 Deep psuedopupil scores for *miR-284*. Exel7317 is the deficiency used for miR-284. The heterozygote mutant allele (*dmiR-284*/+) is used as a control in addition to CS. The rescue was done by expressing *miR-284* in the Rh1 expressing R1-R6 cells. n=30.

3.2.3 *miR-285* mutants have impaired pseudopupils

To make the *miR-285* mutant, the *miR-285* hairpin was replaced with the mini-white gene, which is used as a marker to track the miRNA loss. A rescue transgene was generated by inserting the *miR-285* hairpin, flanked by 2.7 kB upstream and downstream genomic fragments into the genome by P-element mediated transformation (Fig 3.4a). The *miR-285* mutant was verified as null for the *miR-285* miRNA by quantitative RT-PCR. The transgenic rescue line restores mature *miR-285* levels to ~1.5 fold wild type (Fig 3.4b). *miR-285* mutants are viable, fertile, and do not show any morphological defects.

miR-285 mutant animals showed disappearance of the DP 5 days post-eclosion under constant light conditions. In order to minimize background effects due to the knockout generation process, I used several deficiency lines in *trans* with the *miR-285* knockout allele. The deep pseudopupil phenotype was observed using all genetic combinations (Fig 3.5). Additionally, a UAS-*miR-285* transgenic line was generated, and an Rh1-Gal4 mediated expression of *miR-285* restored the loss of deep pseudopupil in the mutants (Fig 3.6). Under normal 12 hours light (~500 lux) and12 hours dark cycle, *miR-285* mutants are slower to lose the deep pseudopupil. By 20 days of age, only 20% mutants still have the intact deep psuedopupil (Fig 3.7).

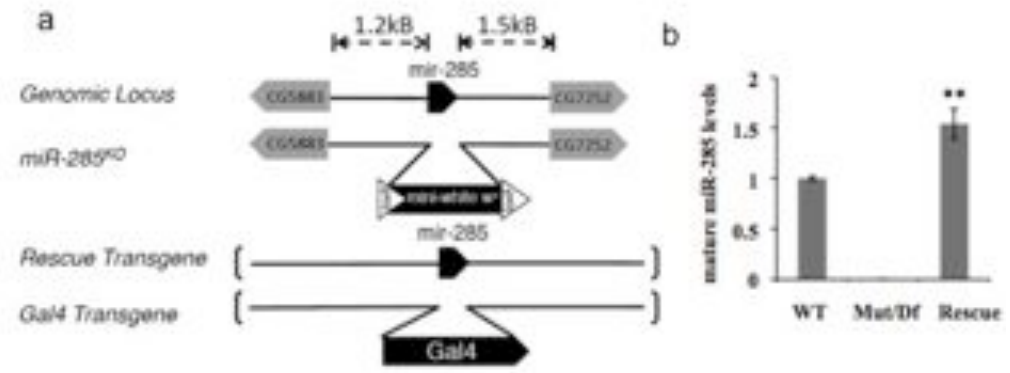

Fig 3.4 a Schematic showing the genomic locus of *miR-285*. Also shows the targeting strategy used to produce the *miR-285* mutant by homologous recombination. *miR-285* is located in the interval between CG5883 and CG7252. The miRNA hairpin was deleted and replaced with a mini-white cassette flanked by loxP sites. A rescue transgene was constructed comprising ~3KB of DNA located between CG5883 and CG7252. This construct was used to produce transgenic flies at landing site 51D. The miR285 gal4 transgene contained the same DNA fragment except that the miRNA hairpin was replaced by Gal4 coding sequences, **b** Mutants lacked detectable mature *miR-285* miRNA measured by quantitative real time PCR. miRNA expression was restored to ~1.5x normal levels using the rescue transgene in the mutant background. This transgene rescued the mutant phenotypes described in the main text. Data were normalized to U27 RNA and represent average ± SD for two biological replicates. ** $p<0.01$ Students t-test.

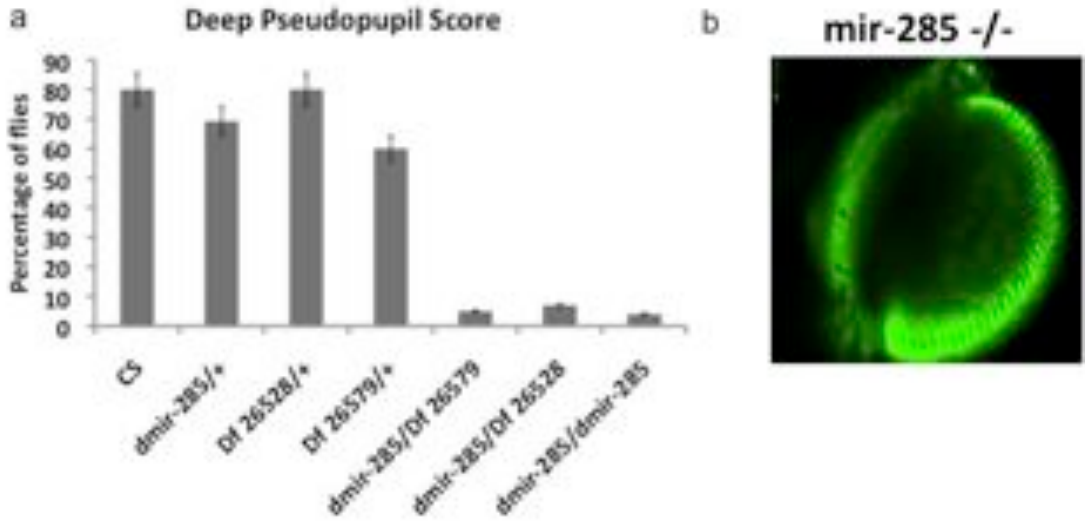

Fig 3.5 Deep psuedopupil scores for *miR-285*. **a** Graph shows the *miR-285* DP phenotype using various homozygous and trans-heterozygous genetic combinations Df 26579 and Df 26528 uncover the *miR-285* locus. **b** Image shows lack of deep psuedopupil in *miR-285* mutant flies (magnification-10x).

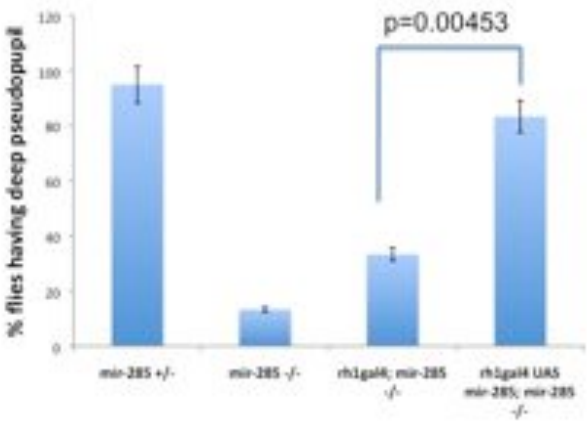

Fig 3.6 Rescue of miR-285 deep psuedopupil phenotype. Graph shows rescue of the DP phenotype using Rh1Gal4 mediated expression of *miR-285* in the mutant genetic background. Error bars represent SD. $p<0.005$ using Student's t-test.

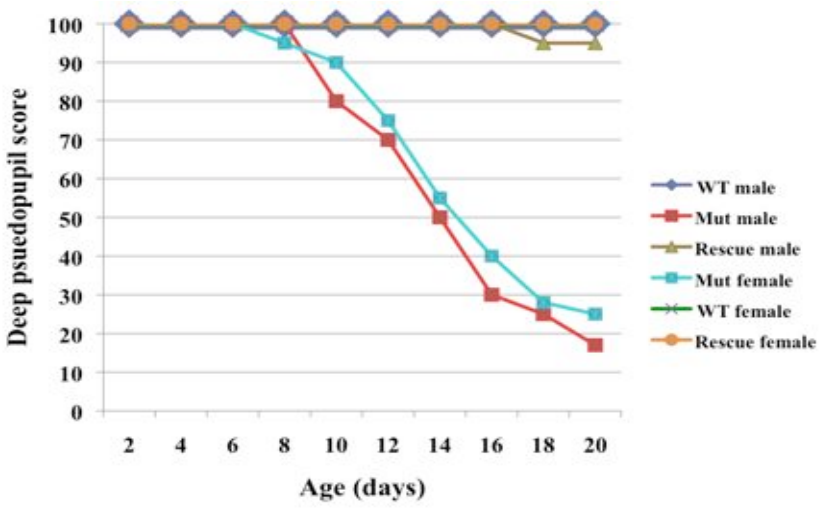

Fig 3.7 Graph shows DP score as a function of age for *miR-285* mutants under normal light-dark (12:12) cycle with light of intensity ~500 lux. WT = CS, Mut = *miR-285*/Df, Res = Genomic Rescue+*miR-285*/Df; n=30.

3.2.3.1 Activity-dependent onset

Either light dependent or independent pathways can trigger retinal degeneration (reviewed in (Wang and Montell, 2007). Mutations in folding and maturation of the light-sensing trans-membrane rhodopsin proteins cause the light-independent form of retinal degeneration. Mutations in the visual transduction pathway lead to light or activity dependent form of degeneration. Visual excitation of retinal photoreceptors begins with the absorption of light by the visual pigment (rhodopsin) which, acting through G proteins, targets the protein *NorpA* encoded by a phosphoinositide-specific phospholipase C (PLC). *NorpA* then catalyzes the breakdown of phospholipids and generates inositol trisphosphate (IP3) and diacylglycerol. These second messengers activate transient receptor potential (trp) channels, causing a high influx of calcium into the neurons, which needs to be extruded quickly to reset the photoreceptors and prevent toxicity. Light-dependent degeneration is typically triggered because of a lack of control of this cycle.

3.2.3.1.1 Suppression in dark

To test for activity dependence of the phenotype, the mutant flies were reared in the dark and kept in complete darkness after eclosion. These flies showed a partial, but significant suppression of the DP phenotype under dark, suggesting an activity-dependent mechanism (Fig 3.8).

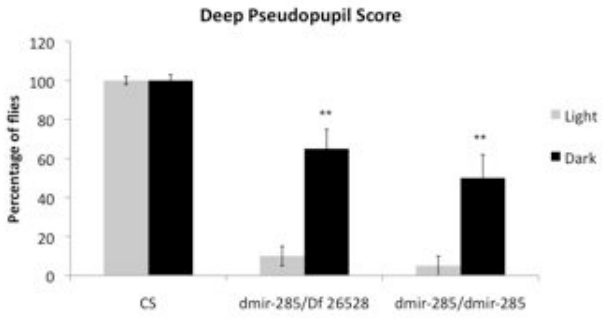

Fig 3.8 Graph shows DP scores for dark-raised mutant flies. n=20 for each condition, with 3 biological replicates each. Error bars represent SD. ** $p<0.01$ by Student's t-test.

3.2.3.1.2 *norpA*^{7} mediated-suppression

Null mutations of *norpA* result in total blindness, resulting from lack of photocurrents as measured by electroretinograms (ERGs) (Harris and Stark, 1977; Inoue et al., 1989). The *norpA*^{7} mutant is a null EMS allele, which has been used to suppress light-dependent retinal degeneration by blocking receptor potentials (Harris and Stark, 1977). Using this allele in combination with the *miR-285* mutant, I observed a significant suppression of the DP phenotype (Fig 3.9). This suggests that the loss of *miR-285* causes activity dependent retinal degeneration.

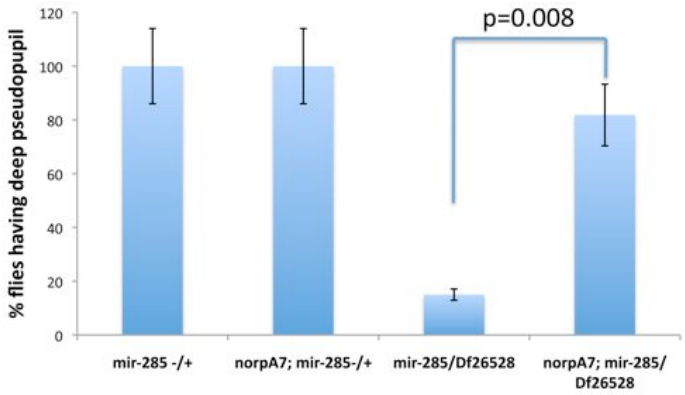

Fig 3.9 norpA-mediated rescue**.** Graph shows percentage of flies with deep pseudopupil is restored to wildtype genotypes when *norpA* mutant allele is used in the mutant. Error bars represent SD.

3.2.4 Semi-thin retinal sections

The deep pseudopupil analysis suggests that photoreceptor integrity is impaired in the *miR-285* mutant flies in a light-dependent manner. In order to directly observe the photoreceptors, I made semi-thin resin sections of adult retina, at 5 and 20 days of age (Fig 3.10). The rhabdomeres looked normal in the mutant retinas at day 5. However, by 20 days, there were gross morphological abnormalities in photoreceptor organization (Fig 3.10). Under normal light, the DP disappeared in *miR-285* mutants by 20 days of age. The rhabdomeres were not lost altogether, however, their arrangement was highly disordered.

3.2.5 Tests for visual function

While the deep pseudopupil analysis together with retinal sections provided ample evidence for loss of photoreceptor integrity, I wanted to test whether this phenotype has functional consequences for fly vision.

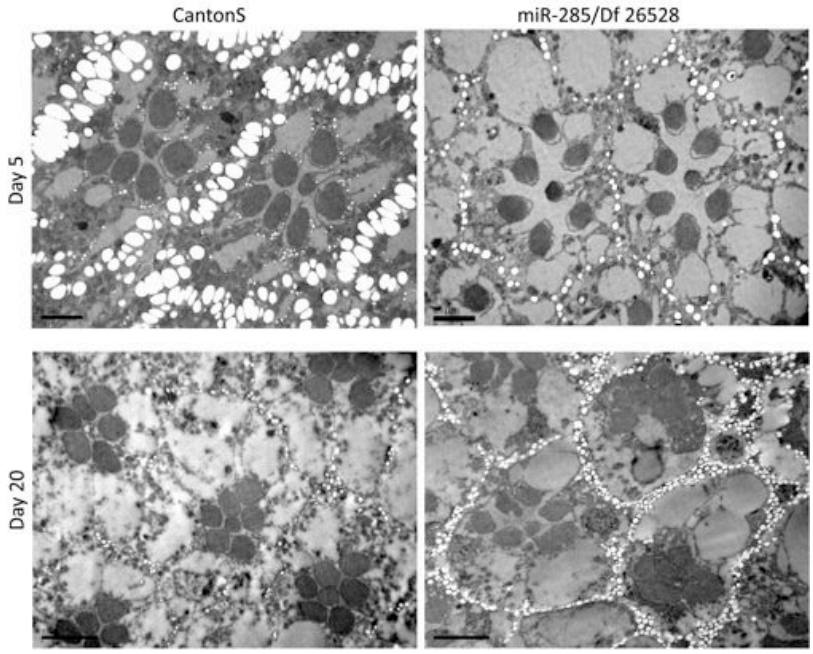

Fig 3.10 Representative electron micrographs of semi-thin retina sections from wildtype and *miR-285* mutant flies at 5 and 20 days of age. Quality of images is slightly compromised due to incomplete infiltration of the resin.

3.2.5.1 Electroretinograms

Loss of photoreceptor integrity usually translates into loss of photocurrents. This can be measured using electroretinograms (ERGs). The ERG recording method uses an extracellular electrode to record a compound field potential from photoreceptors and downstream neurons within the fly eye in response to flashes of light (Dolph et al., 2011). Transient spikes at the onset and offset of a light flash correspond to postsynaptic potentials in photoreceptors, while a sustained potential during the light stimulus results from the depolarization of photoreceptor cells (Hardie and Raghu, 2001; Montell, 1999; Stark and Wasserman, 1972; Wu and Wong, 1977). The ERG experiments were done with the help of Dr Rudy Behnia (NYU). I aged the flies after eclosion under normal light-dark (12:12) cycle with light intensity ~ 500lux. While the DP disappears in *miR-285* mutants by 20 days of age (Fig 3.7), the ERGs

remained intact (Fig 3.11), implying the flies are not functionally blind. The on and off transients indicate that signaling between photoreceptors and laminar neurons is functional. The depolarization during the 1s light stimulus indicates that the photo-transduction cascade is intact. This implies that perhaps *miR-285* is impacting higher visual processing centers. However, the question of what is leading to disorganized photoreceptors is more difficult to explain.

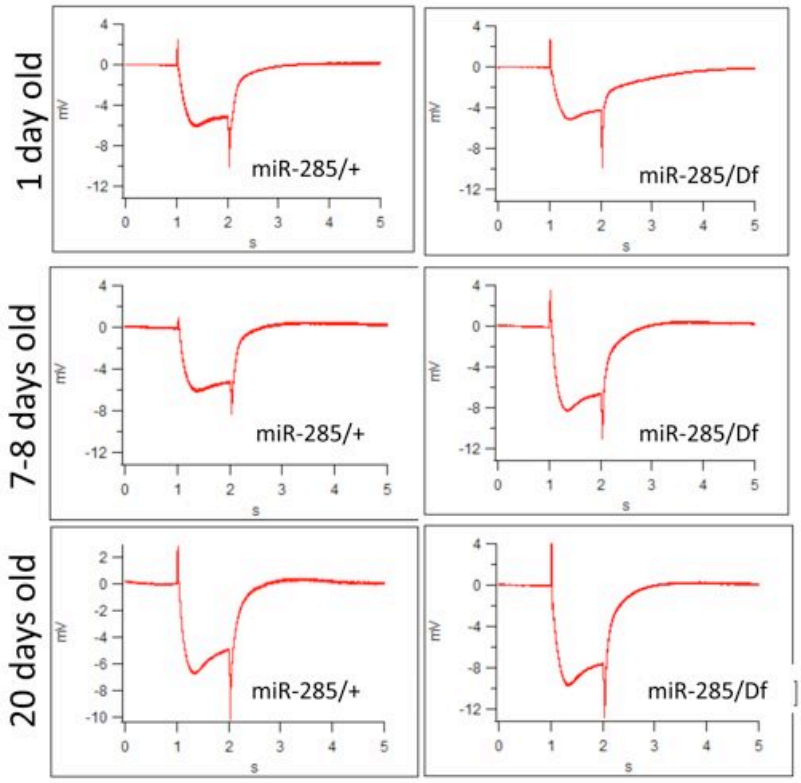

Fig 3.11 Electroretinograms for control (*miR-285*/+) and mutant (*miR-285*/Df) flies at different ages, maintained under normal light-dark (12:12) cycle with light intensity ~ 500lux.

3.2.6 Targets

I took multiple approaches to find target genes for *miR-285*, in the context of the deep pseudopupil phenotype. From the many computational prediction programs, I identified candidate genes with *miR-285* binding sites involved in

some aspect of eye development or function and those genes that are enriched in the WT eye (Table 3.1). Quantitative PCRs for measuring these candidates did not show significant up-regulation for most genes in the mutant heads (Fig 3.12). *Pu* and *bw* were slightly upregulated, but were not followed up for further tests, because these were both involved in pigmentation of the eye, not potentially relevant for the phenotype under study.

TargetScan 3'UTR sites	RNAHybrid 3'UTR sites	Minotar ORF sites
neur	Eip71CD	cnk
wts	CG13409	Dab
W	Ggamma30A	msn
Pu	CG2121	ca
Rh6	CG9317	
bw	trpl	
mbl		
Ras85D		
Dad		
bab2		
tsh		
sna		

Table 3.1 Candidate approach for target genes using *miR-285* binding site prediction programs: TargetScan, RNAHybrid, and MinoTar.

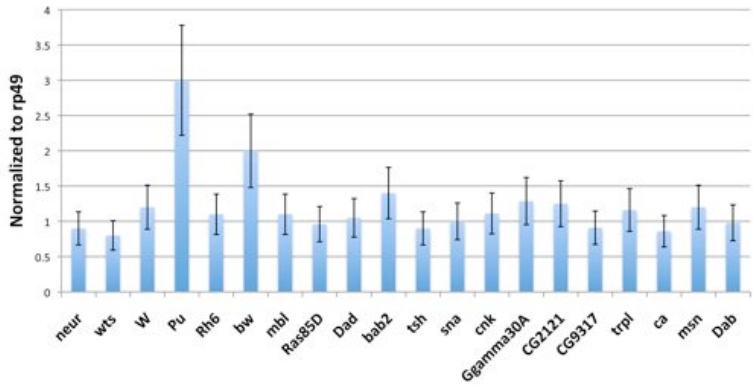

Fig 3.12 qRT-PCRs for candidate target genes. Data from mutant head RNA is normalized to w^{1118} head RNA. Error bars represent SD.

To further my search for a target gene, I performed unbiased microarray analyses on RNA from heads of w^{1118}, *miR-285* mutant and *miR-285* rescue (*miR-285* mutant with Rh1Gal4>UAS-*miR-285*). From the set, I found only 4 genes (Table 3.2), which were upregulated in the mutant, and were downregulated in the rescue; and had weak *miR-285* binding sites using the RNAHybrid program. However, functional genetic tests by reducing expression of these genes in the mutant could not rescue the deep pseudopupil phenotype (data not shown).

Gene	Binding site	Fold up in mutant	Fold down in rescue
CG31909	6 mer GU	1.482218057	0.703097917
m	6 mer	1.397918949	0.666856623
CalpA	6 mer GU	1.389217869	0.808240791
Irp-1B	6 mers	1.249162464	0.634528782

Table 3.2 Genes shortlisted from the microarray analysis. Binding site denotes the kind of binding of *miR-285*; GU pairing weakens the site.

3.2.7 Conclusions

Overall, *miR-285* mutants lost the deep psuedopupils, in an activity dependent manner, and showed morphological abnormalities in rhabdomere arrangement. These slight changes in rhabdomere morphology would be sufficient to lose the formation of the deep pseudopupil image, which is very sensitive to the geometrical arrangement of photoreceptors. However, the ERGs were intact, implying that the photoreceptors and downstream synapses are functional. Additionally, I did not observe any increased apoptosis in the mutant brain

(data not shown), and was unable to rescue the deep pseudopupil phenotype by expressing p35, an anti-apoptotic protein (Fig 3.13). This suggests that the defects were not caused by neuronal degeneration or cell death.

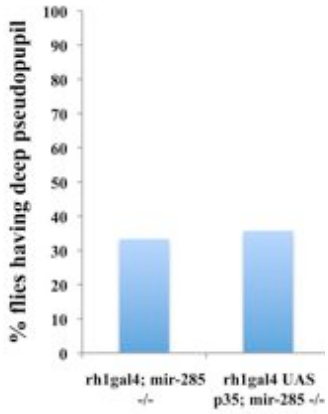

Fig 3.13 p35-mediated rescue. Eye-specific expression of the anti-apoptotic gene p35 could not rescue the *miR-285* deep psuedopupil phenotype (n=30 flies).

3.3 Age-related phenotypes: Lifespan assay

As a part of a general analysis of the *miR-285* mutant, I tested their lifespans and observed that loss of *miR-285* prolonged lifespan by ~25-30% in males (Fig 3.14a, b). This increase in lifespan could be suppressed by adding the miRNA back into the system. A control rescue transgene without the miRNA hairpin did not rescue median lifespan. Lifespan of mutant females was unchanged (Fig 3.14c).

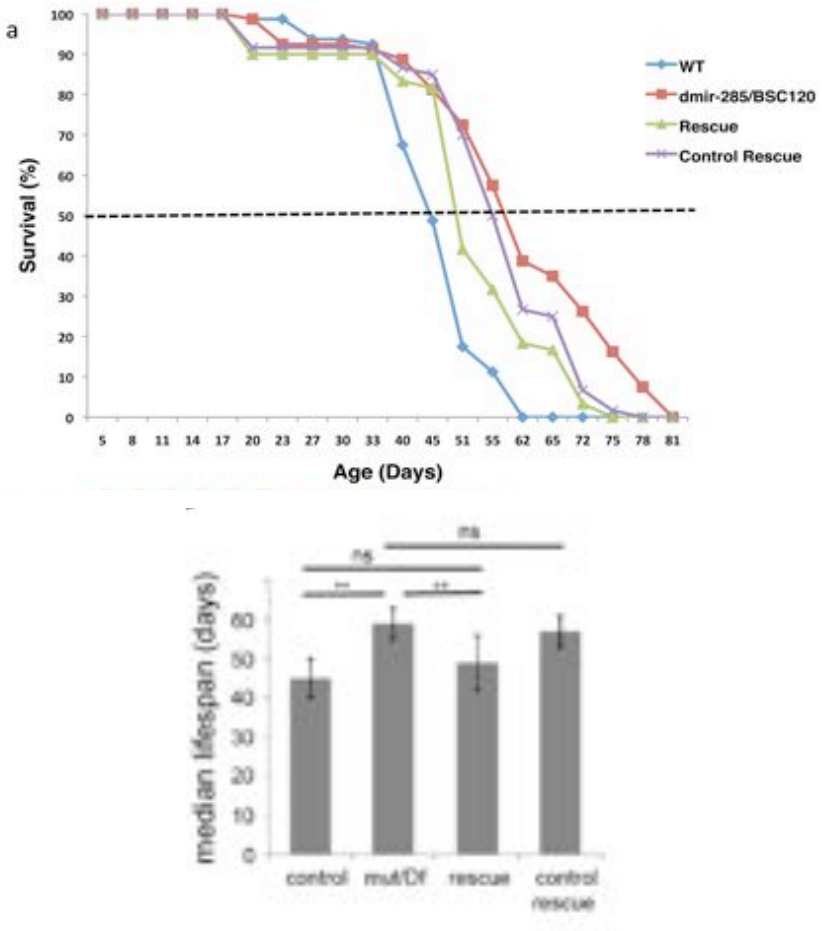

Fig 3.14 a Lifespan curve for males, **b** Median lifespan for the indicated genotypes. n = 180 flies per genotype (3x3x20 flies/vial). Error bars represent SD. ** = p<0.01, ns: not significant; Student's t-test was used. *miR-285* knock-out mutants were used in trans to a wild-type copy of *miR-285* as controls. Mutants are the knock-out allele in trans to *Df(3L)BSC120* which uncovers the *miR-285* locus; rescue indicates the mutant/Df combination carrying one copy of the genomic rescue transgene; control rescue represents

mutant flies with the rescue construct without the *miR-285* hairpin. Data represent the average of at least 3 biological replicates with 3 vials x 20 flies for each genotype.

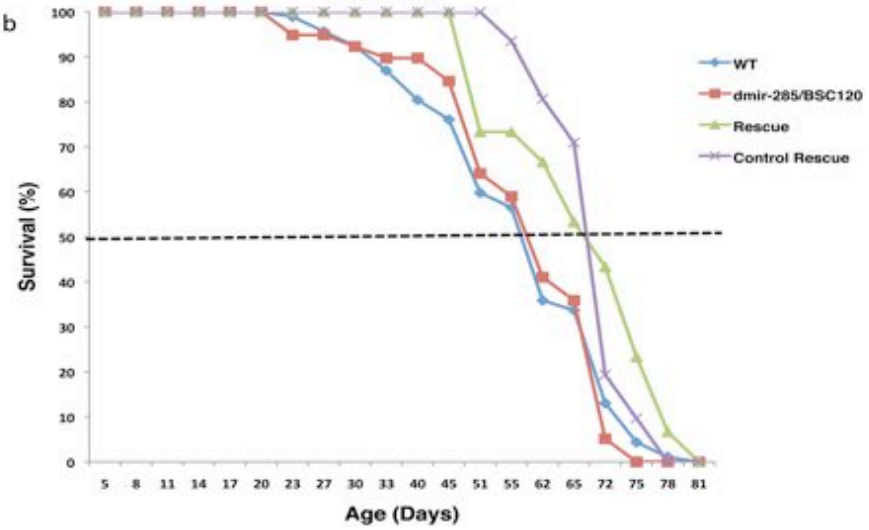

Fig 3.14 c Lifespan curve for females. Genotypes indicate same as Fig 3.14a. n = 180 flies per genotype (3x3x20 flies/vial).

3.4 Locomotor phenotypes

An increase in lifespan raised the possibility of other age-related phenotypes in the *miR-285* mutants. Since *miR-285* mutants have increased lifespans, it is possible that their aging is slowed. Based on this hypothesis, I tested the mutants for age-dependent behaviors. Motor activity is often used as a parameter to assess aging – typically, motor activity declines in animals as they age. I used three kinds of motor activity assays to investigate this.

3.4.1 Climbing assay

The climbing assay is a simple tool to measure negative geotaxis and locomotor behavior in flies. The assay reports a climbing index, which is a measure of how well flies of a given genotype can climb up a fixed distance in

a vial. I measured climbing ability of flies at 3 and 7 weeks of age. Wild type flies showed a decline in performance with age; however, *miR-285* mutant flies continued to do well even at later ages. This age-preserved motor ability could be suppressed by using a rescue transgene (Fig 3.15).

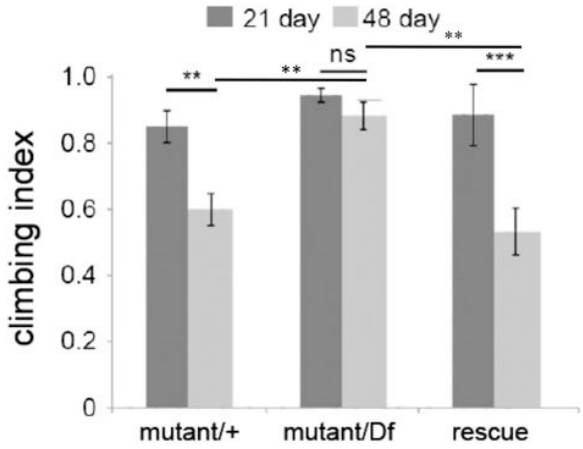

Fig 3.15 Climbing index measures innate climbing behavior and requires motor coordination. *miR-285* knock-out mutants were used in trans to a wild-type copy of *miR-285* as controls. Mutant/Df indicates the knock-out allele in trans to *Df(3L)BSC120* which uncovers the *miR-285* locus; rescue indicates the mutant/Df combination carrying one copy of the genomic rescue transgene; data represent the average of at least 3 biological replicates. n = 40 flies per genotype. Error bars represent SD.

3.4.2 Phototaxis assay

Fruit flies are positively phototactic, implying that they are attracted to and move towards a light source. This requires them to be able to sense light, and have motor coordination. Because *miR-285* is expressed in the eyes (Fig 3.18, 3.19), I tested flies using the phototaxis assay in order to complement the climbing assay. Interestingly, the behavior of flies was similar to that in the climbing assay – older wild type males showed a decline in movement

towards light, whereas older *miR-285* knockout males did not show this difference (Fig 3.16). Females were unaffected.

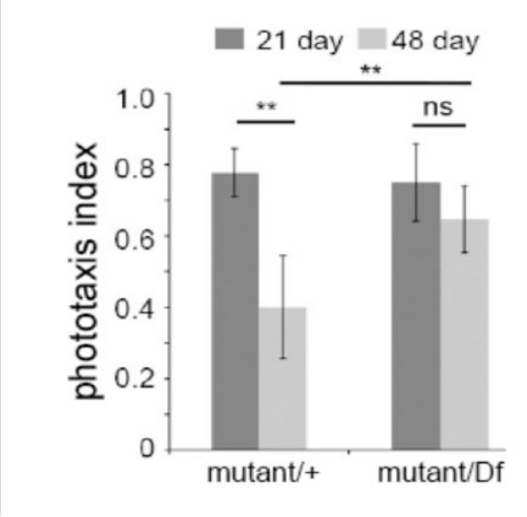

Fig 3.16 Graph depicts phototaxis index of flies, their ability to move towards a light source at 21 and 48 days of age. Mutant/Df indicates the knock-out allele in trans to *Df(3L)BSC120* which uncovers the *miR-285* locus; data represent the average of at least 3 biological replicates. n = 40 flies per genotype. Error bars represent SD.

3.4.3 Population Locomotor assay

Both the climbing and phototaxis assay show that *miR-285* mutants have age-preserved motor abilities. Both these assays have coordinated motor ability as the common denominator, which raised the question whether *miR-285* mutant flies have basally high locomotor activity. I tested the mutants using a population monitor assay, which reports activity of flies every hour. *miR-285* deletion mutants show increased motor activity in a population monitor assay (Fig 3.17). This effect was only observed in males, and could be restored to wild-type levels using a rescue transgene.

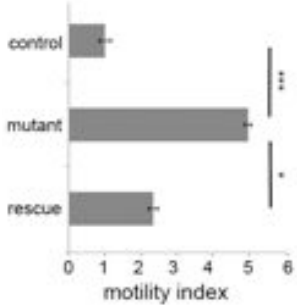

Fig 3.17 Motility index measures locomotor activity normalized to the activity of the control population. *miR-285* knock-out mutants were used in trans to a wild-type copy of *miR-285* as controls. Mutant indicates the knock-out allele in trans to *Df(3L)BSC120* which uncovers the *miR-285* locus; rescue indicates the mutant/Df combination carrying one copy of the genomic rescue transgene; n = 100 flies per sample. Error bars represent SEM.

3.5 Expression analysis

miR-285 is one of the ten most abundant miRNAs in adult fly heads and is expressed almost exclusively in the head (Ruby et al., 2007b) miRBase). I wanted to examine *miR-285* expression in detail at the spatial and temporal levels.

3.5.1 Spatial expression

3.5.1.1 LNA in situ hybridization

LNA (locked nucleic acid) probes are sensitive and have great specificity for miRNAs in situ hybridization (Toledano et al., 2012). ISH for *miR-285* in adult brains showed expression in the retina and in the optic lobe, specifically the lamina (Fig 3.18).

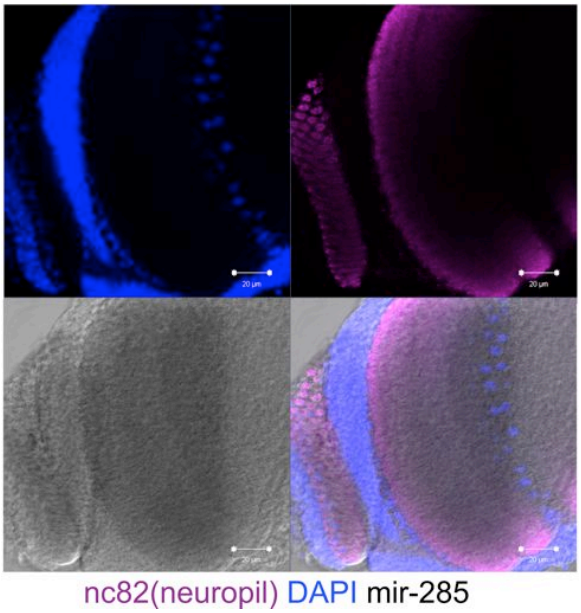

Fig 3.18 LNA in situ hybridization for *miR-285* in the retina and the lamina, using alkaline phosphatase staining at 40x magnification. nc82 marks the neuropil (axons and dendrites), DAPI stains all nuclei.

3.5.1.2 promoter Gal4 mediated-expression

To visualize *miR-285* expression at a greater resolution, I used *miR-285* Gal4 to drive expression of RFP (Fig 3.3). *miR-285* is expressed in the visual system, broadly in the compound eyes and in the ocelli (Fig 3.19). Fig 3.20 top panel shows expression in the retina and the optic lobe, specifically in the R1-R6 photoreceptors, and their connections into the lamina. *miR-285*-expressing cells in the central brain largely co-localize with repo, a glial marker (Xiong et al., 1994). Only some of them co-localize with elav, a post-mitotic neuronal marker (Fig 3.20).

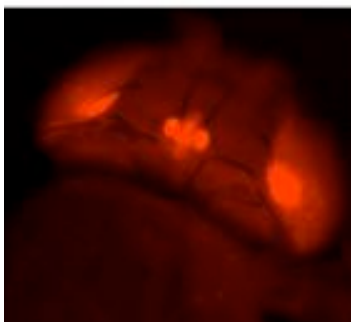

Fig 3.19 Overview of *miR-285* expression using *miR-285*Gal4>UAS mCD8 RFP – expression in ocelli and compound eyes.

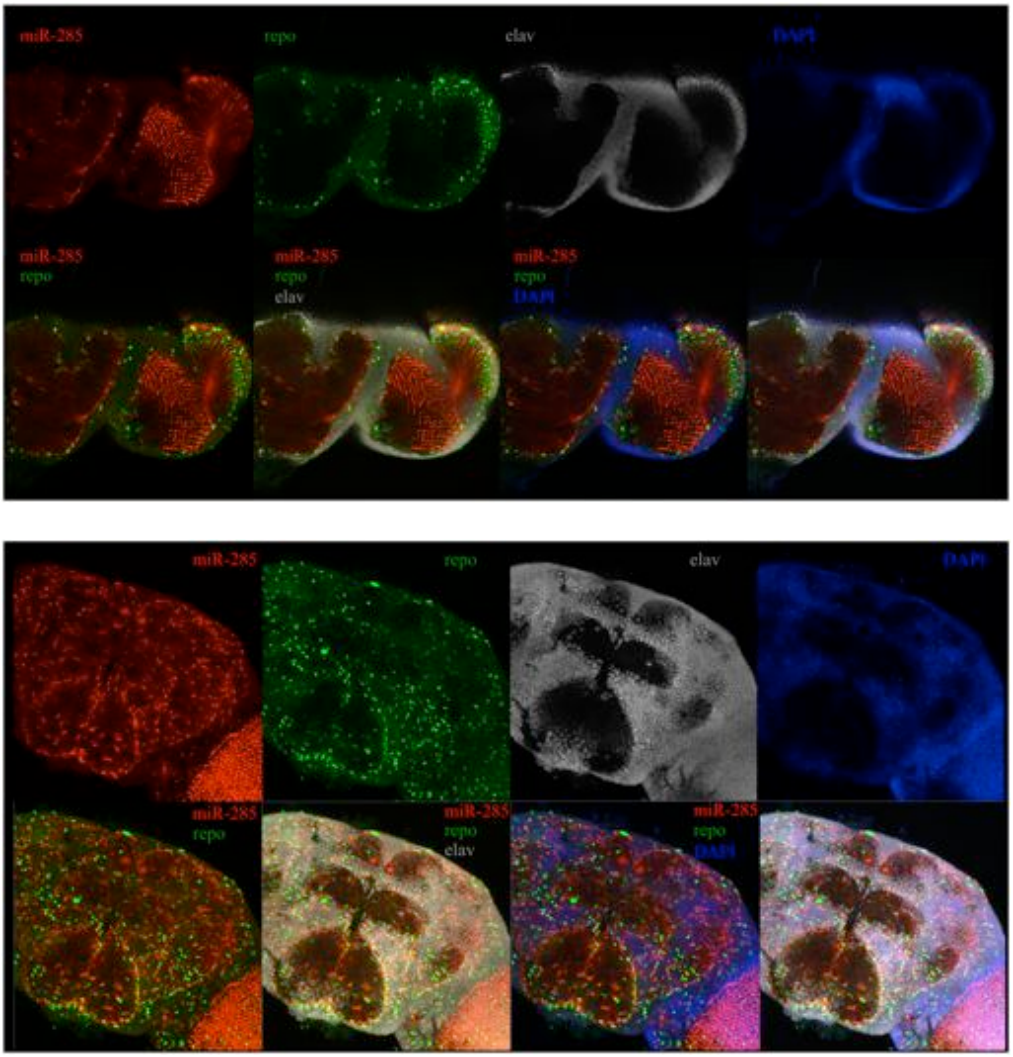

Fig 3.20 Expression of *miR-285* in the adult brain using the promoter-Gal4 driving mCD8-RFP. **Top panel** single plane image of *miR-285* expression in photoreceptors at 20x; **bottom panel** maximum projection image of *miR-285* co-localization with repo (glia) in the central brain at 20x; *miR-285* also co-localizes with a few neuronal cell bodies (elav).

3.5.2 Temporal expression: decline across age

I found that mature *miR-285* expression is age-dependent, and decreases in the head as animals age (Fig 3.21). This age-dependence is sexually dimorphic, and was only observed in males. Females have comparably a much lower abundance (<50% compared to males) of *miR-285* (Fig 3.21). Sequencing data from miRBase also shows a 4 times greater number of reads in male heads as

compared to female heads (http://www.mirbase.org/cgi-bin/get_read.pl?acc=MIMAT0000356).

Interestingly, all the age-related phenotypes are only observed in *miR-285* knockout males, implying that *miR-285* has a specific function at a younger age in males, which comes at a cost of a shorter lifespan.

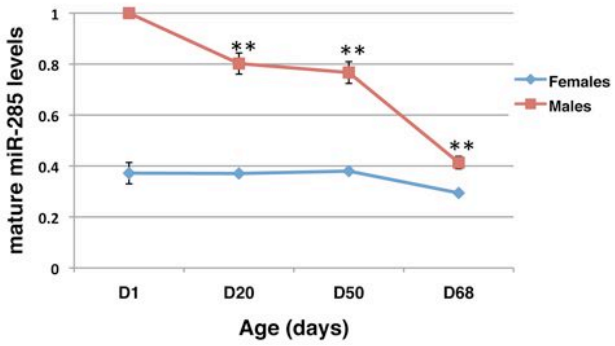

Fig 3.21 Age-dependent decline of *miR-285* expression. *miR-285* miRNA levels in RNA from male and female heads at the indicated ages. Data are normalized to male at day 1; n=4; ** = p<0.01. Error bars represent SD.

3.6 Targets

3.6.1 Unbiased biochemical analyses

To complement computational target predictions, and improve chances of identifying biologically relevant targets, I did two unbiased genome-wide biochemical analyses at the mRNA and the protein levels. Adult heads were the tissue of choice for these experiments, since *miR-285* is highly enriched in adult heads.

3.6.1.1 Microarray

To identify *miR-285* targets, expression profiling was performed using RNA extracted from heads of young mutant and control males. 57 transcripts were upregulated in the mutant by >1.5 fold ($p<0.05$; Fig 3.23a, Table 3.3). 28 of these contained potential *miR-285* target sites as identified using RNAHybrid. Gene Ontology (GO) analysis showed enrichment of genes involved in redox pathways among the upregulated transcripts (Fig 3.22).

Gene	Fold up-regulation	BH	GO Molecular Function
RFeSP	35.148	0.00012	ubiquinol-cytochrome-c reductase activity
CG16713	29.507	0.00021	serine-type endopeptidase inhibitor activity
CG2177	13.074	0.00012	metal ion transmembrane transporter activity
Prx2540-2	12.429	0.00177	thioredoxin peroxidase activity
Actbeta	9.31	0.00006	transforming growth factor beta receptor binding
CG3699	7.516	0.00108	oxidoreductase activity
CG4080	5.772	0.00021	zinc ion binding
CG14798	5.766	0.00013	-
Fbxl4	5.195	0.0003	-
CG17669	4.748	0.00027	-
kdk5	4.492	0.00021	-
CG10924	4.242	0.00021	phosphoenolpyruvate carboxykinase (GTP) activity
CG31704	4.201	0.0003	serine-type endopeptidase inhibitor activity
CG5653	4.13	0.00249	oxidoreductase activity
CG32791	4.121	0.00023	-
CG8193	3.878	0.00023	L-DOPA monooxygenase activity
Cpr50Ca	3.8	0.01103	structural constituent of chitin-based cuticle
Obp56f	3.756	0.0324	odorant binding
CG4650	3.623	0.00237	serine-type endopeptidase activity
Sod3	3.374	0.00179	superoxide dismutase activity
Rh5	3.301	0.00159	G-protein coupled photoreceptor activity
IM10	3.252	0.02952	-
CG8213	3.116	0.00232	serine-type endopeptidase activity
CG16898	2.912	0.03931	transferase activity
Mec2	2.677	0.00237	protein binding
CG4688	2.593	0.00596	glutathione transferase activity
CG16782	2.557	0.02755	-
CG42326	2.524	0.00179	-
Lsp1alpha	2.502	0.04022	nutrient reservoir activity
Pde1c	2.431	0.00346	calmodulin binding
Ance-2	2.428	0.00249	peptidyl-dipeptidase activity
CG14625	2.412	0.01584	-
CG7227	2.393	0.03072	scavenger receptor activity
CG5883	2.379	0.00179	structural constituent of peritrophic membrane
UGP	2.33	0.02462	UTP:glucose-1-phosphate uridylyltransferase activity
simj	2.313	0.00179	protein binding
CG33468	2.311	0.00804	-
CG13130	2.287	0.01821	-
CG1941	2.261	0.01887	transferase activity
CG7173	2.215	0.00596	-
CG4398	2.161	0.00904	-
Rala	2.138	0.00684	GTPase activity
Cpr78Bc	2.066	0.00853	structural constituent of chitin-based cuticle
CG7722	2.04	0.00928	serine-type endopeptidase inhibitor activity
CG7906	2.022	0.0288	-
CG1791	1.952	0.02134	-
CG10178	1.917	0.0211	glucuronosyltransferase activity
CG13594	1.91	0.01186	-
Bmcp	1.817	0.01013	transmembrane transporter activity
tutl	1.791	0.01757	-
CG4593	1.791	0.00596	-
Cyp6a23	1.77	0.01014	electron carrier activity
CG3835	1.679	0.01233	flavin adenine dinucleotide binding
Cyp4p3	1.672	0.01103	electron carrier activity
GIIIspla2	1.667	0.00979	phospholipase A2 activity
mst	1.606	0.01356	-

Table 3.3 Transcripts upregulated in RNA extracted from *miR-285* mutant heads normalized to w^{1118} controls (3 biological replicates). BH represents the adjusted p-values determined using the Benjamini & Hochberg (1995) method.

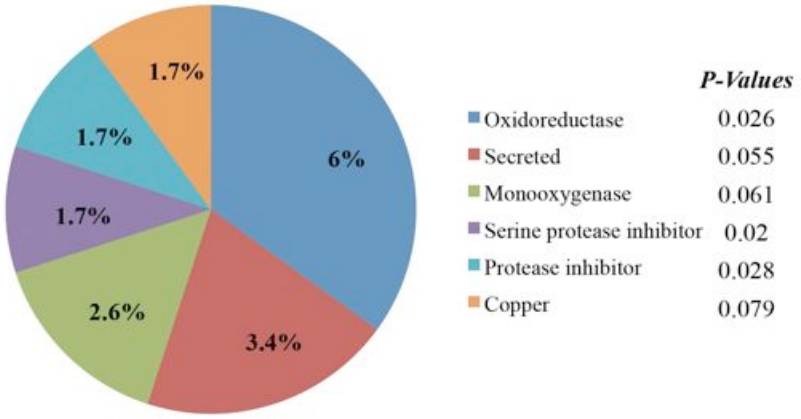

Fig 3.22 Gene Ontology analysis of transcripts that were upregulated >1.5 fold, $p<0.05$ in RNA from *miR-285* mutant heads compared to controls. P-values for GO enrichment are shown above. % indicates the percentage of genes in the catoegory that were upregulated.

3.6.1.2 Proteomics

As a second approach, changes in total head protein levels were compared in mutant and control (w^{1118}) animals using dimethyl dye-swap mass spectrometry. Among ~2500 detectably labeled proteins, 31 were upregulated by >1.5 fold in *miR-285* mutant heads ($p<0.05$; Fig 3.23a, Table 3.4). 12 contained potential *miR-285* sites, based on manual seed complimentarity using RNAHybrid analysis.

Protein IDs	Gene	Fold up-regulation	GO molecular function
A1Z892	Prx2540	13.5	thioredoxin peroxidase activity
B7Z103	CG42323	3.5	-
P07701	Sgs5	3.5	structural molecule activity
Q9VQH2	Duox	3.4	calcium ion binding peroxidase activity
Q6NMY2	CG8343	2.8	mannose binding
Q9VV21	CG4962	2.8	-
Q9U1L2	CG3699	2.8	oxidoreductase activity
Q0E9C3	Sod3	2.6	superoxide dismutase activity
Q9VYX8	CG1572	2.6	-
O97064	Ccp84Ag	2.2	structural constituent of chitin-based larval cuticle
Q9VV13	CG13065	2.2	-
O97059	Ccp84Ab	2.1	structural constituent of chitin-based larval cuticle
Q9V400	Ilk	2.1	protein serine/threonine kinase activity
Q9VT15	CG3088	2.0	serine-type endopeptidase activity
Q5U126	CG34461	2.0	structural constituent of chitin-based cuticle
Q26416	Acp1	1.9	structural constituent of adult chitin-based cuticle
P08570	RpLP1	1.8	structural constituent of ribosome
Q7K511	CG3835	1.8	flavin adenine dinucleotide binding
Q9VZG2	Cpr64Aa	1.8	structural constituent of chitin-based larval cuticle
P23380	Vha16-1	1.8	hydrogen ion transmembrane transporter activity
Q7JZW0	Cpr51A	1.8	structural constituent of chitin-based cuticle
Q9W4W5	CG2680	1.7	4-nitrophenylphosphatase activity
Q0KI21	CG13606	1.7	-
A8DY53	CG30492	1.7	-
Q9VPR1	CG2789	1.7	benzodiazepine receptor activity
Q8IQE9	fd68A	1.7	Mg2+ binding transcription factor activity
Q9VMR6	CG12512	1.7	long-chain fatty acid-CoA ligase activity
Q9VSF0	Atg18	1.6	phosphatidylinositol-3,5-bisphosphate binding
Q9VXR5	CG9281	1.6	ATPase activity, coupled to transmembrane
Q9W1D9	CG3860	1.6	oxysterol binding
Q9V9R3	Ac3	1.6	adenylate cyclase activity
Q09103-3	rdgA	1.6	diacylglycerol kinase activity

Table 3.4 Proteins upregulated in *miR-285* mutant heads normalized to w^{1118} controls. Fold-change data are from four biological replicates, with proteins counted as upregulated >1.5 fold reliably ($p<0.05$) in at least 3 samples.

3.6.2 Working list of targets

The datasets from both the biochemical approaches were processed – genes upregulated >1.5-fold were shortlisted and their transcript sequences were downloaded from FlyBase (http://flybase.org/). *miR-285* mature transcript

sequence was downloaded from miRBase (Griffith-Jones 2006; http://www.mirbase.org/). These sequences were tested for target sites using RNAHybrid (http://bibiserv.techfak.uni-bielefeld.de/rnahybrid/), and analyzed for *miR-285* binding sites both in the 3'UTRs and the ORFs of upregulated genes. Unusually for a miRNA, most of the predicted *miR-285* target sites were found in the open reading frames of the upregulated proteins. The two datasets overlap on 4 genes - *Prx2540-2*, *Sod3*, CG3835 and CG3699; of which *Prx2540-2*, *Sod3* and CG3835 have binding sites for *miR-285* (Fig 3.23a). All 3 of these are involved in redox metabolism. Based on this, I then looked for other upregulated genes (mRNA and protein) involved in redox metabolism. Six shortlisted genes were re-confirmed by quantitative RT-PCR, a more sensitive method for mRNA measurements on RNA isolated from control and *miR-285* mutant male heads (Fig 3.23b).

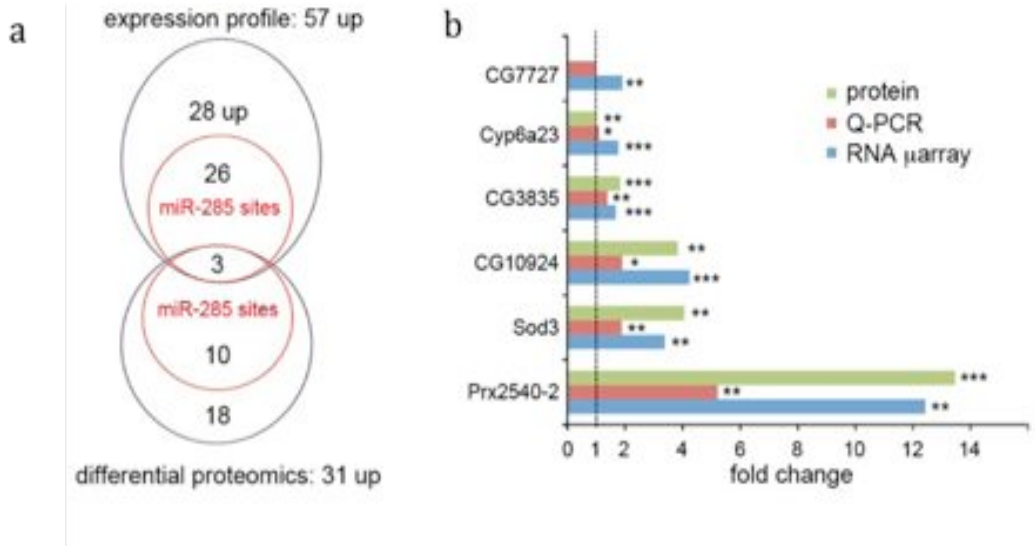

Fig 3.23 a Diagram summarizing transcripts and proteins upregulated in the *miR-285* mutant. Data in Tables 3.1 and 3.2, **b** Upregulation of selected candidate targets. Blue: microarray analysis of RNA from mutant heads, compared to controls. Red: quantitative real time PCR analysis using RNA from mutant heads, compared to controls. Green: proteins measured by differential proteomics.

3.6.2.1 Genetic tests

miRNA repress their targets, therefore there should be a genetic interaction between the putative target and the miRNA. Reduction of expression of putative target genes that are upregulated in the mutant should rescue the mutant phenotypes, and serves as a means of identifying such interactions.

3.6.2.1.1 Locomotor Rescue

I used the *miR-285* Gal4 driver to express UAS-RNAi transgenes to reduce expression of the selected targets in the *miR-285*-expressing cells. Of the 6 genes tested using this strategy, 2 genes showed a significant reduction in locomotor activity (Fig 3.24a): *Sod3* and *Prx2540-2*, both of which are important for reactive oxygen species metabolism. To confirm the efficacy of RNAi, I tested mRNA levels of *Sod3* and *Prx2540-2* using qRT-PCR with RNA from the heads of *Sod3* and *Prx2540-2* RNAi flies (Fig 3.24b). Surprisingly, *Prx2540-2* was reduced upon decreasing *Sod3* while the reverse was not observed. This suggests some influence of Sod3 activity on *Prx2540-2* expression.

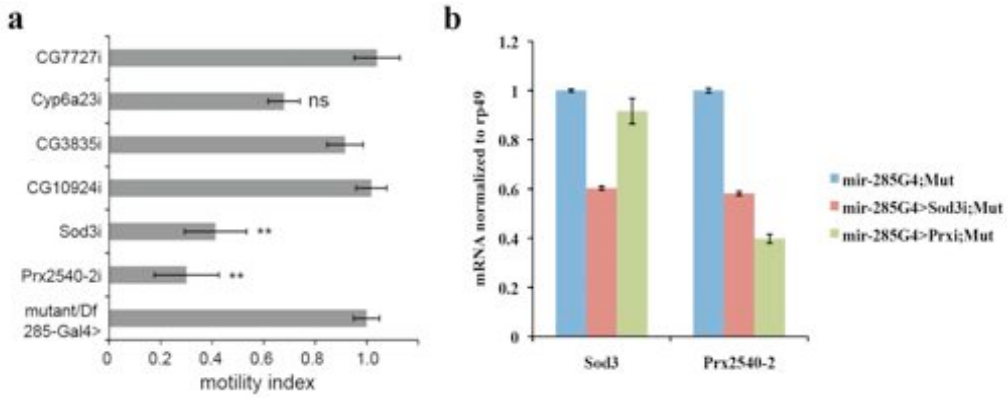

Fig 3.24 a Effect of selective depletion of the candidate targets in *miR-285* expressing cells on locomotor activity. Locomotor activity was normalized to the activity level of the mutant/Df carrying the Gal4 driver, but without RNAi transgenes. **=p<0.01; ns: not significant. **b** Test of RNAi efficacy by qRT-PCR for *Sod3* and *Prx2540-2* in the genotypes shown.

3.6.2.1.2 Lifespan Rescue

Reducing *Sod3* and *Prx2540-2* in the *miR-285* expressing cells also rescued the increased lifespan of the mutants (Fig 3.25a, b). The median lifespan of mutant flies with reduced levels of *Sod3* and *Prx2540-2* was ~7 weeks, similar to that of control flies.

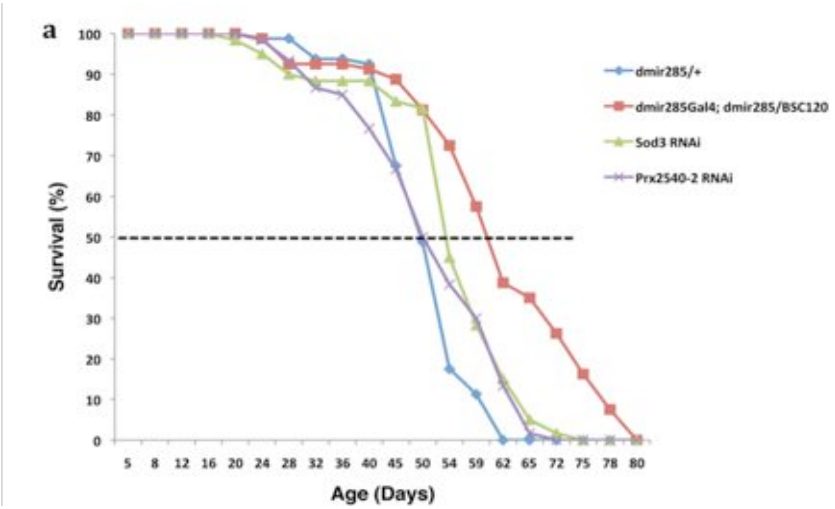

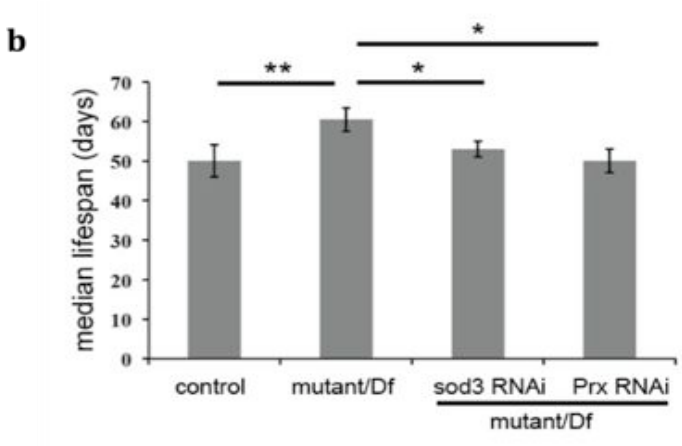

Fig 3.25 Effect of selective depletion of the candidate targets in *miR-285* expressing cells on **a** survival and, **b** median lifespan. Total 180 flies per genotype (3x3x20 flies/vial). *=p<0.05; **=p<0.01.

3.6.2.2 Direct targets of *miR-285* – Luciferase assays

Genetic interactions of *miR-285* with *Sod3* and *Prx2540-2* are consistent with the possibility that *miR-285* directly regulates their expression, as is the observation that *Sod3* and *Prx2540-2* have *miR-285* binding sites in their coding regions. To test direct regulation, I cloned the full-length endogenous coding sequences of the two genes downstream of the firefly luciferase gene, using them as artificial 3'-UTRs in an S2 cell-based assay. These reporters should show decreased luminescence when *miR-285* is also expressed, if there is direct regulation. At the same time, I cloned the same sequences with mutated binding sites to disrupt *miR-285* binding (Fig 3.26a, c). For *Sod3*, the magnitude of down-regulation of luciferase activity was small, but statistically significant, and was lost in the construct where the site was mutated to disrupt seed pairing (Fig 3.26b). Down-regulation of the *Prx2540-2* reporter was greater and also was statistically significant, and was lost in the construct where the site was mutated to disrupt seed pairing (Fig 3.26d). Together, these

results show that the sites in *Sod3* and *Prx2540-2* CDS are directly regulatable by *miR-285*.

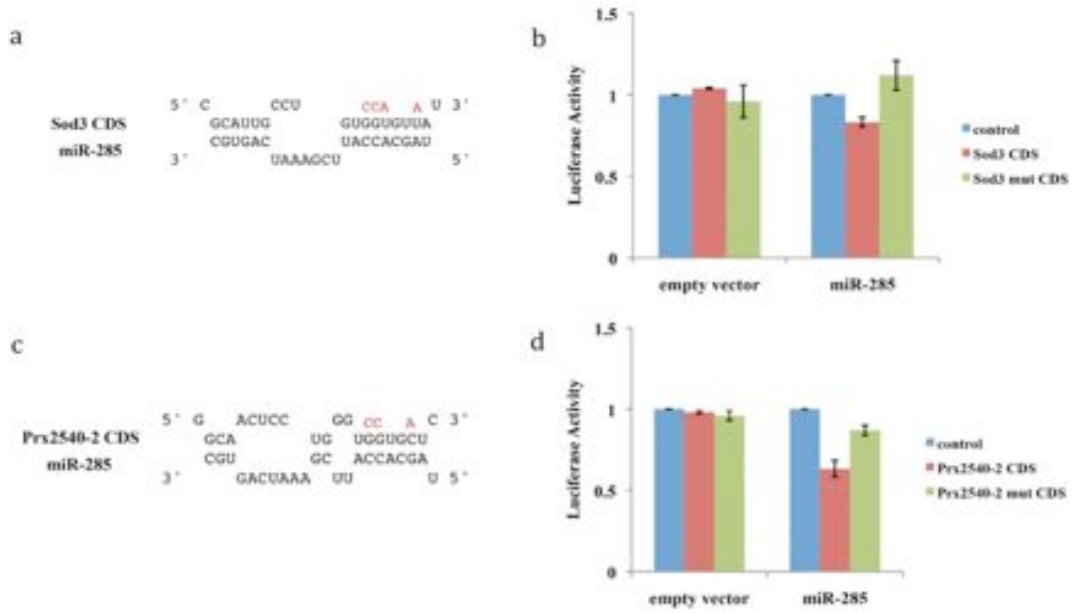

Fig 3.26 a Predicted *miR-285* target site in the ORF of *Sod3*. The site shows extensive seed pairing, but contains 2 G:U base pairs. Residues shown in red were mutated to disrupt seed pairing for the luciferase assay. **b** Luciferase reporter assay to test regulation of the *Sod3* sites by *miR-285* (comparing *Sod3* CDS with the luciferase control, p=0.037 using two-tailed unpaired Student's t-test) **c** Predicted *miR-285* target site in the ORF of *Prx2540-2*. The site shows 7-mer seed pairing. Residues shown in red were mutated to disrupt seed pairing for the luciferase assay. **d** Luciferase reporter assay to test regulation of the *Prx2540-2* site by *miR-285* (comparing *Prx2540-2* CDS with the luciferase control, p=0.0009 using two-tailed unpaired Student's t-test). All data represent the average of at least three biological replicates. Error bars: standard deviation.

3.7 The reactive oxygen species pathway

Sod3 and *Prx2540-2* are both members of the reactive oxygen species pathway.

3.8 Reactive Oxygen Species and *miR-285*

The functional targets encode enzymes involved in metabolism of reactive oxygen species (ROS). *Sod3* encodes an extracellular copper/zinc superoxide dismutase (Jung et al., 2011) that converts extracellular superoxide anion (O_2^-) to hydrogen peroxide (H_2O_2). H_2O_2 readily enters the cell where it can be metabolized by peroxiredoxin, a cytosolic thioredoxin peroxidase enzyme encoded by *Prx2540-2* (Fig 3.27). The *miR-285* mutant exhibited elevated superoxide dismutase activity, which could be partially corrected by restoring miRNA expression in the mutant background (Fig 3.28). Duox, a third enzyme involved in extracellular superoxide metabolism, encodes a transmembrane protein with NADPH oxidase activity that produces extracellular superoxide anion. Although d*Duox* transcript lacks *miR-285* target sites, a *miR-285* site was found in the coding sequence of its maturation factor Mol, the ortholog of DuoxA. *mol* and d*Duox* mRNA levels were increased in the mutant, along with *Sod3* and *Prx2540-2* (Fig 3.29). Thus, multiple enzymes involved in production and metabolism of ROS are upregulated in the *miR-285* mutant, both as direct and indirect consequences.

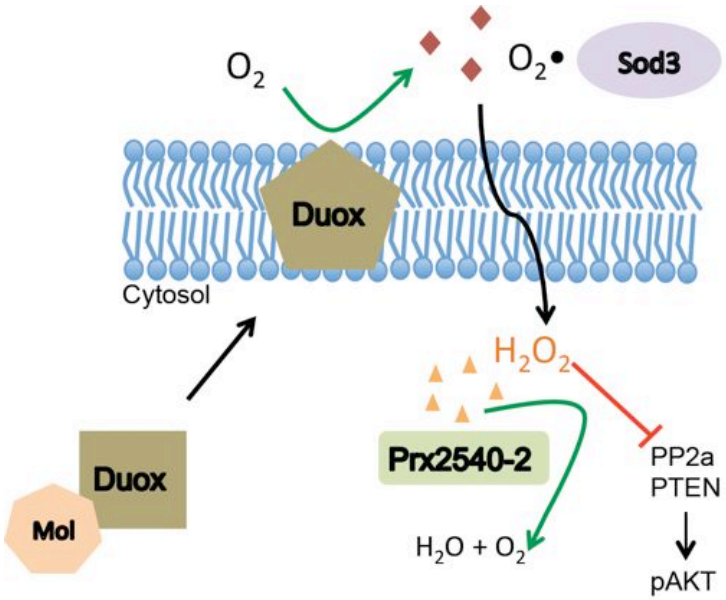

Fig 3.27 Schematic of the enzymes involved metabolism of extracellular superoxide. Duox is a transmembrane NADPH oxidase that produces anionic superoxide. O_2^- Is catabolized by extracellular *Sod3* into H_2O_2 and water. H_2O_2 diffuses freely across the plasma membrane and is converted to molecular oxygen and water in the cytoplasm by Thioredoxin peroxidase, *Prx2540-2*. Mol is an ER-resident transmembrane maturation factor for Duox.

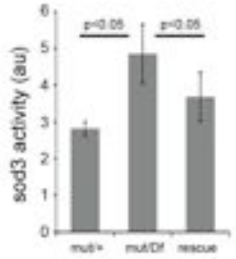

Fig 3.28 Superoxide dismutase activity (in arbitrary units) measured in lysates of adult heads from flies of the indicated genotypes. Error bars represent SD.

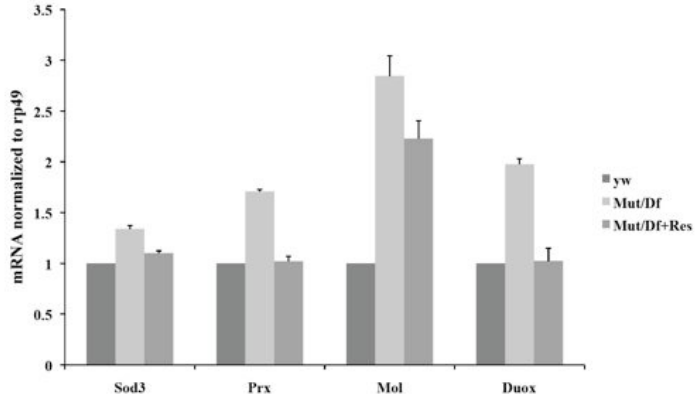

Fig 3.29 mRNA levels of *mol, Duox Prx2540-2* and *Sod3* measured by quantitative real time PCR in RNA isolated from heads of *yw* control flies, *miR-285* mutants (knock-out/*Df(3L)BSC120*) and rescued mutant flies carrying one copy of the rescue transgene. Data represent the average of three biological replicates and 3 technical replicates each. Error bars: standard deviation. $p<0.05$ for mut/Df compared to yw, and rescue (Student's t-test).

3.8.1 Target levels increase with age

Since *miR-285* expression decreases with age, I wanted to test if wild type flies show an age-dependent increase in the target genes. Fig 3.30 shows qRT-PCR data using RNA from w^{1118} heads. There is a modest increase in *Sod3* and *Prx2540-2* levels in older flies; however, levels of mol and dDuox remain largely unchanged.

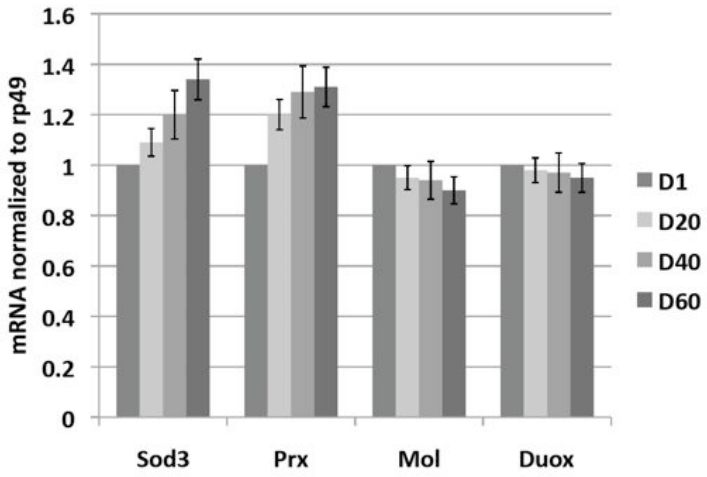

Fig 3.30 Age-dependent change in ROS gene expression. Graph shows *Sod3*, *Prx2540-2* (Prx), mol and Duox expression levels in w1118 head RNA as a function of age at 1-day, 20-, 40- and 60-days of age. Error bars represent standard deviation.

3.8.2 ROS signaling in the *miR-285* mutant

Although excess ROS can cause oxidative damage, at physiological levels ROS play important roles as modulators of signal transduction pathways. One mechanism by which ROS act involves oxidation of catalytically important cysteine residues in phosphatases, such as PTEN and PP2A (Leslie, 2006).

ROS-mediated reduction of PTEN and PP2A activity can lead to increased levels of AKT phosphorylation (Coant et al., 2010; Naughton et al., 2009). I observed an increase in AKT phosphorylation in the *miR-285* mutant, which was restored toward normal by RNAi mediated depletion of either *Sod3* or *Prx2540-2* in *miR-285*-expressing cells (Fig 3.31a). Expression of the FOXO target *4E-BP* was reduced (Fig 3.31b), consistent with an increase in AKT activity leading to reduction of nuclear FOXO activity (Teleman et al., 2008). Other known regulators of AKT were not altered in the mutant mRNA and proteome analyses. These observations suggest that coordinated increase in the expression of *mol*/*Duox*, *Sod3* and *Prx2540-2* leads to an increase in ROS signaling via the AKT pathway.

Elevated ROS signaling may provide an explanation for the hyperactive phenotype that I observed in the *miR-285* mutant. Treatment of flies with low levels of H_2O_2 has been reported to induce locomotor activity (Grover et al., 2009). Superoxide dismutase over-expression has also been reported to induce greater locomotor activity and higher walking speeds, especially in older flies (Martin et al., 2009; Parkes et al., 1998; Phillips et al., 2000; Spencer et al., 2003).

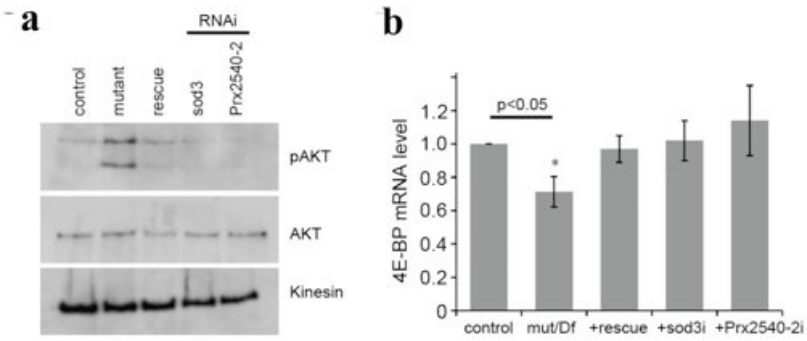

Fig 3.31 a Immunoblot showing total Akt levels and activated Akt detected by antibody specific to phosphorylated S505. *miR-285* knock-out mutants were used in trans to a wild-type copy of *miR-285* as controls in this and subsequent figures unless otherwise indicated. Mutant/Df indicates the knock-out allele in trans to *Df(3L)BSC120* which uncovers the *miR-285* locus; rescue indicates the mutant/Df combination carrying one copy of the genomic rescue transgene. RNAi indicates the UAS-RNAi transgene expressed under *miR-285 Gal4* control in the *miR-285* mutant background. Antibody to Kinesin was used to control for loading. **b** 4E-BP transcript levels measured by quantitative real time RT-PCR in RNA isolated from heads of the indicated genotypes. +rescue indicates mutant with a rescue transgene; +*Sod3*i or +*Prx2540-2*i indicate mutant expressing the UAS RNAi transgene under *miR-285 Gal4* control.

3.8.3 Oxidative stress and ROS turnover in the *miR-285* mutant male

The elevated expression of enzymes involved in ROS metabolism prompted me to ask whether *miR-285* mutants might be protected from oxidative damage. Large amounts of H_2O_2 are lethal to flies and they die quickly within hours. However, *miR-285* mutants survived significantly longer (median survival ~50 hours) than control flies (median survival ~32 hours) on medium containing 5% H_2O_2 (Fig 3.32). Sensitivity to H_2O_2 was restored toward normal by depletion of *Sod3* or *Prx2540-2*. This protection from oxidative stress likely results from increased levels of ROS scavenging enzymes in the mutant, thus, increasing total ROS turnover (Fig 3.29).

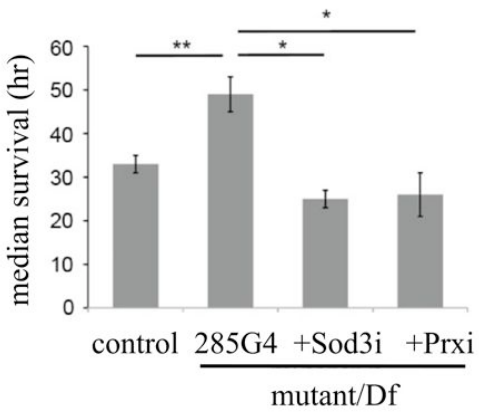

Fig 3.32 Oxidative stress assay. Median survival (hours) of flies on food containing 5% H_2O_2. 285G4 +*Sod3*i or +*Prx2540-2*i indicate mutant/Df expressing the UAS RNAi transgene under *miR-285 Gal4* control. n = 20 flies/replicate/genotype. Error bars represent standard error.

3.9 Male-specific function of *miR-285*

Male flies lacking *miR-285* show improved resistance to oxidative stress, extended lifespan and reduced age-progressive decline in performance of various behavioral tasks. The presence of the miRNA therefore seems to impair male fitness while having little effect on females. This apparent conundrum prompted me to look for defects that might be associated with the absence of the miRNA. *miR-285* is expressed at higher levels in young adult males and its level declines with age (Fig 3.21). Expression in female flies is relatively constant with age, and similar in appearance to older males. Female *miR-285* mutant flies exhibit normal lifespan and performance in behavior assays. Presumably, having the miRNA provides some benefit to young males to offset the obvious costs that its activity causes in later life.

To study this aspect, I explored phenotypes specific to males. I did not observe any outward morphological abnormalities in the *miR-285* mutant males. Since *miR-285* is predominantly expressed in the male brain, I examined several aspects of male behavior to get clues about function of the miRNA. *Drosophila* male courtship behavior is a hard-wired stereotypical behavior. When a male is paired with a virgin female, the male performs a series of behaviors, which require multi-modal sensory processing, mainly from visual, olfactory and gustatory cues. Mutant males paired with wild type females did not show an obvious defect in mating behavior. Overall performance,

measured by the time taken to initiate courtship, was faster than control males (Fig 3.33). This appears to be consistent with the overall higher activity level in the young mutant males.

However, when female flies were provided with a choice between a *miR-285* mutant male and a CS control male, the females copulated with the control male in ~2/3 of encounters (Fig 3.34a). The females' ability to discriminate between the control and mutant males was statistically significant (p=0.013, Fisher's exact test). Female discrimination between control and rescued mutant males was not significant (p= 0.75). Next, I asked whether depletion of the targets *Sod3* and *Prx-2540-2* in the *miR-285* mutant background would affect mate choice. Females were able to discriminate between control males and the *miR-285* mutant carrying the *miR-285 Gal4* transgene (Fig 3.34b; p=0.038). Depletion of *Sod3* in the mutant background by *miR-285 Gal4* driven expression of the *Sod3* UAS-RNAi transgene had little effect, but depletion of *Prx-2540-2* reduced the difference between mutant and control males. Females did not significantly distinguish between control males and mutant males with *Prx-2540-2* depleted (p=0.28).

Overall, *miR-285* functions to keep males in the mating competition, at the cost of a shorter life and impaired motor fitness.

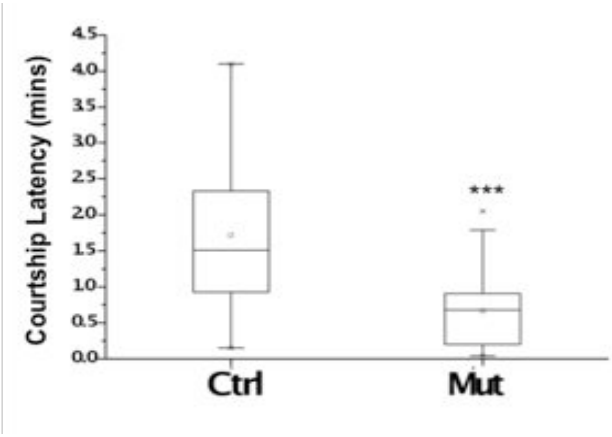

Fig 3.33 Boxplot of courtship latency showing time to initiate courtship by control (mutant/+) and mutant males towards CS virgin females. Mann-Whitney U_a=161, p<0.0001. Error bars represent data maxima and minima.

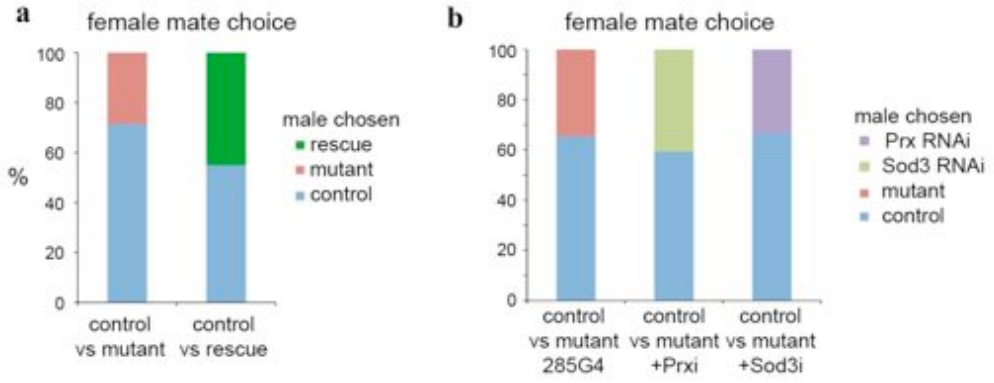

Fig 3.34 a Preference of CS females in a female mate choice assay between control vs mutant males and control vs rescue males. **b** Preference of CS females in a female mate choice assay between control vs mutant males carrying the *miR-285-Gal4* transgene. +*Sod3*i or +Prxi indicate mutant expressing the UAS RNAi transgene under *miR-285 Gal4* control.

3.10 Sex-specific expression of *miR-285*

The sex-specific difference in miR-285 expression levels prompted me to ask if this expression is dependent upon the sex-determining pathway. Many genes show soma-biased sex-differential expression in adult flies (Goldman and Arbeitman, 2007), dependent upon FRU^M (fruitless), a male-specific transcription factor (Manoli et al., 2005). *miR-285* expression also showed

reduction in *fru P1* males, which lack FRU^{M} (Fig 3.35), suggesting that it is under the control of sex-determining genes. *Sod3* and d*Duox* also show sex-specific expression levels, being higher in males, reflecting the stronger male-specific transcriptional silencing by *miR-285* (Fig 3.36).

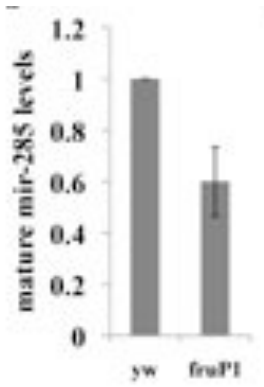

Fig 3.35 *miR-285* expression is partially dependent on sex-determination pathway via *fruitless*. mature *miR-285* levels normalized to U14 in the fru^{P1} fruitless mutant. Error bars represent SD.

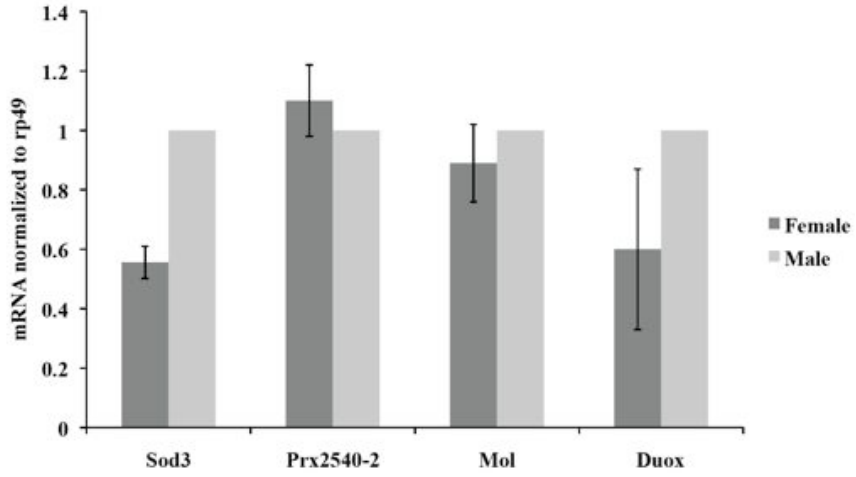

Fig 3.36 Sex-differential expression of *Sod3, Prx2540-2*, d*Duox* and *mol.* Expression levels of the ROS pathway genes in male and female w1118 heads. Error bars represent SD.

3.11 Deep psuedopupil phenotype is being partially mediated by ROS

This thesis presents my work in a chronological order, and thus after identifying *Prx2540-2* and *Sod3* as bona fide targets of *miR-285* in the context

of lifespan and locomotion, I wondered if upregulation of the same targets was responsible for the age-dependent loss of deep psueodpupil, which results from disorganization of the photoreceptors in the eye. Deep psuedopupil loss was partially suppressed by reducing *Sod3* and *Prx2540-2* expression by RNAi in both males and females under normal conditions of light/dark (Fig 3.37). The partial suppression could very well be because of incomplete reduction of gene expression by RNAi (Fig 3.24b). Alternatively, there could be additional targets regulated by *miR-285*, which might be important for this phenotype.

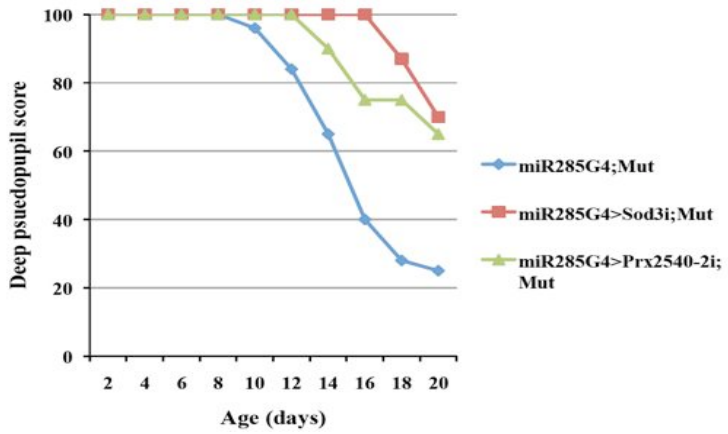

Fig 3.37 Deep psuedopupil score (%flies having deep psuedopupil) of flies with RNAi-mediated depletion of *Sod3* and *Prx2540-2* in the *miR-285* mutant.

Chapter 4 Discussion

4.1 Reactive oxygen species

Reactive oxygen species is a collective term that describes chemical species that are formed upon incomplete reduction of oxygen and includes the superoxide anion (O_2^-), hydrogen peroxide (H_2O_2) and the hydroxyl radical ($HO^{\cdot}$). Most reactive oxygen species (ROS) are generated as natural by-products of the mitochondrial electron transport chain. In addition, ROS are formed as necessary intermediates of metal catalyzed oxidation reactions in peroxisomes and the endoplasmic reticulum. In phagocytic cells, ROS production is stimulated by the presence of pathogens, and is catalyzed by the action of NADPH oxidase, a multicomponent membrane bound enzyme complex, and is necessary for the bactericidal action of phagocytes (Babior et al., 1973). NOX2 was identified as the catalytic subunit of this complex. To date five NOX isoforms and two related enzymes DUOX1 and DUOX2 have been discovered in mammals. *Drosophila* functional orthologs are d*Nox* (NADPH oxidase) and d*Duox* (Dual oxidase) – both are highly homologous but d*Duox* has an additional peroxidase domain that can produce H_2O_2. In recent years, it has been reported that O_2^- is produced in non-phagocytic cells as well such as vascular muscle cells and gastrointestinal epithelial cells in a NOX/DUOX dependent manner. In *Drosophila*, d*Duox* has been reported to function in the mucosal barrier epithelia, producing ROS to combat pathogens (Ha et al., 2009; Ha et al., 2005). There are studies that report their expression in other tissues too, including the brain (Katsuyama et al., 2012).

Cells have endogenous systems to deal with these free radicals in the form of antioxidant enzymes like superoxide dismutases, which can convert superoxide anions into hydrogen peroxide that is detoxified into water and molecular oxygen by catalases and peroxidases. Cells also employ non-enzymatic small molecule antioxidants like glutathione, vitamin C, and vitamin E to detoxify free radicals.

4.2 Good ROS, Bad ROS

Reactive oxygen species were initially identified as having toxic effects on physiology – the first traceable paper reported deleterious effects of hydrogen peroxide on brain tissue (Mann and Quastel, 1946). Indeed, high concentrations of ROS are harmful, causing DNA damage, lipid peroxidation, and harmful protein oxidation. ROS also stands at an important position with respect to aging – Denham Harman proposed the free radical theory of aging in 1956, stating that organisms age because cells accumulate oxidative damage during their lives. Consistent with this theory, flies lacking antioxidant enzymes can shorten lifespan, and reducing oxidative damage in yeast and *Drosophila* can extend lifespan (Fontana et al., 2010) (Martin et al., 2009; Parkes et al., 1998; Phillips et al., 2000; Spencer et al., 2003). However, there are studies in *Drosophila* and mice, where over-expression of antioxidant enzymes did not show any effect. Also, in *C. elegans*, deletion of mitochondrial SOD2 can extend lifespan, but deleting all the 5 SOD genes has no effect on lifespan suggesting antagonistic effects among the homologs (Van Raamsdonk and Hekimi, 2009, 2012). Therefore while there is evidence that supports the free radical theory of aging, the question whether reducing

oxidative damage below normal levels is sufficient to extend lifespan is rather contentious.

Since the discovery of NOX-mediated superoxide production, the view of ROS being only harmful has changed. Recent work has shown that ROS can modulate diverse physiological functions beyond innate immunity, such as the biosynthesis of thyroid hormones, cellular signaling, gene expression, cellular growth and death (reviewed in Bedard and Krause, 2007; D'Autreaux and Toledano, 2007). Of all the free radical species, H_2O_2 fulfills two criteria to be a second messenger – first, it is enzymatically produced and degraded, providing spatio-temporal specificity; second, it has the ability and specificity for thiol oxidation on proteins such as phosphatases, thus triggering downstream signaling (Forman et al., 2010). Additionally, it is relatively stable with a half-life of ~1ms and steady state levels ~10^{-7} M. Diffusion of H_2O_2 can be modulated by changes in membrane permeability or by aquaporin-mediated transport. Overall, stability, controlled production, selective reactivity and diffusivity make H_2O_2 fit for signaling, and it is produced in almost all cell types (Finkel, 2011). Signaling occurs by oxidation of cysteine residues in phosphatases, such as PTEN and PP2A (Leslie, 2006).

4.3 NADPH oxidase – generated ROS and the brain

There are a few studies that investigate the endogenous role of ROS in neuronal development, physiology and function. Evidence is accumulating pointing towards a role for ROS produced by NADPH oxidases in cell-signaling functions in CNS modulating neuronal differentiation (Tsatmali et

al., 2006). Another recent study showed that high ROS levels promote neural stem cell renewal and neurogenesis in mice (Le Belle et al., 2011). ROS have also been demonstrated to have some roles for synaptic activity, learning, memory and long term potentiation (Gahtan et al., 1998; Hu et al., 2007; Kishida et al., 2006; Massaad and Klann, 2011; Milton and Sweeney, 2012; Thiels and Klann, 2002; Thiels et al., 2000). Most of these studies provide a role for ROS produced by NOX enzymes, whose expression in CNS is well established (Knapp and Klann, 2002). In contrast, DUOX enzymes are not well understood in the neuronal context. There is some evidence that DUOX have roles in astrocytes upon stress induction such as ischemia and osmotic stress (Reinehr et al., 2007)**.** In *Drosophila*, d*Nox* has been shown to have a role in smooth muscle (Ritsick et al., 2007) and d*Duox* in host defense (Ha et al., 2009; Ha et al., 2005; Razzell et al., 2013) – their role in the brain is largely unexplored.

4.4 Maintaining the right level of ROS activity in the brain

Of all the genes tested in this study, *Prx2540-2* and *Sod3* were found to behave as functional targets mediating activity of the microRNA. Depletion of these genes suppressed the increased locomotor activity and lifespan of the mutants. *Prx2540-2* and *Sod3* are both genes involved in ROS metabolism. Increased expression of two enzymes in the same pathway suggests an overall increase in ROS turnover. In addition to these ROS scavengers, d*Duox*, an NADPH oxidase and *mol*, d*Duox* maturation factor, are also upregulated indirectly in the mutants, also consistent with an increased flux of ROS signaling. miRNAs function to regulate the robustness of cellular processes,

and to maintain balance in gene expression. This study suggests that *miR-285* functions to balance superoxide production and breakdown, because a direct increase in superoxide breakdown is being offset by an indirect increase in superoxide production via *Duox* in the mutants.

The concerted action of *miR-285* to regulate multiple members of the extracellular ROS pathway suggests that fine-tuning of ROS signaling is needed to mediate appropriate CNS function. Cytoplasmic NADPH oxidase (Nox)-generated-H_2O_2 plays a key role as a mediator of growth factor signaling during neuronal stem cell proliferation and neurogenesis, as well as supporting cell survival (Dickinson et al., 2011). In mammals, cytoplasmic Nox enzymes are a source of brain ROS implicated in seizures and neurodegeneration (Bedard and Krause, 2007; Lambeth, 2004). Specific roles of the plasma membrane d*Duox* enzyme and extracellular ROS in the CNS are less well studied. Failure to maintain an appropriate level of extracellular ROS activity by *miR-285*-expressing cells of the young male brain leads to reduced reproductive success, presumably through subtle alterations in behavior.

4.5 The ROS theory of aging

Discovering the biological basis of aging is an important remaining challenge in science. A long-standing assumption is that aging occurs due to wear and tear, and molecular and cellular damage by free radicals has long been thought to be a causative agent. However, since the discovery of beneficial roles of ROS signaling, the question of whether free radicals are ‘friends or foes’, or both, is being reassessed. Recently, this theory has come under serious

question because of evidence from *C. elegans* (Gems and Doonan, 2009; Van Raamsdonk and Hekimi, 2009, 2012). However, studies from flies and mice are still supportive of this theory of aging (Liochev, 2013).

Young male *Drosophila* have higher *miR-285* levels, hence a reduced level of ROS signaling. This seems to impair male attractiveness, suggesting a normal role for ROS in CNS functions related to courtship success. As males age, *miR-285* levels reduce, increasing the ROS signaling, and possibly ROS turnover – just as in the *miR-285* mutant. This mechanism might help deal with the age-increasing oxidative damage in the CNS. This study adds onto the body of evidence that reports increases in lifespan in *Drosophila* by over-expression of ROS scavengers. Additionally, this work shows that an endogenous miRNA-mediated mechanism exists to increase ROS scavenger levels in biological systems in an age-dependent manner.

4.6 Function and significance of *miR-285* in male *Drosophila*

The presence of *miR-285* sites in the coding sequences of three separate proteins involved in extracellular ROS metabolism suggests that this regulation has been selected for during evolution. As a consequence, male flies lacking *miR-285* show improved resistance to oxidative stress, extended lifespan and reduced age-progressive decline in performance of various behavioral tasks. Hyperactive locomotor behavior can be considered a potential evolutionary disadvantage because hyperactive, longer-lived flies would likely consume more resources, and would need to forage better.

However, the presence of the miRNA seems to impair only male fitness while having little effect on females.

This conundrum is resolved by the finding that *miR-285* knockout males are less attractive to females in the context of mating. In a natural setting, where competition for mate choice is expected, *miR-285* mutant males would likely be at a disadvantage. Thus, the activity of the miRNA in promoting reproductive success in the young male appears to provide a selective advantage that has outweighed the cost of accelerated impairment of CNS function later in life. These effects appear to be mediated through regulation of ROS metabolism, though there may also be other *miR-285* targets mediating this subtle behavior. The question of why the mutant male is less attractive to the female remains to be addressed – it could have defects in courtship song production, or its pheromonal profile. It is also possible that hyperactivity itself might be acting as a 'mating deterrent'.

Lifespan is unlikely to be under direct selective pressure unless it interferes with the reproductive potential of the organism. There is a growing body of evidence that **s**ignals from the gonad affect lifespan in *C. elegans* and *Drosophila* through modulation of the insulin-signaling pathway (Arantes-Oliveira et al., 2002; Flatt et al., 2008; Hsin and Kenyon, 1999). These have recently been linked to function of the heterochronic miRNA *let-7*, in the nematode (Shen et al., 2012). This study provides evidence for a different type of link between reproduction and lifespan: selection for reproductive success, through miRNA mediated modulation of ROS metabolism in the brain, which comes at a cost in terms of aging and lifespan.

4.7 Function of *miR-285* in glia

miR-285 co-localizes largely with glial markers in the brain, and *miR-285* repression in glia using a sponge transgene could reproduce lifespan extension as observed in *miR-285* mutant males, indicating functional association of *miR-285* and glia. It would be interesting to explore the exact nature of these glia, and the cellular function of the miRNA in them. *miR-285* expressed in glia in the central brain is able to control male behavioral output of altered locomotion and mate attractiveness, which is directed by neurons. It is tempting to hypothesize that *miR-285* could be mediating communication between glia and neurons by transmitting signals to neurons via changes in gene expression profiles in glia. Morphologically, astrocytes associate closely with neurons – they are abundant in the cortex, they surround synaptic terminals, are interconnected via gap junctions and modulate neuronal activity by releasing neurotransmitters (Alvarez-Maubecin et al., 2000; Ventura and Harris, 1999) (Fields and Stevens-Graham, 2002). Thus it is possible that *miR-285* mediates communication by extracellular ROS production. Interest has been growing in the potential roles of ROS signaling in the developed brain in recent years - ROS have been demonstrated to have some roles for synaptic activity, learning, memory and long term potentiation (Gahtan et al., 1998; Hu et al., 2007; Kishida et al., 2006; Massaad and Klann, 2011; Milton and Sweeney, 2012; Thiels and Klann, 2002; Thiels et al., 2000). There is some evidence that DUOX have roles in astrocytes upon stress induction such as ischemia and osmotic stress (Reinehr et al., 2007)**.** It is interesting to note that

miR-29a, the vertebrate homolog of *miR-285*, is enriched in astrocytes, and was recently shown to prevent ROS accumulation in primary mouse astrocytes under glucose deprivation (Ouyang et al., 2013). This exciting finding points to probable functional conservation of the *miR-285/miR-29* family in astrocytes, which remains to be tested.

4.8 Sexual dimorphism of *miR-285*

The sexual dimorphism observed in *miR-285* expression is interesting. Due to this peculiar expression pattern, there are some phenotypes common to both sexes, and some only restricted to males. While aberrant lifespan, locomotor and mating behaviors are only observed in males, the deep psuedopupil phenotype does not show this gender bias - both males and females exhibited it. Additionally, locomotor activity itself has been shown to have sexually dimorphic features. Female flies constantly adjust their activity pattern whereas males usually show a steadier, walking pace (Gatti et al., 2000). Taken together, these suggest that perhaps *miR-285* might also function to steady the male locomotion behavior by suppressing ROS signaling. This possibility remains to be tested.

4.9 ROS targets in the context of deep pseudopupil

Prx2540-2 and *Sod3* were able to partially suppress the deep pseudopupil phenotype observed in both mutant males and females. This indicates that elevated *Sod3* and *Prx2540-2* levels impair visual function in the animal, and the miRNA limits this. Increased oxidative signaling is known to be harmful to cellular integrity. The defect is exacerbated by light, suggesting that it is

dependent on the visual signal transduction pathway. Oxidative damage appears to be a byproduct of rhodopsin-mediated photo-activation (Wiegand et al., 1983), because animals lacking functional rhodopsin are resistant to oxidative damage (Grimm et al., 2000). *miR-285* appears to act by protecting against such ROS damage.

It is interesting that *miR-285* is highly enriched in the photoreceptors, and that *norpA* deletion can rescue the deep pseudopupil phenotype. *norpA* is a phospholipase C, which gets activated by a G-protein coupled receptor, and is expressed in the photoreceptors and the gut. In the photoreceptors, light is the activating trigger, whereas microbes activate *norpA* in the gut epithelia. There is evidence that *norpA* activates d*Duox* to produce ROS in the gut (Ha et al., 2009). It is possible that they function similarly in the photoreceptors – *miR-285* keeps ROS signaling low in the eye, failing which, leads to the cellular dismorpholgy that is reflected by loss of deep pseudopupil.

In this context, it is really remarkable that the signaling between photoreceptors and laminar neurons is intact, even though the deep pseudopupil disappears in the mutants in a light-dependent manner. As a simple assay for visual function, I measured the male mutant flies' ability to locate a wild type female in the dark. Functionally blind males take much longer to locate the female, and typically trace a distinct zigzag path towards the female (Krstic et al., 2009). However, *miR-285* mutant males did not show any such disadvantage in locating the females in dark conditions (data not shown). It is still possible that there is some effect at higher visual centers,

which is reflected in the disappearance of the deep pseudopupil. Fruit flies require complex coordination between visual processing and motor output centers for steering flight courses (McCann and MacGinitie, 1965). Optomotor response is a useful measure of such higher order processing, and it would be interesting to test optomotor performance of *miR-285* mutants as readout for visual function.

4.10 Conclusions and Future Work

Overall, this work explores the role of *miR-285* in neural physiology and behavior. The aspect of *miR-285* functioning to impart precision to courtship at the cost of a shortened lifespan and reduced general fitness is novel and interesting. The question of why the mutant male is less attractive to the female remains to be addressed – there could be several potential reasons, concerning male behavior or its pheromonal profile. Also, since the ROS genes-mediated rescue of the male rejection is only partial, it is very likely that other targets are acting to modulate mate-choice behavior.

REFERENCES

Agostini, M., Tucci, P., Killick, R., Candi, E., Sayan, B.S., Rivetti di Val Cervo, P., Nicotera, P., McKeon, F., Knight, R.A., Mak, T.W.*, et al.* (2011). Neuronal differentiation by TAp73 is mediated by microRNA-34a regulation of synaptic protein targets. Proc Natl Acad Sci U S A *108*, 21093-21098.

Alvarez-Maubecin, V., Garcia-Hernandez, F., Williams, J.T., and Van Bockstaele, E.J. (2000). Functional coupling between neurons and glia. J Neurosci *20*, 4091-4098.

Arantes-Oliveira, N., Apfeld, J., Dillin, A., and Kenyon, C. (2002). Regulation of life-span by germ-line stem cells in Caenorhabditis elegans. Science *295*, 502-505.

Babior, B.M., Kipnes, R.S., and Curnutte, J.T. (1973). Biological defense mechanisms. The production by leukocytes of superoxide, a potential bactericidal agent. J Clin Invest *52*, 741-744.

Baek, D., Villen, J., Shin, C., Camargo, F.D., Gygi, S.P., and Bartel, D.P. (2008). The impact of microRNAs on protein output. Nature *455*, 64-71.

Bail, S., Swerdel, M., Liu, H., Jiao, X., Goff, L.A., Hart, R.P., and Kiledjian, M. (2010). Differential regulation of microRNA stability. RNA *16*, 1032-1039.

Bak, M., Silahtaroglu, A., Moller, M., Christensen, M., Rath, M.F., Skryabin, B., Tommerup, N., and Kauppinen, S. (2008). MicroRNA expression in the adult mouse central nervous system. RNA *14*, 432-444.

Bartel, D.P. (2009). MicroRNAs: target recognition and regulatory functions. Cell *136*, 215-233.

Bartel, D.P., and Chen, C.Z. (2004). Micromanagers of gene expression: the potentially widespread influence of metazoan microRNAs. Nat Rev Genet *5*, 396-400.

Bateman, J.R., Lee, A.M., and Wu, C.T. (2006). Site-specific transformation of Drosophila via phiC31 integrase-mediated cassette exchange. Genetics *173*, 769-777.

Bazzini, A.A., Lee, M.T., and Giraldez, A.J. (2012). Ribosome profiling shows that miR-430 reduces translation before causing mRNA decay in zebrafish. Science *336*, 233-237.

Becam, I., Rafel, N., Hong, X., Cohen, S.M., and Milan, M. (2011). Notch-mediated repression of bantam miRNA contributes to boundary formation in the Drosophila wing. Development *138*, 3781-3789.

Bedard, K., and Krause, K.H. (2007). The NOX family of ROS-generating NADPH oxidases: physiology and pathophysiology. Physiol Rev *87*, 245-313.

Behm-Ansmant, I., Rehwinkel, J., Doerks, T., Stark, A., Bork, P., and Izaurralde, E. (2006a). mRNA degradation by miRNAs and GW182 requires both CCR4:NOT deadenylase and DCP1:DCP2 decapping complexes. Genes Dev *20*, 1885-1898.

Behm-Ansmant, I., Rehwinkel, J., and Izaurralde, E. (2006b). MicroRNAs silence gene expression by repressing protein expression and/or by promoting mRNA decay. Cold Spring Harb Symp Quant Biol *71*, 523-530.

Beitzinger, M., Peters, L., Zhu, J.Y., Kremmer, E., and Meister, G. (2007). Identification of human microRNA targets from isolated argonaute protein complexes. RNA Biol *4*, 76-84.

Benzer, S. (1967). BEHAVIORAL MUTANTS OF Drosophila ISOLATED BY COUNTERCURRENT DISTRIBUTION. Proc Natl Acad Sci U S A *58*, 1112-1119.

Berdnik, D., Fan, A.P., Potter, C.J., and Luo, L. (2008). MicroRNA processing pathway regulates olfactory neuron morphogenesis. Curr Biol *18*, 1754-1759.

Berezikov, E., Robine, N., Samsonova, A., Westholm, J.O., Naqvi, A., Hung, J.H., Okamura, K., Dai, Q., Bortolamiol-Becet, D., Martin, R.*, et al.* (2011). Deep annotation of Drosophila melanogaster microRNAs yields insights into their processing, modification, and emergence. Genome Res *21*, 203-215.

Berezikov, E., Thuemmler, F., van Laake, L.W., Kondova, I., Bontrop, R., Cuppen, E., and Plasterk, R.H. (2006). Diversity of microRNAs in human and chimpanzee brain. Nat Genet *38*, 1375-1377.

Bernstein, E., Kim, S.Y., Carmell, M.A., Murchison, E.P., Alcorn, H., Li, M.Z., Mills, A.A., Elledge, S.J., Anderson, K.V., and Hannon, G.J. (2003). Dicer is essential for mouse development. Nat Genet *35*, 215-217.

Bischof, J., Maeda, R.K., Hediger, M., Karch, F., and Basler, K. (2007). An optimized transgenesis system for Drosophila using germ-line-specific phiC31 integrases. Proc Natl Acad Sci U S A *104*, 3312-3317.

Boersema, P.J., Raijmakers, R., Lemeer, S., Mohammed, S., and Heck, A.J. (2009). Multiplex peptide stable isotope dimethyl labeling for quantitative proteomics. Nat Protoc *4*, 484-494.

Bogerd, H.P., Karnowski, H.W., Cai, X., Shin, J., Pohlers, M., and Cullen, B.R. (2010). A mammalian herpesvirus uses noncanonical expression and processing mechanisms to generate viral MicroRNAs. Mol Cell *37*, 135-142.

Brennecke, J., Hipfner, D.R., Stark, A., Russell, R.B., and Cohen, S.M. (2003). bantam encodes a developmentally regulated microRNA that controls cell

proliferation and regulates the proapoptotic gene hid in Drosophila. Cell *113*, 25-36.

Brennecke, J., Stark, A., Russell, R.B., and Cohen, S.M. (2005). Principles of microRNA-target recognition. PLoS Biol *3*, e85.

Bushati, N., Stark, A., Brennecke, J., and Cohen, S.M. (2008). Temporal reciprocity of miRNAs and their targets during the maternal-to-zygotic transition in Drosophila. Curr Biol *18*, 501-506.

Caygill, E.E., and Johnston, L.A. (2008). Temporal regulation of metamorphic processes in Drosophila by the let-7 and miR-125 heterochronic microRNAs. Curr Biol *18*, 943-950.

Cazalla, D., Xie, M., and Steitz, J.A. (2011). A primate herpesvirus uses the integrator complex to generate viral microRNAs. Mol Cell *43*, 982-992.

Chatterjee, S., Fasler, M., Bussing, I., and Grosshans, H. (2011). Target-mediated protection of endogenous microRNAs in C. elegans. Dev Cell *20*, 388-396.

Chatterjee, S., and Grosshans, H. (2009). Active turnover modulates mature microRNA activity in Caenorhabditis elegans. Nature *461*, 546-549.

Cheloufi, S., Dos Santos, C.O., Chong, M.M., and Hannon, G.J. (2010). A dicer-independent miRNA biogenesis pathway that requires Ago catalysis. Nature *465*, 584-589.

Chen, Y.W., Weng, R., and Cohen, S.M. (2011). Protocols for use of homologous recombination gene targeting to produce microRNA mutants in Drosophila. Methods Mol Biol *732*, 99-120.

Chiang, H.R., Schoenfeld, L.W., Ruby, J.G., Auyeung, V.C., Spies, N., Baek, D., Johnston, W.K., Russ, C., Luo, S., Babiarz, J.E.*, et al.* (2010). Mammalian microRNAs: experimental evaluation of novel and previously annotated genes. Genes Dev *24*, 992-1009.

Choi, P.S., Zakhary, L., Choi, W.Y., Caron, S., Alvarez-Saavedra, E., Miska, E.A., McManus, M., Harfe, B., Giraldez, A.J., Horvitz, H.R.*, et al.* (2008). Members of the miRNA-200 family regulate olfactory neurogenesis. Neuron *57*, 41-55.

Cifuentes, D., Xue, H., Taylor, D.W., Patnode, H., Mishima, Y., Cheloufi, S., Ma, E., Mane, S., Hannon, G.J., Lawson, N.D.*, et al.* (2010). A novel miRNA processing pathway independent of Dicer requires Argonaute2 catalytic activity. Science *328*, 1694-1698.

Coant, N., Ben Mkaddem, S., Pedruzzi, E., Guichard, C., Treton, X., Ducroc, R., Freund, J.N., Cazals-Hatem, D., Bouhnik, Y., Woerther, P.L.*, et al.* (2010). NADPH oxidase 1 modulates WNT and NOTCH1 signaling to control the

fate of proliferative progenitor cells in the colon. Mol Cell Biol *30*, 2636-2650.

Coller, J., and Parker, R. (2004). Eukaryotic mRNA decapping. Annu Rev Biochem *73*, 861-890.

D'Ambrogio, A., Gu, W., Udagawa, T., Mello, C.C., and Richter, J.D. (2012). Specific miRNA stabilization by Gld2-catalyzed monoadenylation. Cell Rep *2*, 1537-1545.

D'Autreaux, B., and Toledano, M.B. (2007). ROS as signalling molecules: mechanisms that generate specificity in ROS homeostasis. Nat Rev Mol Cell Biol *8*, 813-824.

Damiani, D., Alexander, J.J., O'Rourke, J.R., McManus, M., Jadhav, A.P., Cepko, C.L., Hauswirth, W.W., Harfe, B.D., and Strettoi, E. (2008). Dicer inactivation leads to progressive functional and structural degeneration of the mouse retina. J Neurosci *28*, 4878-4887.

Davis, C.J., Clinton, J.M., Taishi, P., Bohnet, S.G., Honn, K.A., and Krueger, J.M. (2011). MicroRNA 132 alters sleep and varies with time in brain. J Appl Physiol *111*, 665-672.

Davis, T.H., Cuellar, T.L., Koch, S.M., Barker, A.J., Harfe, B.D., McManus, M.T., and Ullian, E.M. (2008). Conditional loss of Dicer disrupts cellular and tissue morphogenesis in the cortex and hippocampus. J Neurosci *28*, 4322-4330.

Demir, E., and Dickson, B.J. (2005). fruitless splicing specifies male courtship behavior in Drosophila. Cell *121*, 785-794.

Dickinson, B.C., Peltier, J., Stone, D., Schaffer, D.V., and Chang, C.J. (2011). Nox2 redox signaling maintains essential cell populations in the brain. Nat Chem Biol *7*, 106-112.

Diederichs, S., and Haber, D.A. (2007). Dual role for argonautes in microRNA processing and posttranscriptional regulation of microRNA expression. Cell *131*, 1097-1108.

Djuranovic, S., Nahvi, A., and Green, R. (2011). A parsimonious model for gene regulation by miRNAs. Science *331*, 550-553.

Doench, J.G., and Sharp, P.A. (2004). Specificity of microRNA target selection in translational repression. Genes Dev *18*, 504-511.

Dolph, P., Nair, A., and Raghu, P. (2011). Electroretinogram recordings of Drosophila. Cold Spring Harb Protoc *2011*, pdb prot5549.

Dorval, V., Smith, P.Y., Delay, C., Calvo, E., Planel, E., Zommer, N., Buee, L., and Hebert, S.S. (2012). Gene network and pathway analysis of mice with conditional ablation of Dicer in post-mitotic neurons. PLoS One *7*, e44060.

Dudai, Y. (2008). Seymour Benzer (1921-2007). Neuron *57*, 24-26.

Easow, G., Teleman, A.A., and Cohen, S.M. (2007). Isolation of microRNA targets by miRNP immunopurification. RNA *13*, 1198-1204.

Ebert, M.S., and Sharp, P.A. (2010). MicroRNA sponges: progress and possibilities. RNA *16*, 2043-2050.

Edbauer, D., Neilson, J.R., Foster, K.A., Wang, C.F., Seeburg, D.P., Batterton, M.N., Tada, T., Dolan, B.M., Sharp, P.A., and Sheng, M. (2010). Regulation of synaptic structure and function by FMRP-associated microRNAs miR-125b and miR-132. Neuron *65*, 373-384.

Feany, M.B., and Bender, W.W. (2000). A Drosophila model of Parkinson's disease. Nature *404*, 394-398.

Fields, R.D., and Stevens-Graham, B. (2002). New insights into neuron-glia communication. Science *298*, 556-562.

Finkel, T. (2011). Signal transduction by reactive oxygen species. J Cell Biol *194*, 7-15.

Flatt, T., Min, K.J., D'Alterio, C., Villa-Cuesta, E., Cumbers, J., Lehmann, R., Jones, D.L., and Tatar, M. (2008). Drosophila germ-line modulation of insulin signaling and lifespan. Proc Natl Acad Sci U S A *105*, 6368-6373.

Fontana, L., Partridge, L., and Longo, V.D. (2010). Extending healthy life span--from yeast to humans. Science *328*, 321-326.

Forman, H.J., Maiorino, M., and Ursini, F. (2010). Signaling functions of reactive oxygen species. Biochemistry *49*, 835-842.

Franceschini, N., and Kirschfeld, K. (1971a). [In vivo optical study of photoreceptor elements in the compound eye of Drosophila]. Kybernetik *8*, 1-13.

Franceschini, N., and Kirschfeld, K. (1971b). [Pseudopupil phenomena in the compound eye of drosophila]. Kybernetik *9*, 159-182.

Friedman, R.C., Farh, K.K., Burge, C.B., and Bartel, D.P. (2009). Most mammalian mRNAs are conserved targets of microRNAs. Genome Res *19*, 92-105.

Gaengel, K., and Mlodzik, M. (2008). Microscopic analysis of the adult Drosophila retina using semithin plastic sections. Methods Mol Biol *420*, 277-287.

Gahtan, E., Auerbach, J.M., Groner, Y., and Segal, M. (1998). Reversible impairment of long-term potentiation in transgenic Cu/Zn-SOD mice. Eur J Neurosci *10*, 538-544.

Gandhi, R., Healy, B., Gholipour, T., Egorova, S., Musallam, A., Shuja, M., Nejad, P., Patel, B., Hei, H., Khoury, S.*, et al.* (2013). Circulating microRNAs as biomarkers for disease staging in multiple sclerosis. Ann Neurol.

Gatti, S., Ferveur, J.F., and Martin, J.R. (2000). Genetic identification of neurons controlling a sexually dimorphic behaviour. Curr Biol *10*, 667-670.

Ge, W., Chen, Y.W., Weng, R., Lim, S.F., Buescher, M., Zhang, R., and Cohen, S.M. (2012). Overlapping functions of microRNAs in control of apoptosis during Drosophila embryogenesis. Cell Death Differ *19*, 839-846.

Gems, D., and Doonan, R. (2009). Antioxidant defense and aging in C. elegans: is the oxidative damage theory of aging wrong? Cell Cycle *8*, 1681-1687.

Goldman, T.D., and Arbeitman, M.N. (2007). Genomic and functional studies of Drosophila sex hierarchy regulated gene expression in adult head and nervous system tissues. PLoS Genet *3*, e216.

Greenberg, J.K., Xia, J., Zhou, X., Thatcher, S.R., Gu, X., Ament, S.A., Newman, T.C., Green, P.J., Zhang, W., Robinson, G.E.*, et al.* (2012). Behavioral plasticity in honey bees is associated with differences in brain microRNA transcriptome. Genes Brain Behav *11*, 660-670.

Greenspan, R.J. (2008). Seymour Benzer (1921-2007). Curr Biol *18*, R106-110.

Grimm, C., Wenzel, A., Hafezi, F., Yu, S., Redmond, T.M., and Reme, C.E. (2000). Protection of Rpe65-deficient mice identifies rhodopsin as a mediator of light-induced retinal degeneration. Nat Genet *25*, 63-66.

Groth, A.C., Fish, M., Nusse, R., and Calos, M.P. (2004). Construction of transgenic Drosophila by using the site-specific integrase from phage phiC31. Genetics *166*, 1775-1782.

Grover, D., Ford, D., Brown, C., Hoe, N., Erdem, A., Tavare, S., and Tower, J. (2009). Hydrogen peroxide stimulates activity and alters behavior in Drosophila melanogaster. PLoS One *4*, e7580.

Guo, H., Ingolia, N.T., Weissman, J.S., and Bartel, D.P. (2010a). Mammalian microRNAs predominantly act to decrease target mRNA levels. Nature *466*, 835-840.

Guo, L., Liu, Y., Bai, Y., Sun, Y., Xiao, F., and Guo, Y. (2010b). Gene expression profiling of drug-resistant small cell lung cancer cells by combining microRNA and cDNA expression analysis. Eur J Cancer *46*, 1692-1702.

Ha, E.M., Lee, K.A., Park, S.H., Kim, S.H., Nam, H.J., Lee, H.Y., Kang, D., and Lee, W.J. (2009). Regulation of DUOX by the Galphaq-phospholipase Cbeta-Ca2+ pathway in Drosophila gut immunity. Dev Cell *16*, 386-397.

Ha, E.M., Oh, C.T., Bae, Y.S., and Lee, W.J. (2005). A direct role for dual oxidase in Drosophila gut immunity. Science *310*, 847-850.

Hafner, M., Landthaler, M., Burger, L., Khorshid, M., Hausser, J., Berninger, P., Rothballer, A., Ascano, M., Jr., Jungkamp, A.C., Munschauer, M., *et al.* (2010). Transcriptome-wide identification of RNA-binding protein and microRNA target sites by PAR-CLIP. Cell *141*, 129-141.

Hansen, K.F., Sakamoto, K., Wayman, G.A., Impey, S., and Obrietan, K. (2010). Transgenic miR132 alters neuronal spine density and impairs novel object recognition memory. PLoS One *5*, e15497.

Hansen, T.B., Jensen, T.I., Clausen, B.H., Bramsen, J.B., Finsen, B., Damgaard, C.K., and Kjems, J. (2013). Natural RNA circles function as efficient microRNA sponges. Nature *495*, 384-388.

Hardie, R.C., and Raghu, P. (2001). Visual transduction in Drosophila. Nature *413*, 186-193.

Harris, W.A., and Stark, W.S. (1977). Hereditary retinal degeneration in Drosophila melanogaster. A mutant defect associated with the phototransduction process. J Gen Physiol *69*, 261-291.

Hatfield, S.D., Shcherbata, H.R., Fischer, K.A., Nakahara, K., Carthew, R.W., and Ruohola-Baker, H. (2005). Stem cell division is regulated by the microRNA pathway. Nature *435*, 974-978.

Hebert, S.S., Papadopoulou, A.S., Smith, P., Galas, M.C., Planel, E., Silahtaroglu, A.N., Sergeant, N., Buee, L., and De Strooper, B. (2010). Genetic ablation of Dicer in adult forebrain neurons results in abnormal tau hyperphosphorylation and neurodegeneration. Hum Mol Genet *19*, 3959-3969.

Hendrickson, D.G., Hogan, D.J., Herschlag, D., Ferrell, J.E., and Brown, P.O. (2008). Systematic identification of mRNAs recruited to argonaute 2 by specific microRNAs and corresponding changes in transcript abundance. PLoS One *3*, e2126.

Herranz, H., and Cohen, S.M. (2010). MicroRNAs and gene regulatory networks: managing the impact of noise in biological systems. Genes Dev *24*, 1339-1344.

Herranz, H., Hong, X., and Cohen, S.M. (2012a). Mutual repression by bantam miRNA and Capicua links the EGFR/MAPK and Hippo pathways in growth control. Curr Biol *22*, 651-657.

Herranz, H., Hong, X., Hung, N.T., Voorhoeve, P.M., and Cohen, S.M. (2012b). Oncogenic cooperation between SOCS family proteins and EGFR identified using a Drosophila epithelial transformation model. Genes Dev *26*, 1602-1611.

Hilgers, V., Bushati, N., and Cohen, S.M. (2010). Drosophila microRNAs 263a/b confer robustness during development by protecting nascent sense organs from apoptosis. PLoS Biol *8*, e1000396.

Hong, X., Hammell, M., Ambros, V., and Cohen, S.M. (2009). Immunopurification of Ago1 miRNPs selects for a distinct class of microRNA targets. Proc Natl Acad Sci U S A *106*, 15085-15090.

Hsin, H., and Kenyon, C. (1999). Signals from the reproductive system regulate the lifespan of C. elegans. Nature *399*, 362-366.

Hsu, J.L., Huang, S.Y., Chow, N.H., and Chen, S.H. (2003). Stable-isotope dimethyl labeling for quantitative proteomics. Anal Chem *75*, 6843-6852.

Hu, D., Klann, E., and Thiels, E. (2007). Superoxide dismutase and hippocampal function: age and isozyme matter. Antioxid Redox Signal *9*, 201-210.

Hu, K., Xie, Y.Y., Zhang, C., Ouyang, D.S., Long, H.Y., Sun, D.N., Long, L.L., Feng, L., Li, Y., and Xiao, B. (2012). MicroRNA expression profile of the hippocampus in a rat model of temporal lobe epilepsy and miR-34a-targeted neuroprotection against hippocampal neurone cell apoptosis post-status epilepticus. BMC Neurosci *13*, 115.

Hua, D., Mo, F., Ding, D., Li, L., Han, X., Zhao, N., Foltz, G., Lin, B., Lan, Q., and Huang, Q. (2012). A catalogue of glioblastoma and brain MicroRNAs identified by deep sequencing. OMICS *16*, 690-699.

Hutvagner, G., and Simard, M.J. (2008). Argonaute proteins: key players in RNA silencing. Nat Rev Mol Cell Biol *9*, 22-32.

Ilieva, H., Polymenidou, M., and Cleveland, D.W. (2009). Non-cell autonomous toxicity in neurodegenerative disorders: ALS and beyond. J Cell Biol *187*, 761-772.

Inoue, H., Yoshioka, T., and Hotta, Y. (1989). Diacylglycerol kinase defect in a Drosophila retinal degeneration mutant rdgA. J Biol Chem *264*, 5996-6000.

Jakymiw, A., Lian, S., Eystathioy, T., Li, S., Satoh, M., Hamel, J.C., Fritzler, M.J., and Chan, E.K. (2005). Disruption of GW bodies impairs mammalian RNA interference. Nat Cell Biol *7*, 1267-1274.

Jones, W.D., Cayirlioglu, P., Kadow, I.G., and Vosshall, L.B. (2007). Two chemosensory receptors together mediate carbon dioxide detection in Drosophila. Nature *445*, 86-90.

Jung, I., Kim, T.Y., and Kim-Ha, J. (2011). Identification of Drosophila SOD3 and its protective role against phototoxic damage to cells. FEBS Lett *585*, 1973-1978.

Junn, E., and Mouradian, M.M. (2012). MicroRNAs in neurodegenerative diseases and their therapeutic potential. Pharmacol Ther *133*, 142-150.

Kadener, S., Menet, J.S., Sugino, K., Horwich, M.D., Weissbein, U., Nawathean, P., Vagin, V.V., Zamore, P.D., Nelson, S.B., and Rosbash, M. (2009). A role for microRNAs in the Drosophila circadian clock. Genes Dev *23*, 2179-2191.

Kai, Z.S., and Pasquinelli, A.E. (2010). MicroRNA assassins: factors that regulate the disappearance of miRNAs. Nat Struct Mol Biol *17*, 5-10.

Kapsimali, M., Kloosterman, W.P., de Bruijn, E., Rosa, F., Plasterk, R.H., and Wilson, S.W. (2007). MicroRNAs show a wide diversity of expression profiles in the developing and mature central nervous system. Genome Biol *8*, R173.

Karginov, F.V., Conaco, C., Xuan, Z., Schmidt, B.H., Parker, J.S., Mandel, G., and Hannon, G.J. (2007). A biochemical approach to identifying microRNA targets. Proc Natl Acad Sci U S A *104*, 19291-19296.

Karres, J.S., Hilgers, V., Carrera, I., Treisman, J., and Cohen, S.M. (2007). The conserved microRNA miR-8 tunes atrophin levels to prevent neurodegeneration in Drosophila. Cell *131*, 136-145.

Katoh, T., Sakaguchi, Y., Miyauchi, K., Suzuki, T., Kashiwabara, S., and Baba, T. (2009). Selective stabilization of mammalian microRNAs by 3' adenylation mediated by the cytoplasmic poly(A) polymerase GLD-2. Genes Dev *23*, 433-438.

Katsuyama, M., Matsuno, K., and Yabe-Nishimura, C. (2012). Physiological roles of NOX/NADPH oxidase, the superoxide-generating enzyme. J Clin Biochem Nutr *50*, 9-22.

Katz, B., and Minke, B. (2009). Drosophila photoreceptors and signaling mechanisms. Front Cell Neurosci *3*, 2.

Khvorova, A., Reynolds, A., and Jayasena, S.D. (2003). Functional siRNAs and miRNAs exhibit strand bias. Cell *115*, 209-216.

Kim, J., Inoue, K., Ishii, J., Vanti, W.B., Voronov, S.V., Murchison, E., Hannon, G., and Abeliovich, A. (2007). A MicroRNA feedback circuit in midbrain dopamine neurons. Science *317*, 1220-1224.

Kishida, K.T., Hoeffer, C.A., Hu, D., Pao, M., Holland, S.M., and Klann, E. (2006). Synaptic plasticity deficits and mild memory impairments in mouse models of chronic granulomatous disease. Mol Cell Biol *26*, 5908-5920.

Klein, U., Lia, M., Crespo, M., Siegel, R., Shen, Q., Mo, T., Ambesi-Impiombato, A., Califano, A., Migliazza, A., Bhagat, G.*, et al.* (2010). The DLEU2/miR-15a/16-1 cluster controls B cell proliferation and its deletion leads to chronic lymphocytic leukemia. Cancer Cell *17*, 28-40.

Knapp, L.T., and Klann, E. (2002). Role of reactive oxygen species in hippocampal long-term potentiation: contributory or inhibitory? J Neurosci Res *70*, 1-7.

Koh, K., Joiner, W.J., Wu, M.N., Yue, Z., Smith, C.J., and Sehgal, A. (2008). Identification of SLEEPLESS, a sleep-promoting factor. Science *321*, 372-376.

Krek, A., Grun, D., Poy, M.N., Wolf, R., Rosenberg, L., Epstein, E.J., MacMenamin, P., da Piedade, I., Gunsalus, K.C., Stoffel, M.*, et al.* (2005). Combinatorial microRNA target predictions. Nat Genet *37*, 495-500.

Krstic, D., Boll, W., and Noll, M. (2009). Sensory integration regulating male courtship behavior in Drosophila. PLoS One *4*, e4457.

Kye, M.J., Neveu, P., Lee, Y.S., Zhou, M., Steen, J.A., Sahin, M., Kosik, K.S., and Silva, A.J. (2011). NMDA mediated contextual conditioning changes miRNA expression. PLoS One *6*, e24682.

Lambeth, J.D. (2004). NOX enzymes and the biology of reactive oxygen. Nat Rev Immunol *4*, 181-189.

Landgraf, P., Rusu, M., Sheridan, R., Sewer, A., Iovino, N., Aravin, A., Pfeffer, S., Rice, A., Kamphorst, A.O., Landthaler, M.*, et al.* (2007). A mammalian microRNA expression atlas based on small RNA library sequencing. Cell *129*, 1401-1414.

Le Belle, J.E., Orozco, N.M., Paucar, A.A., Saxe, J.P., Mottahedeh, J., Pyle, A.D., Wu, H., and Kornblum, H.I. (2011). Proliferative neural stem cells have high endogenous ROS levels that regulate self-renewal and neurogenesis in a PI3K/Akt-dependant manner. Cell Stem Cell *8*, 59-71.

Lee, I., Ajay, S.S., Yook, J.I., Kim, H.S., Hong, S.H., Kim, N.H., Dhanasekaran, S.M., Chinnaiyan, A.M., and Athey, B.D. (2009). New class of microRNA targets containing simultaneous 5'-UTR and 3'-UTR interaction sites. Genome Res *19*, 1175-1183.

Lee, R.C., Feinbaum, R.L., and Ambros, V. (1993). The C. elegans heterochronic gene lin-4 encodes small RNAs with antisense complementarity to lin-14. Cell *75*, 843-854.

Lee, Y., Ahn, C., Han, J., Choi, H., Kim, J., Yim, J., Lee, J., Provost, P., Radmark, O., Kim, S.*, et al.* (2003). The nuclear RNase III Drosha initiates microRNA processing. Nature *425*, 415-419.

Lee, Y.S., Nakahara, K., Pham, J.W., Kim, K., He, Z., Sontheimer, E.J., and Carthew, R.W. (2004). Distinct roles for Drosophila Dicer-1 and Dicer-2 in the siRNA/miRNA silencing pathways. Cell *117*, 69-81.

Leslie, N.R. (2006). The redox regulation of PI 3-kinase-dependent signaling. Antioxid Redox Signal *8*, 1765-1774.

Lewis, B.P., Burge, C.B., and Bartel, D.P. (2005). Conserved seed pairing, often flanked by adenosines, indicates that thousands of human genes are microRNA targets. Cell *120*, 15-20.

Lewis, B.P., Shih, I.H., Jones-Rhoades, M.W., Bartel, D.P., and Burge, C.B. (2003). Prediction of mammalian microRNA targets. Cell *115*, 787-798.

Li, N., You, X., Chen, T., Mackowiak, S.D., Friedlander, M.R., Weigt, M., Du, H., Gogol-Doring, A., Chang, Z., Dieterich, C.*, et al.* (2013). Global profiling of miRNAs and the hairpin precursors: insights into miRNA processing and novel miRNA discovery. Nucleic Acids Res *41*, 3619-3634.

Li, X., and Carthew, R.W. (2005). A microRNA mediates EGF receptor signaling and promotes photoreceptor differentiation in the Drosophila eye. Cell *123*, 1267-1277.

Lim, L.P., Glasner, M.E., Yekta, S., Burge, C.B., and Bartel, D.P. (2003). Vertebrate microRNA genes. Science *299*, 1540.

Ling, K.H., Brautigan, P.J., Hahn, C.N., Daish, T., Rayner, J.R., Cheah, P.S., Raison, J.M., Piltz, S., Mann, J.R., Mattiske, D.M.*, et al.* (2011). Deep sequencing analysis of the developing mouse brain reveals a novel microRNA. BMC Genomics *12*, 176.

Liochev, S.I. (2013). Reactive oxygen species and the free radical theory of aging. Free Radic Biol Med *60C*, 1-4.

Liu, J., Carmell, M.A., Rivas, F.V., Marsden, C.G., Thomson, J.M., Song, J.J., Hammond, S.M., Joshua-Tor, L., and Hannon, G.J. (2004). Argonaute2 is the catalytic engine of mammalian RNAi. Science *305*, 1437-1441.

Liu, J., Rivas, F.V., Wohlschlegel, J., Yates, J.R., 3rd, Parker, R., and Hannon, G.J. (2005). A role for the P-body component GW182 in microRNA function. Nat Cell Biol *7*, 1261-1266.

Liu, N., Landreh, M., Cao, K., Abe, M., Hendriks, G.J., Kennerdell, J.R., Zhu, Y., Wang, L.S., and Bonini, N.M. (2012). The microRNA miR-34 modulates ageing and neurodegeneration in Drosophila. Nature *482*, 519-523.

Loya, C.M., Lu, C.S., Van Vactor, D., and Fulga, T.A. (2009). Transgenic microRNA inhibition with spatiotemporal specificity in intact organisms. Nat Methods *6*, 897-903.

Luo, W., and Sehgal, A. (2012). Regulation of circadian behavioral output via a MicroRNA-JAK/STAT circuit. Cell *148*, 765-779.

Mann, M. (2006). Functional and quantitative proteomics using SILAC. Nat Rev Mol Cell Biol *7*, 952-958.

Mann, P.J., and Quastel, J.H. (1946). Toxic effects of oxygen and of hydrogen peroxide on brain metabolism. Biochem J *40*, 139-144.

Manoli, D.S., Foss, M., Villella, A., Taylor, B.J., Hall, J.C., and Baker, B.S. (2005). Male-specific fruitless specifies the neural substrates of Drosophila courtship behaviour. Nature *436*, 395-400.

Martin, I., Jones, M.A., and Grotewiel, M. (2009). Manipulation of Sod1 expression ubiquitously, but not in the nervous system or muscle, impacts age-related parameters in Drosophila. FEBS Lett *583*, 2308-2314.

Martinez, J., Patkaniowska, A., Urlaub, H., Luhrmann, R., and Tuschl, T. (2002). Single-stranded antisense siRNAs guide target RNA cleavage in RNAi. Cell *110*, 563-574.

Massaad, C.A., and Klann, E. (2011). Reactive oxygen species in the regulation of synaptic plasticity and memory. Antioxid Redox Signal *14*, 2013-2054.

Maurin, T., Cazalla, D., Yang, S., Jr., Bortolamiol-Becet, D., and Lai, E.C. (2012). RNase III-independent microRNA biogenesis in mammalian cells. RNA *18*, 2166-2173.

McCann, G.D., and MacGinitie, G.F. (1965). Optomotor response studies of insect vision. Proc R Soc Lond B Biol Sci *163*, 369-401.

McNeill, E., and Van Vactor, D. (2012). MicroRNAs shape the neuronal landscape. Neuron *75*, 363-379.

Meister, G., Landthaler, M., Patkaniowska, A., Dorsett, Y., Teng, G., and Tuschl, T. (2004). Human Argonaute2 mediates RNA cleavage targeted by miRNAs and siRNAs. Mol Cell *15*, 185-197.

Mellios, N., Sugihara, H., Castro, J., Banerjee, A., Le, C., Kumar, A., Crawford, B., Strathmann, J., Tropea, D., Levine, S.S.*, et al.* (2011). miR-132, an experience-dependent microRNA, is essential for visual cortex plasticity. Nat Neurosci *14*, 1240-1242.

Memczak, S., Jens, M., Elefsinioti, A., Torti, F., Krueger, J., Rybak, A., Maier, L., Mackowiak, S.D., Gregersen, L.H., Munschauer, M.*, et al.* (2013). Circular RNAs are a large class of animal RNAs with regulatory potency. Nature *495*, 333-338.

Milton, V.J., and Sweeney, S.T. (2012). Oxidative stress in synapse development and function. Dev Neurobiol *72*, 100-110.

Miska, E.A., Alvarez-Saavedra, E., Abbott, A.L., Lau, N.C., Hellman, A.B., McGonagle, S.M., Bartel, D.P., Ambros, V.R., and Horvitz, H.R. (2007). Most Caenorhabditis elegans microRNAs are individually not essential for development or viability. PLoS Genet *3*, e215.

Mollet, S., Cougot, N., Wilczynska, A., Dautry, F., Kress, M., Bertrand, E., and Weil, D. (2008). Translationally repressed mRNA transiently cycles through stress granules during stress. Mol Biol Cell *19*, 4469-4479.

Montell, C. (1999). Visual transduction in Drosophila. Annu Rev Cell Dev Biol *15*, 231-268.

Moore, L.M., Kivinen, V., Liu, Y., Annala, M., Cogdell, D., Liu, X., Liu, C.G., Sawaya, R., Yli-Harja, O., Shmulevich, I.*, et al.* (2013). Transcriptome and small RNA deep sequencing reveals deregulation of miRNA biogenesis in human glioma. J Pathol *229*, 449-459.

Mori, M.A., Raghavan, P., Thomou, T., Boucher, J., Robida-Stubbs, S., Macotela, Y., Russell, S.J., Kirkland, J.L., Blackwell, T.K., and Kahn, C.R. (2012). Role of microRNA processing in adipose tissue in stress defense and longevity. Cell Metab *16*, 336-347.

Moss, E.G., Lee, R.C., and Ambros, V. (1997). The cold shock domain protein LIN-28 controls developmental timing in C. elegans and is regulated by the lin-4 RNA. Cell *88*, 637-646.

Naughton, R., Quiney, C., Turner, S.D., and Cotter, T.G. (2009). Bcr-Abl-mediated redox regulation of the PI3K/AKT pathway. Leukemia *23*, 1432-1440.

Noren Hooten, N., Abdelmohsen, K., Gorospe, M., Ejiogu, N., Zonderman, A.B., and Evans, M.K. (2010). microRNA expression patterns reveal differential expression of target genes with age. PLoS One *5*, e10724.

Nudelman, A.S., DiRocco, D.P., Lambert, T.J., Garelick, M.G., Le, J., Nathanson, N.M., and Storm, D.R. (2010). Neuronal activity rapidly induces transcription of the CREB-regulated microRNA-132, in vivo. Hippocampus *20*, 492-498.

O'Carroll, D., Mecklenbrauker, I., Das, P.P., Santana, A., Koenig, U., Enright, A.J., Miska, E.A., and Tarakhovsky, A. (2007). A Slicer-independent role for Argonaute 2 in hematopoiesis and the microRNA pathway. Genes Dev *21*, 1999-2004.

Okamura, K., Hagen, J.W., Duan, H., Tyler, D.M., and Lai, E.C. (2007). The mirtron pathway generates microRNA-class regulatory RNAs in Drosophila. Cell *130*, 89-100.

Okamura, K., Ishizuka, A., Siomi, H., and Siomi, M.C. (2004). Distinct roles for Argonaute proteins in small RNA-directed RNA cleavage pathways. Genes Dev *18*, 1655-1666.

Ong, S.E., Blagoev, B., Kratchmarova, I., Kristensen, D.B., Steen, H., Pandey, A., and Mann, M. (2002). Stable isotope labeling by amino acids in cell culture, SILAC, as a simple and accurate approach to expression proteomics. Mol Cell Proteomics *1*, 376-386.

Ouyang, Y.B., Xu, L., Lu, Y., Sun, X., Yue, S., Xiong, X.X., and Giffard, R.G. (2013). Astrocyte-enriched miR-29a targets PUMA and reduces neuronal vulnerability to forebrain ischemia. Glia *61*, 1784-1794.

Pandey, A.C., Semon, J.A., Kaushal, D., O'Sullivan, R.P., Glowacki, J., Gimble, J.M., and Bunnell, B.A. (2011). MicroRNA profiling reveals age-dependent differential expression of nuclear factor kappaB and mitogen-activated protein kinase in adipose and bone marrow-derived human mesenchymal stem cells. Stem Cell Res Ther *2*, 49.

Park, C.Y., Jeker, L.T., Carver-Moore, K., Oh, A., Liu, H.J., Cameron, R., Richards, H., Li, Z., Adler, D., Yoshinaga, Y.*, et al.* (2012). A resource for the conditional ablation of microRNAs in the mouse. Cell Rep *1*, 385-391.

Parkes, T.L., Elia, A.J., Dickinson, D., Hilliker, A.J., Phillips, J.P., and Boulianne, G.L. (1998). Extension of Drosophila lifespan by overexpression of human SOD1 in motorneurons. Nat Genet *19*, 171-174.

Pasquinelli, A.E., Reinhart, B.J., Slack, F., Martindale, M.Q., Kuroda, M.I., Maller, B., Hayward, D.C., Ball, E.E., Degnan, B., Muller, P.*, et al.* (2000). Conservation of the sequence and temporal expression of let-7 heterochronic regulatory RNA. Nature *408*, 86-89.

Pereira, J.A., Baumann, R., Norrmen, C., Somandin, C., Miehe, M., Jacob, C., Luhmann, T., Hall-Bozic, H., Mantei, N., Meijer, D.*, et al.* (2010). Dicer in Schwann cells is required for myelination and axonal integrity. J Neurosci *30*, 6763-6775.

Phillips, J.P., Parkes, T.L., and Hilliker, A.J. (2000). Targeted neuronal gene expression and longevity in Drosophila. Exp Gerontol *35*, 1157-1164.

Pillai, R.S., Bhattacharyya, S.N., Artus, C.G., Zoller, T., Cougot, N., Basyuk, E., Bertrand, E., and Filipowicz, W. (2005). Inhibition of translational initiation by Let-7 MicroRNA in human cells. Science *309*, 1573-1576.

Port, J.D., Walker, L.A., Polk, J., Nunley, K., Buttrick, P.M., and Sucharov, C.C. (2011). Temporal expression of miRNAs and mRNAs in a mouse model of myocardial infarction. Physiol Genomics *43*, 1087-1095.

Poy, M.N., Hausser, J., Trajkovski, M., Braun, M., Collins, S., Rorsman, P., Zavolan, M., and Stoffel, M. (2009). miR-375 maintains normal pancreatic alpha- and beta-cell mass. Proc Natl Acad Sci U S A *106*, 5813-5818.

Prinz, M., Priller, J., Sisodia, S.S., and Ransohoff, R.M. (2011). Heterogeneity of CNS myeloid cells and their roles in neurodegeneration. Nat Neurosci *14*, 1227-1235.

Prosser, H.M., Koike-Yusa, H., Cooper, J.D., Law, F.C., and Bradley, A. (2011). A resource of vectors and ES cells for targeted deletion of microRNAs in mice. Nat Biotechnol *29*, 840-845.

Rainer, J., Sanchez-Cabo, F., Stocker, G., Sturn, A., and Trajanoski, Z. (2006). CARMAweb: comprehensive R- and bioconductor-based web service for microarray data analysis. Nucleic Acids Res *34*, W498-503.

Rasmussen, K.D., Simmini, S., Abreu-Goodger, C., Bartonicek, N., Di Giacomo, M., Bilbao-Cortes, D., Horos, R., Von Lindern, M., Enright, A.J., and O'Carroll, D. (2010). The miR-144/451 locus is required for erythroid homeostasis. J Exp Med *207*, 1351-1358.

Razzell, W., Evans, I.R., Martin, P., and Wood, W. (2013). Calcium flashes orchestrate the wound inflammatory response through DUOX activation and hydrogen peroxide release. Curr Biol *23*, 424-429.

Reinehr, R., Gorg, B., Becker, S., Qvartskhava, N., Bidmon, H.J., Selbach, O., Haas, H.L., Schliess, F., and Haussinger, D. (2007). Hypoosmotic swelling and ammonia increase oxidative stress by NADPH oxidase in cultured astrocytes and vital brain slices. Glia *55*, 758-771.

Reinhart, B.J., Slack, F.J., Basson, M., Pasquinelli, A.E., Bettinger, J.C., Rougvie, A.E., Horvitz, H.R., and Ruvkun, G. (2000). The 21-nucleotide let-7 RNA regulates developmental timing in Caenorhabditis elegans. Nature *403*, 901-906.

Ritsick, D.R., Edens, W.A., Finnerty, V., and Lambeth, J.D. (2007). Nox regulation of smooth muscle contraction. Free Radic Biol Med *43*, 31-38.

Rong, H., Liu, T.B., Yang, K.J., Yang, H.C., Wu, D.H., Liao, C.P., Hong, F., Yang, H.Z., Wan, F., Ye, X.Y.*, et al.* (2011). MicroRNA-134 plasma levels before and after treatment for bipolar mania. J Psychiatr Res *45*, 92-95.

Rong, Y.S., and Golic, K.G. (2000). Gene targeting by homologous recombination in Drosophila. Science *288*, 2013-2018.

Rong, Y.S., and Golic, K.G. (2001). A targeted gene knockout in Drosophila. Genetics *157*, 1307-1312.

Rong, Y.S., and Golic, K.G. (2003). The homologous chromosome is an effective template for the repair of mitotic DNA double-strand breaks in Drosophila. Genetics *165*, 1831-1842.

Ruby, J.G., Jan, C.H., and Bartel, D.P. (2007a). Intronic microRNA precursors that bypass Drosha processing. Nature *448*, 83-86.

Ruby, J.G., Stark, A., Johnston, W.K., Kellis, M., Bartel, D.P., and Lai, E.C. (2007b). Evolution, biogenesis, expression, and target predictions of a substantially expanded set of Drosophila microRNAs. Genome Res *17*, 1850-1864.

Ruegger, S., and Grosshans, H. (2012). MicroRNA turnover: when, how, and why. Trends Biochem Sci *37*, 436-446.

Sadegh, M.K., Ekman, M., Rippe, C., Uvelius, B., Sward, K., and Albinsson, S. (2012). Deletion of Dicer in smooth muscle affects voiding pattern and reduces detrusor contractility and neuroeffector transmission. PLoS One *7*, e35882.

Saito, K., Ishizuka, A., Siomi, H., and Siomi, M.C. (2005). Processing of pre-microRNAs by the Dicer-1-Loquacious complex in Drosophila cells. PLoS Biol *3*, e235.

Schaefer, A., O'Carroll, D., Tan, C.L., Hillman, D., Sugimori, M., Llinas, R., and Greengard, P. (2007). Cerebellar neurodegeneration in the absence of microRNAs. J Exp Med *204*, 1553-1558.

Schnall-Levin, M., Zhao, Y., Perrimon, N., and Berger, B. (2010). Conserved microRNA targeting in Drosophila is as widespread in coding regions as in 3'UTRs. Proc Natl Acad Sci U S A *107*, 15751-15756.

Schwarz, D.S., Hutvagner, G., Du, T., Xu, Z., Aronin, N., and Zamore, P.D. (2003). Asymmetry in the assembly of the RNAi enzyme complex. Cell *115*, 199-208.

Selbach, M., Schwanhausser, B., Thierfelder, N., Fang, Z., Khanin, R., and Rajewsky, N. (2008). Widespread changes in protein synthesis induced by microRNAs. Nature *455*, 58-63.

Sen, G.L., and Blau, H.M. (2005). Argonaute 2/RISC resides in sites of mammalian mRNA decay known as cytoplasmic bodies. Nat Cell Biol *7*, 633-636.

Shen, Y., Wollam, J., Magner, D., Karalay, O., and Antebi, A. (2012). A steroid receptor-microRNA switch regulates life span in response to signals from the gonad. Science *338*, 1472-1476.

Shin, D., Shin, J.Y., McManus, M.T., Ptacek, L.J., and Fu, Y.H. (2009). Dicer ablation in oligodendrocytes provokes neuronal impairment in mice. Ann Neurol *66*, 843-857.

Silber, J., Lim, D.A., Petritsch, C., Persson, A.I., Maunakea, A.K., Yu, M., Vandenberg, S.R., Ginzinger, D.G., James, C.D., Costello, J.F.*, et al.* (2008). miR-124 and miR-137 inhibit proliferation of glioblastoma multiforme cells and induce differentiation of brain tumor stem cells. BMC Med *6*, 14.

Smibert, P., Bejarano, F., Wang, D., Garaulet, D.L., Yang, J.S., Martin, R., Bortolamiol-Becet, D., Robine, N., Hiesinger, P.R., and Lai, E.C. (2011). A Drosophila genetic screen yields allelic series of core microRNA biogenesis factors and reveals post-developmental roles for microRNAs. RNA *17*, 1997-2010.

Sokol, N.S., Xu, P., Jan, Y.N., and Ambros, V. (2008). Drosophila let-7 microRNA is required for remodeling of the neuromusculature during metamorphosis. Genes Dev *22*, 1591-1596.

Somel, M., Guo, S., Fu, N., Yan, Z., Hu, H.Y., Xu, Y., Yuan, Y., Ning, Z., Hu, Y., Menzel, C.*, et al.* (2010). MicroRNA, mRNA, and protein expression link development and aging in human and macaque brain. Genome Res *20*, 1207-1218.

Spencer, C.C., Howell, C.E., Wright, A.R., and Promislow, D.E. (2003). Testing an 'aging gene' in long-lived drosophila strains: increased longevity depends on sex and genetic background. Aging Cell *2*, 123-130.

Stark, W.S., and Thomas, C.F. (2004). Microscopy of multiple visual receptor types in Drosophila. Mol Vis *10*, 943-955.

Stark, W.S., and Wasserman, G.S. (1972). Transient and receptor potentials in the electroretinogram of Drosophila. Vision Res *12*, 1771-1775.

Sury, M.D., Chen, J.X., and Selbach, M. (2010). The SILAC fly allows for accurate protein quantification in vivo. Mol Cell Proteomics *9*, 2173-2183.

Szulwach, K.E., Li, X., Smrt, R.D., Li, Y., Luo, Y., Lin, L., Santistevan, N.J., Li, W., Zhao, X., and Jin, P. (2010). Cross talk between microRNA and epigenetic regulation in adult neurogenesis. J Cell Biol *189*, 127-141.

Tang, K.F., and Ren, H. (2012). The role of dicer in DNA damage repair. Int J Mol Sci *13*, 16769-16778.

Tao, J., Wu, H., Lin, Q., Wei, W., Lu, X.H., Cantle, J.P., Ao, Y., Olsen, R.W., Yang, X.W., Mody, I.*, et al.* (2011). Deletion of astroglial Dicer causes non-cell-autonomous neuronal dysfunction and degeneration. J Neurosci *31*, 8306-8319.

Teleman, A.A., Hietakangas, V., Sayadian, A.C., and Cohen, S.M. (2008). Nutritional control of protein biosynthetic capacity by insulin via Myc in Drosophila. Cell Metab *7*, 21-32.

Teleman, A.A., Maitra, S., and Cohen, S.M. (2006). Drosophila lacking microRNA miR-278 are defective in energy homeostasis. Genes Dev *20*, 417-422.

Thiels, E., and Klann, E. (2002). Hippocampal memory and plasticity in superoxide dismutase mutant mice. Physiol Behav *77*, 601-605.

Thiels, E., Urban, N.N., Gonzalez-Burgos, G.R., Kanterewicz, B.I., Barrionuevo, G., Chu, C.T., Oury, T.D., and Klann, E. (2000). Impairment of long-term potentiation and associative memory in mice that overexpress extracellular superoxide dismutase. J Neurosci *20*, 7631-7639.

Tognini, P., Putignano, E., Coatti, A., and Pizzorusso, T. (2011). Experience-dependent expression of miR-132 regulates ocular dominance plasticity. Nat Neurosci *14*, 1237-1239.

Toledano, H., D'Alterio, C., Loza-Coll, M., and Jones, D.L. (2012). Dual fluorescence detection of protein and RNA in Drosophila tissues. Nat Protoc *7*, 1808-1817.

Tsatmali, M., Walcott, E.C., Makarenkova, H., and Crossin, K.L. (2006). Reactive oxygen species modulate the differentiation of neurons in clonal cortical cultures. Mol Cell Neurosci *33*, 345-357.

Valencia-Sanchez, M.A., Liu, J., Hannon, G.J., and Parker, R. (2006). Control of translation and mRNA degradation by miRNAs and siRNAs. Genes Dev *20*, 515-524.

Van Raamsdonk, J.M., and Hekimi, S. (2009). Deletion of the mitochondrial superoxide dismutase sod-2 extends lifespan in Caenorhabditis elegans. PLoS Genet *5*, e1000361.

Van Raamsdonk, J.M., and Hekimi, S. (2012). Superoxide dismutase is dispensable for normal animal lifespan. Proc Natl Acad Sci U S A *109*, 5785-5790.

Varghese, J., and Cohen, S.M. (2007). microRNA miR-14 acts to modulate a positive autoregulatory loop controlling steroid hormone signaling in Drosophila. Genes Dev *21*, 2277-2282.

Varghese, J., Lim, S.F., and Cohen, S.M. (2010). Drosophila miR-14 regulates insulin production and metabolism through its target, sugarbabe. Genes Dev *24*, 2748-2753.

Ventura, A., Young, A.G., Winslow, M.M., Lintault, L., Meissner, A., Erkeland, S.J., Newman, J., Bronson, R.T., Crowley, D., Stone, J.R.*, et al.* (2008). Targeted deletion reveals essential and overlapping functions of the miR-17 through 92 family of miRNA clusters. Cell *132*, 875-886.

Ventura, R., and Harris, K.M. (1999). Three-dimensional relationships between hippocampal synapses and astrocytes. J Neurosci *19*, 6897-6906.

Verrier, J.D., Semple-Rowland, S., Madorsky, I., Papin, J.E., and Notterpek, L. (2010). Reduction of Dicer impairs Schwann cell differentiation and myelination. J Neurosci Res *88*, 2558-2568.

Wang, C.H., Lee, D.Y., Deng, Z., Jeyapalan, Z., Lee, S.C., Kahai, S., Lu, W.Y., Zhang, Y., and Yang, B.B. (2008). MicroRNA miR-328 regulates zonation morphogenesis by targeting CD44 expression. PLoS One *3*, e2420.

Wang, J.W., Humphreys, J.M., Phillips, J.P., Hilliker, A.J., and Wu, C.F. (2000). A novel leg-shaking Drosophila mutant defective in a voltage-

gated K(+)current and hypersensitive to reactive oxygen species. J Neurosci *20*, 5958-5964.

Wang, T., and Montell, C. (2007). Phototransduction and retinal degeneration in Drosophila. Pflugers Arch *454*, 821-847.

Weinmann, L., Hock, J., Ivacevic, T., Ohrt, T., Mutze, J., Schwille, P., Kremmer, E., Benes, V., Urlaub, H., and Meister, G. (2009). Importin 8 is a gene silencing factor that targets argonaute proteins to distinct mRNAs. Cell *136*, 496-507.

Weng, R., Chen, Y.W., Bushati, N., Cliffe, A., and Cohen, S.M. (2009). Recombinase-mediated cassette exchange provides a versatile platform for gene targeting: knockout of miR-31b. Genetics *183*, 399-402.

Weng, R., Chin, J.S., Yew, J.Y., Bushati, N., and Cohen, S.M. (2013). controls male reproductive success in. Elife *2*, e00640.

Weng, R., and Cohen, S.M. (2012). Drosophila miR-124 regulates neuroblast proliferation through its target anachronism. Development *139*, 1427-1434.

Westholm, J.O., and Lai, E.C. (2011). Mirtrons: microRNA biogenesis via splicing. Biochimie *93*, 1897-1904.

Wiegand, R.D., Giusto, N.M., Rapp, L.M., and Anderson, R.E. (1983). Evidence for rod outer segment lipid peroxidation following constant illumination of the rat retina. Invest Ophthalmol Vis Sci *24*, 1433-1435.

Wightman, B., Ha, I., and Ruvkun, G. (1993). Posttranscriptional regulation of the heterochronic gene lin-14 by lin-4 mediates temporal pattern formation in C. elegans. Cell *75*, 855-862.

Winter, J., and Diederichs, S. (2011). Argonaute proteins regulate microRNA stability: Increased microRNA abundance by Argonaute proteins is due to microRNA stabilization. RNA Biol *8*, 1149-1157.

Wisniewski, J.R., Zougman, A., Nagaraj, N., and Mann, M. (2009). Universal sample preparation method for proteome analysis. Nat Methods *6*, 359-362.

Wu, C.F., and Wong, F. (1977). Frequency characteristics in the visual system of Drosophila: genetic dissection of electroretinogram components. J Gen Physiol *69*, 705-724.

Wu, D., Raafat, A., Pak, E., Clemens, S., and Murashov, A.K. (2012). Dicer-microRNA pathway is critical for peripheral nerve regeneration and functional recovery in vivo and regenerative axonogenesis in vitro. Exp Neurol *233*, 555-565.

Xiao, C., Calado, D.P., Galler, G., Thai, T.H., Patterson, H.C., Wang, J., Rajewsky, N., Bender, T.P., and Rajewsky, K. (2007). MiR-150 controls B cell differentiation by targeting the transcription factor c-Myb. Cell *131*, 146-159.

Xiong, W.C., Okano, H., Patel, N.H., Blendy, J.A., and Montell, C. (1994). repo encodes a glial-specific homeo domain protein required in the Drosophila nervous system. Genes Dev *8*, 981-994.

Xu, G., Fewell, C., Taylor, C., Deng, N., Hedges, D., Wang, X., Zhang, K., Lacey, M., Zhang, H., Yin, Q.*, et al.* (2010). Transcriptome and targetome analysis in MIR155 expressing cells using RNA-seq. RNA *16*, 1610-1622.

Yang, J.S., and Lai, E.C. (2011). Alternative miRNA biogenesis pathways and the interpretation of core miRNA pathway mutants. Mol Cell *43*, 892-903.

Yang, J.S., Maurin, T., and Lai, E.C. (2012). Functional parameters of Dicer-independent microRNA biogenesis. RNA *18*, 945-957.

Yang, J.S., Maurin, T., Robine, N., Rasmussen, K.D., Jeffrey, K.L., Chandwani, R., Papapetrou, E.P., Sadelain, M., O'Carroll, D., and Lai, E.C. (2010). Conserved vertebrate mir-451 provides a platform for Dicer-independent, Ago2-mediated microRNA biogenesis. Proc Natl Acad Sci U S A *107*, 15163-15168.

Yang, J.S., Nam, H.J., Seo, M., Han, S.K., Choi, Y., Nam, H.G., Lee, S.J., and Kim, S. (2011). OASIS: online application for the survival analysis of lifespan assays performed in aging research. PLoS One *6*, e23525.

Yang, M., Lee, J.E., Padgett, R.W., and Edery, I. (2008). Circadian regulation of a limited set of conserved microRNAs in Drosophila. BMC Genomics *9*, 83.

Yao, B., La, L.B., Chen, Y.C., Chang, L.J., and Chan, E.K. (2012). Defining a new role of GW182 in maintaining miRNA stability. EMBO Rep *13*, 1102-1108.

Zhang, N., and Bevan, M.J. (2010). Dicer controls CD8+ T-cell activation, migration, and survival. Proc Natl Acad Sci U S A *107*, 21629-21634.

Zhao, Y., Ransom, J.F., Li, A., Vedantham, V., von Drehle, M., Muth, A.N., Tsuchihashi, T., McManus, M.T., Schwartz, R.J., and Srivastava, D. (2007). Dysregulation of cardiogenesis, cardiac conduction, and cell cycle in mice lacking miRNA-1-2. Cell *129*, 303-317.

Zhou, B., Wang, S., Mayr, C., Bartel, D.P., and Lodish, H.F. (2007). miR-150, a microRNA expressed in mature B and T cells, blocks early B cell development when expressed prematurely. Proc Natl Acad Sci U S A *104*, 7080-7085.

Ziu, M., Fletcher, L., Rana, S., Jimenez, D.F., and Digicaylioglu, M. (2011). Temporal differences in microRNA expression patterns in astrocytes and neurons after ischemic injury. PLoS One *6*, e14724.

Zovoilis, A., Agbemenyah, H.Y., Agis-Balboa, R.C., Stilling, R.M., Edbauer, D., Rao, P., Farinelli, L., Delalle, I., Schmitt, A., Falkai, P.*, et al.* (2011). microRNA-34c is a novel target to treat dementias. EMBO J *30*, 4299-4308.

Griffiths-Jones S, Saini HK, van Dongen S, Enright AJ. (2008) miRBase: tools for microRNA genomics. NAR 2008 36(Database Issue):D154-D158

APPENDIX I

Permission to re-use Fig 3.1a from Dr William Stark. Following is the series of emails for the same.

Devika Garg <devika.garg@gmail.com> Fri, Apr 19, 2013 at 12:41 PM
To: starkws@slu.edu
Dear Dr Stark,

I am a graduate student in Dr Steve Cohen's lab in Singapore. I have been working with fruit flies, and studying retinal degeneration for the first part of my thesis. I also received the norpA P24 mutant flies from your lab a couple of years ago. I used deep pseudopupil analysis as a method to screen possible mutations. In order to explain this optical phenomenon in my thesis, I wish to use figure 2 from your paper -

Stark and Thomas Molecular Vision 2004; 10:943-955

I wish to ask your permission if it would please be okay for me to use it without any modifications from my end. I would attach my correspondence with you with my final volume. I would be very grateful.

Many thanks
Regards
Devika

--
Devika Garg
Graduate Student
Stephen Cohen Laboratory
Institute of Molecular and Cell Biology
61 Biopolis Drive, Proteos
Singapore 138673

William Stark <starkws@slu.edu> Sun, Apr 21, 2013 at 11:40 PM
To: Devika Garg <devika.garg@gmail.com>, Doekele Stavenga <D.G.Stavenga@rug.nl>

the caption reads:

This diagram is redrawn from one used in the laboratory of Dr. Doekele G. Stavenga where WSS was a research fellow in 1978. The original was drawn by Jan Witpaard, a former student of Dr. Stavenga. This drawing helps to demonstrate the optics of the deep pseudopupil as characterized by Franceschini and Kirschfeld [32,47].

and so I am Cc'ing to Doekele Stavenga to see if it is OK with him.
Frankly, in addition to thinking that the material is not really "mine,"
I really do not think my student's art work was very good, but I wanted
to put his picture in so I could acknowledge him

--
"When it comes to brains, remember that the simpler electric, molecular and cellular forces and laws, though still present and operating, have been superseded by the configurational forces of higher level mechanisms" - Roger Sperry (1981 Nobel Prize)

William S. Stark, Ph.D.
Professor of Biology
Saint Louis Univ.
3507 Laclede Ave.
St. Louis MO 63103-2010
(314) 977-7151
starkws@slu.edu
http://starklab.slu.edu

William Stark <starkws@slu.edu> Fri, Apr 26, 2013 at 12:31 AM
To: Devika Garg <devika.garg@gmail.com>

yes, use the figure and thank you for your interest

--
"What if you knew her and found her dead on the ground?" - CSNY (RIP Allison Krause, Jeffrey Miller, William Schroeder & Sandra Scheuer, Kent State May 4, 1970)

William S. Stark, Ph.D.
Professor of Biology
Saint Louis Univ.
3507 Laclede Ave.
St. Louis MO 63103-2010
(314) 977-7151
starkws@slu.edu
http://starklab.slu.edu